The Role of The Non-Canonical NF-κB Pathway during Steady State and Autoimmune Inflammation

Dissertation

Zur Erlangung des Grades

Doktor der Naturwissenschaften

Am Fachbereich Biologie

Der Johannes Gutenberg-Universität in Mainz

Vorgelegt von

Nishada S. K. Ramphal

Geb. am 13. Oktober 1991 in Ede, Niederlanden

Mainz, 2024

Dekan*:* [redacted]

1. Berichterstatter: [redacted]
2. Berichterstatter: [redacted]

Tag der mündlichen Prüfung: 17.09.2024

TABLE OF CONTENTS

TABLE OF FIGURES

LIST OF ABBREVIATIONS

ADP	Adenosine Diphosphate
APC	Antigen-Presenting Cells
ATP	Adenosine Triphosphate
BAMs	Border-Associated Macrophages
BBB	Blood Brain Barrier
BCR	B Cell Receptor
BTKi	Bruton's Tyrosine Kinase Inhibitors
CCR	Chemokine Receptor
cDC	Conventional Dendritic Cell
CDP	Common Dc Precursors
CFA	Complete Freud's Adjuvant
CIS	Clinically Isolated Syndrome
CLIP	Class Ii-Associated Ii Peptide
cMoP	Common Monocyte Progenitors
CMP	Common Myeloid Progenitor
CNS	Central Nervous System
CSF	Cerebrospinal Fluid
DAPI	4',6-Diamidino-2-Fenylindool
DC	Dendritic Cell
DEG	Differentially Expressed Gene
dLN	Skin-Draining Lymph Node
DMT	Disease-Modifying Therapy
EAE	Experimental Autoimmune Encephalomyelitis
EBV	Epstein-Barr Viru
GMP	Granulocyte-Monocyte Progenitor
GWAS	Genome-Wide Association Studies
HLA	Human Leukocyte Antigen Complex
Iba1	Ionized Calcium-Binding Adapter Molecule 1
IFNγ	Interferon-Gamma
LN	Lymph Node
LYVE1	Lymphatic Vessel Endothelial Hyaluronan Receptor 1
MCM	Medullary Cord Macrophages
MFI	Median Fluorescent Intensity
MHCII	Major Histocompatibility Complex Ii
MHCII	Major Histocompatibility Complex
MOG	Myelin Oligodendrocyte Glycoprotein
MS	Multiple Sclerosis
MSM	Medullary Sinus Macrophages
NF-κB	Nuclear Factor Kappa B
NIK	NF-κB Inducing Kinase
pDC	Plasmacytiod Dendritic Cell
pDCs	Plasmacytoid Dcs
$PLP_{139-151}$	Proteolipid Protein139-151
PPMS	Primary Progressive Disease

Ptx	Pertussis Toxin
RRMS	Relapsing-Remitting MS
scRNA-seq	Single-Cell RNA Sequencing
SCS	Subcapsular Sinus
Siglec1	Sialic Acid Binding Ig Like Lectin 1
SPMS	Secondary Progressive MS
TCR	T Cell Receptors
$T_H(1)$	T Helper(1)
TLR	Toll-Like Receptor
TNF-α	Tumour Necrosis Factor Alpha
UMAP	Uniform Manifold Approximation And Projection

1.

INTRODUCTION

1.1 Multiple Sclerosis

1.1.1 Clinical course of MS

Multiple sclerosis (MS) is a chronic autoimmune disease of the central nervous system (CNS) which affects over 700.000 people in Europe[1]. It is one of the most common causes of neurological disability in young and middle-aged adults, and the prevalence has increased in every world region since 2013[1,2]. MS causes disruptions to the nervous system, resulting in various symptoms such as fatigue, weakness, numbness, tingling, and difficulty with coordination and balance. The first episode of these neurological symptoms is defined as clinically isolated syndrome (CIS), which often progresses into a relapsing-remitting MS (RRMS). Approximately 85% of MS patients have RRMS, characterised by episodes of relapse and remission[3]. This typically leads to non-relapsing progression, i.e. secondary progressive MS (SPMS)[4]. In the RRMS stage, patients may experience distinct episodes of neurological dysfunction such as optic neuritis, sensory disturbances, or motor and cerebellar function impairments. During the progressive stage, the neurological dysfunction worsens, particularly affecting the patient's gait[5]. An estimated 10-15% of individuals with MS are diagnosed with primary progressive disease (PPMS). This type of MS is characterised by a progressive decline in function from the beginning, with no relapses and remissions. It is uncertain whether PPMS is a distinct type of MS or simply SPMS without clinically evident relapses[6]. Diagnosing MS involves a combination of clinical, MRI, and laboratory findings. This includes examining the cerebrospinal fluid (CSF) and utilising gadolinium enhancement to visualise the inflammatory components in MS lesions[7].

1.1.2 Mechanisms of MS

MS is characterised by a cascade of pathological events within the CNS, including inflammation, demyelination, blood-brain barrier (BBB) breakdown, gliosis, and scar tissue (sclerosis) formation[4]. However, the sequence of these events and the initiation of MS are still subjects of debate among researchers. Two opposing hypotheses, the "outside-in" and "inside-out" hypotheses, have been proposed.

The outside-in hypothesis suggests that there is first a CNS antigen-specific immune activation in the periphery, which then spreads to the previously unaffected CNS. It is believed that

autoreactive T cells in peripheral tissues may be activated due to direct cross-reactivity, molecular mimicry, or bystander activation. After migrating to the lymph nodes (LNs), a small number of these antigen-specific T cells and B cells will enter the CNS compartment during the early phase of lesion development. $CD4^+$ T cells that enter the perivascular space release cytokines locally, affecting astroglial endfeet and disrupting oligodendroglial and astroglial homeostasis[8]. The release of inflammatory mediators compromises the BBB, causing an influx of immune cells across the BBB, leading to targeted destruction of myelin, damage to oligodendrocytes, and neuroaxonal degeneration[9].

The infiltrating immune cells include autoreactive lymphocytes that respond against CNS autoantigens and were found to consist mainly of T cells, in particular, T helper (T_H)1 cells, which produce the pro-inflammatory cytokines Interferon-gamma (IFNγ) and tumour necrosis factor-alpha (TNF-α)[10]. T_H17 cells are another subset of CD4 T cells that induce a wide range of cytokines, including Interleukin (IL)-17A, IL-21, IL-22 and IL-26, all of which are capable of promoting inflammation. Specifically, IL-17A has been associated with neutrophil expansion and BBB disruption in MS patients[11]. In addition, cytotoxic $CD8^+$ T cells have been found in the lesions of MS patients, which play a role in oligodendrocyte death, demyelination and axonal death[12]. A study by C. Cruciani and colleagues has demonstrated a link between reactivity to autoantigens and different patterns of inflammation, which implies that T cell specificity is a crucial factor in MS[13]. B cells, plasmablasts, and plasma cells are also found in the lesions, meninges, and CSF of most MS patients. They are thought to play a role in the pathogenesis of MS through proinflammatory cytokine and chemokine production, antibody formation, and antigen presentation to T cells[14].

In response to CNS inflammation, resident glial cells, including microglia and astrocytes, become activated and contribute to the immune response. Prolonged neuroinflammation and demyelination can lead to the activation of repair mechanisms, as well as to chronic glial activation and the formation of lesions[15]. Both macrophages and microglia accumulate at sites of active lesions in MS where they release inflammatory mediators which can further amplify neuroinflammation and CNS pathology[16,17]. Interestingly, microglial activation is more pronounced in the normal-appearing white matter of MS patients as compared to healthy controls and increases with disease duration[18]. As the disease progresses, it can lead to gradual neuroaxonal loss, often linked to the patient's disability [4].

In the second hypothesis, it is believed that the initiating event within the CNS causes the activation of microglia[19]. The alternative inside-out hypothesis proposes that an initial event in the CNS triggers microglia activation, leading to an amplification of the immune reaction and the subsequent recruitment of adaptive and innate immune cells[19]. This hypothesis suggests that a primary defect of oligodendrocytes, such as a genetic mutation, results in spontaneous

oligodendrocyte death and the activation of microglial cells. This would explain the initial changes observed in the pre-phagocytic lesion stage or normal-appearing white matter with oligodendrocyte loss and microglia activation without major lymphocyte infiltrates. According to this hypothesis, antigens drain out of the CNS into deep cervical LNs, where they induce a secondary adaptive immune response in the periphery[19,20]. There is supporting evidence for both hypotheses, suggesting that the aetiology of MS likely arises from a combination of both models.

1.1.3 Etiology and Therapeutic Advances in MS

The precise cause of MS remains unknown, yet a variety of risk factors, such as genetic predispositions, viral infections, and environmental factors are associated with disease development. Genetic predisposition plays a role, as evidenced by a higher risk of the disease among individuals with a family history of MS[21]. Furthermore, genome-wide association studies (GWAS) have linked polymorphisms in various genes to MS susceptibility. Interestingly, the majority of the variants lie within genes associated with immune functions[22,23]. In addition to genetic factors, certain environmental influences have been identified as contributing to the risk of developing MS. For instance, MS is more common in areas farther from the equator, suggesting that lack of sunlight and low vitamin D levels may play a role[24]. Lifestyle factors such as smoking and obesity have also been associated with an increased risk of MS[21].

Moreover, viral infections, particularly those caused by the Epstein-Barr virus (EBV), have been suggested as potential triggers for the immune system[25–27]. One study showed a 32-fold increased risk of MS diagnosis in individuals who converted to EBV seropositivity compared with those who remained seronegative[28]. Various mechanisms could be involved in MS pathophysiology through EBV infection. These include the EBV-driven natural movement of autoreactive B cells and T cells into the CNS, molecular mimicry resulting from chronic EBV infection, and inflammatory cytokines and exosomes triggered by EBV[25,26]. In conclusion, the aetiology of MS is complex and involves multiple factors. The interplay of these genetic, lifestyle, and environmental risk factors contributes to the disease's complexity. This underscores the need for further research to understand the mechanisms behind MS and develop effective treatments.

While there is no known cure, there are several treatment options available to manage symptoms and slow the progression of the disease (reviewed in Yang et al., 2022[29]). The therapeutic landscape for MS has evolved significantly over the years, with strategies now targeting key elements contributing to MS pathogenesis: the peripheral immune system, BBB permeability, and leukocyte migration into the CNS[29].

The first Disease-Modifying Therapy (DMT) approved by the FDA in 1993 is IFN-β. It plays a crucial role in managing MS by down-regulating antigen presentation and anti-inflammatory cytokines, suppressing T cell activity and reducing infiltration of immune cells across the BBB [30]. This modulation of the immune response helps to reduce the frequency and severity of MS flare-ups. Another MS therapy approach under investigation in clinical trials is Bruton's tyrosine kinase inhibitors (BTKi). These inhibitors suppress B cell maturation, proliferation, antigen presentation, and the release of cytokines and inflammatory mediators by myeloid cells. Interestingly, BTKi also targets microglia, making them an attractive option for treating both progressive and relapsing forms of MS[31].

Furthermore, there are S1P receptor modulators, such as Fingolimod, which alter the migration of lymphocytes out of the LNs, effectively reducing the inflammatory response in MS[32]. Natalizumab, an antibody against VLA-4, also targets the migration of leukocytes and inhibits their infiltration into the CNS, helping to reduce inflammation and damage in the CNS and thereby slowing the progression of MS[33]. Lastly, B-cell depleting therapies, such as Rituximab, Ocrelizumab, and Ofatumumab, have emerged as effective treatments for MS. By depleting B cells, these therapies help to modulate the immune response, reduce inflammation, and minimise damage in the CNS. This approach has shown promise in reducing relapse rates and slowing disease progression in MS patients[34].

In summary, the current therapeutic strategies for MS are diverse and target different aspects of the disease pathogenesis. These therapies have significantly improved the quality of life for MS patients and continue to evolve with ongoing research and clinical trials.

1.2 Experimental Autoimmune Encephalomyelitis (EAE)

Multiple animal models to study the mechanisms of MS have been developed over the years. However, none of the models used today cover the full spectrum of MS-underlying processes mentioned earlier. One of the most used models is the experimental autoimmune encephalomyelitis (EAE) model[35]. The origin of these models dates back to an experimental attempt to explain the occasional occurrence of neuroparalytic complications in patients receiving rabies vaccination using inactivated viruses insufficiently purified from brain cells or brain tissues. Inflammatory infiltrates were observed in these patients, which suggests an MS-like disease[36,37]. The first animal models were injected with homogenised brain tissue dissolved in saline to mimic this MS-like disease after auto-sensitization in humans. They observed signs of ataxia and paralysis, accompanied by leukocyte infiltration into the CNS, gliosis and demyelination [38]. The foundation for the EAE model was established based on these observations.

To induce EAE, animals are immunised with a CNS-related antigen in combination with a potent adjuvant such as complete Freud's adjuvant (CFA). EAE is most commonly induced in

rodents, and various protocols have been published. The combination of the antigen and the animal species/strain used determines the clinical course of EAE [39,40]. For example, immunising the SJL mouse strain with the proteolipid protein $(PLP)_{139-151}$ peptide results in a relapse remitting EAE course. On the other hand, immunising the C57BL6 mouse strain with the Myelin oligodendrocyte glycoprotein $(MOG)_{35-55}$ peptide results in a monophasic chronic disease course[41].

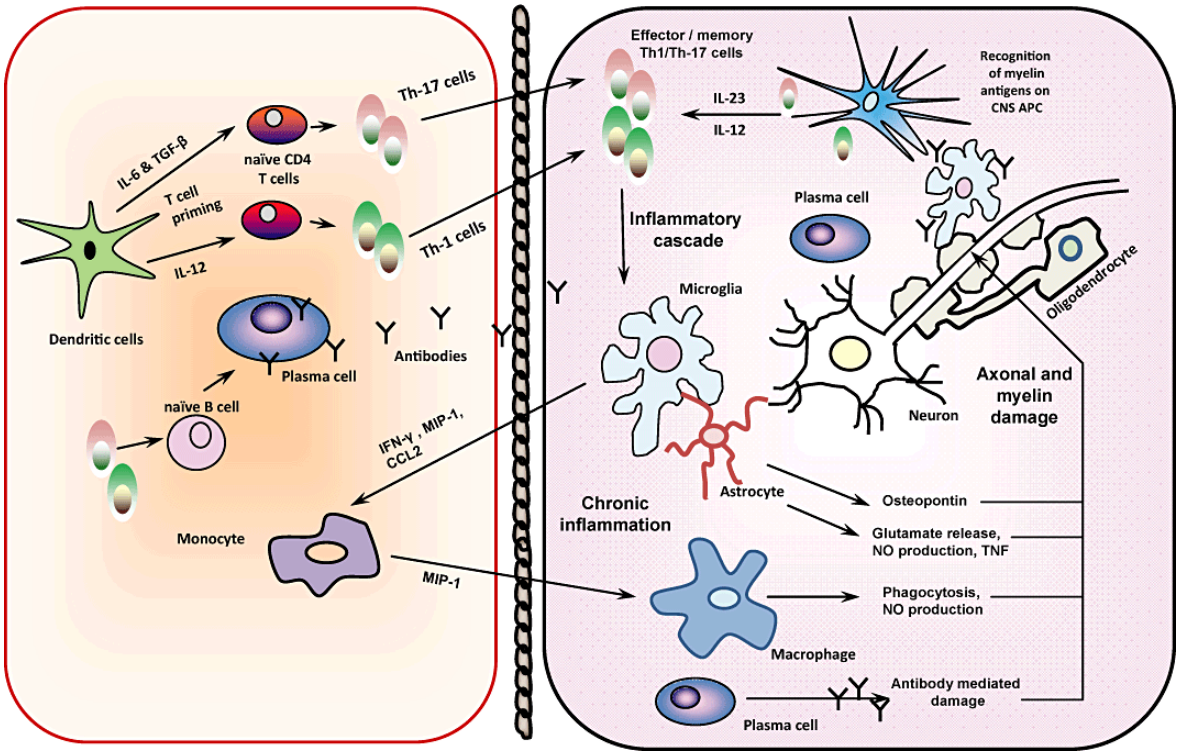

Figure i: Schematic diagram of some of the key pathological features of EAE pathogenesis (From C.S. Constantinescu et al., 2011[42]).

Antigen-presenting dendritic cells (DCs) activate T cells by presenting the antigen peptide. This priming process causes T cells to differentiate into IFNγ-producing and IL-17A-producing T cells. Subsequently, these effector T cells cross the blood-brain barrier and infiltrate the CNS. Once inside the CNS, they are reactivated and initiate an inflammatory response, leading to the destruction of myelin sheaths. Additionally, antibodies and B cells can enter the CNS, and plasma cells produce antibodies within the CNS, contributing to inflammatory demyelination and neurodegeneration.

In this active form of EAE, the CNS antigens are phagocytised by local antigen-presenting cells (APCs) in the skin before travelling to the draining (d)LNs and spleen. Here, the APCs activate T cells through the presentation of the antigen peptide. This priming process will cause the differentiation of T cells into IFNγ-producing T_H1 cells and IL-17A-producing T_H17 cells. Subsequently, these effector T cells will cross the blood-brain barrier and infiltrate the CNS [43,44]. Once inside the CNS, they are reactivated and initiate an inflammatory response, leading to the destruction of myelin sheaths (Fig. i). This progressive loss of myelin results in a range of clinical signs in the mouse, including paralysis of the tail, hind paws and eventually, front paws[41,45]. In some strains of mice, an extra boost to the immune system may be needed to

initiate the disease. This boost comes from pertussis toxin (Ptx), which is derived from the bacterium Bordetella pertussis[46]. Although the exact function of Ptx in the context of EAE induction is not fully understood, it is believed that Ptx enhances EAE by affecting autoreactive T cells and by inducing changes in the BBB[43,44].

Another EAE model is achieved by the transfer of encephalitogenic MOG-activated T cells into mice. In this model, EAE is induced in donor animals, as in the active EAE model. Before or during disease onset, immune cells are isolated from the spleen and dLNs. These cells can be cultured *in vitro* to raise and expand encephalitogenic T cells, which then are transferred into naïve mice[47–49]. Upon transfer, the activated myelin-specific T cells from the donor animals initiate an immune response in the recipient animals, leading to the development of EAE. This allows researchers to study mechanisms of immune surveillance of the CNS and T cell-mediated inflammatory tissue damage[40,50]. One of the significant benefits of using passive transfer models is that the T cells are already raised and expanded before being transferred. This means that the outcome of CNS inflammation is not affected by immune activation in peripheral lymphoid tissue. However, a major drawback of this model is that it is mainly limited to inflammation that is mediated by $CD4^+$ T cells and is not suitable for studying the initial triggering events of CNS inflammation[50,51].

Another experimental model for MS is the spontaneous EAE model, which is useful to study the initiation phase of the disease. For this, transgenic mice, which overexpress myelin-specific T or B cell receptors, were developed. These mice models can be entirely murine or "humanised" for the TCR and associated antigen-presenting molecules and develop spontaneous neurological symptoms with varied incidence and clinical patterns (reviewed in A. Ben-nun et al., 2014)[51].

1.3 Antigen Processing, Presentation and T Cell Activation

As mentioned in the MS and EAE chapters, antigen presentation plays a crucial role in the development of disease in both humans and mice. It is an essential part of the adaptive immune system, which involves the presentation of peptides on Major Histocompatibility Complex (MHC) molecules (human leukocyte antigen complex; HLA in humans) to specific T cell receptors (TCRs) on T cells [52]. There are two major classes of MHC molecules: MHC class I and MHC class II. The MHCI molecule is expressed in almost all cell types, and its primary function is to report intracellular events, such as viral or bacterial infection, to $CD8^+$ T cells have the ability to kill these infected cells[53]. This mechanism is pivotal in alerting the immune system to the presence of virally infected cells. The MHCII molecule is mainly expressed by APCs, which include B cells, dendritic cells (DCs), macrophages, and thymic epithelial cells. Its main function is to present exogenous antigens to $CD4^+$ T cells. The MHCII pathway is essential to warning

the adaptive immune system of foreign antigens and also plays a central role in tolerance against self-antigens[54].

While both MHCI and MHCII pathways are essential for antigen presentation, the focus here will be on the MHCII pathway, as it plays a more critical role in the context of EAE. The process of antigen presentation can be broken down into steps[55]. The first step is the acquisition of exogenous antigens through phagocytosis and endocytosis. This step involves various receptors, including the B cell receptor (BCR), the mannose receptor (CD206; Mrc1), complement receptors and Fc receptors[56,57]. Next, endosomes containing the proteins will fuse with a lysosome, which is rich in proteolytic enzymes and disulphide reductases and has a low pH, which activates the proteases for antigen proteolysis [52,54]. Next, the endosomes containing the peptides will fuse with an endosomal compartment containing the MHCII complex with a class II-associated Ii peptide (CLIP) in the peptide-binding groove. The molecule H2-DM (HLA-DM in humans) is required to exchange the MHCII-bound CLIP for a specific peptide[58,59]. After the binding of a specific peptide derived from a protein degraded by the endosomal pathway, the MHCII complex will be transported to the plasma membrane, where it will present its peptide to the peptide-specific TCR on $CD4^+$ cells[55,60].

The presentation of antigens alone to T cells is not sufficient to activate them; they also need a second co-stimulatory signal. Co-stimulatory molecules may deliver either a stimulatory or inhibitory signal for T cell activation and proliferation, thereby regulating a specific immune response[61]. Some of the positive costimulatory molecules on T cells include CD28, CD40L, and ICOS, while CTLA-4 and PD-1 are two negative co-stimulatory molecules. These molecules can be activated by the ligands CD80, CD86, CD40, and PD-L1 on APCs[62,63]. This tightly regulated mechanism is also implicated in MS and EAE, where APCs present myelin-derived peptides (such as MOG_{35-55}) via MHCII to autoreactive $CD4^+$ T cells. The aberrant activation of these T cells due to co-stimulatory signals leads to an inflammatory response against myelin [64].

1.4 A Short Introduction to Myeloid Cells: Origins And Subtypes.

1.4.1 Origins of myeloid cells

Myeloid cells are part of the innate immune system and have a crucial role in defending the body against pathogens and maintaining tissue homeostasis. These cells originate from hematopoietic stem cells in the bone marrow and are involved in various immune functions, such as phagocytosis, antigen presentation, and cytokine production[65]. Myeloid cells are a diverse group of cell types, including monocytes, macrophages, DCs, neutrophils, eosinophils, basophils, and mast cells, which all arise from a common myeloid progenitor (CMP)[66]. Each of these cell types has distinct functions and contributes to the body's immune response in different ways. Here, we will delve deeper into the functions and origins of macrophages,

monocytes, and DCs, which are part of the mononuclear phagocyte system, a body-wide, specialised system of phagocytic cells.

These three cell types, except certain tissue-resident macrophages, share a common precursor in the bone marrow known as the 'monocyte-macrophage DC progenitor' (MDP). The MDPs are a critical population of cells that have the potential to differentiate into several key immune cells. They give rise to two distinct types of progenitors: the common DC precursors (CDP) and the unipotent common monocyte progenitors (cMoP)[66,67]. The cMoP, as their name suggests, give rise to monocyte populations, which circulate the bloodstream and can further differentiate into macrophages or DCs when entering specific tissues. On the other hand, CDPs have the capacity to develop into different types of DCs: plasmacytoid DCs (pDCs) and conventional (c)DCs (Fig. iiB)[68,69].

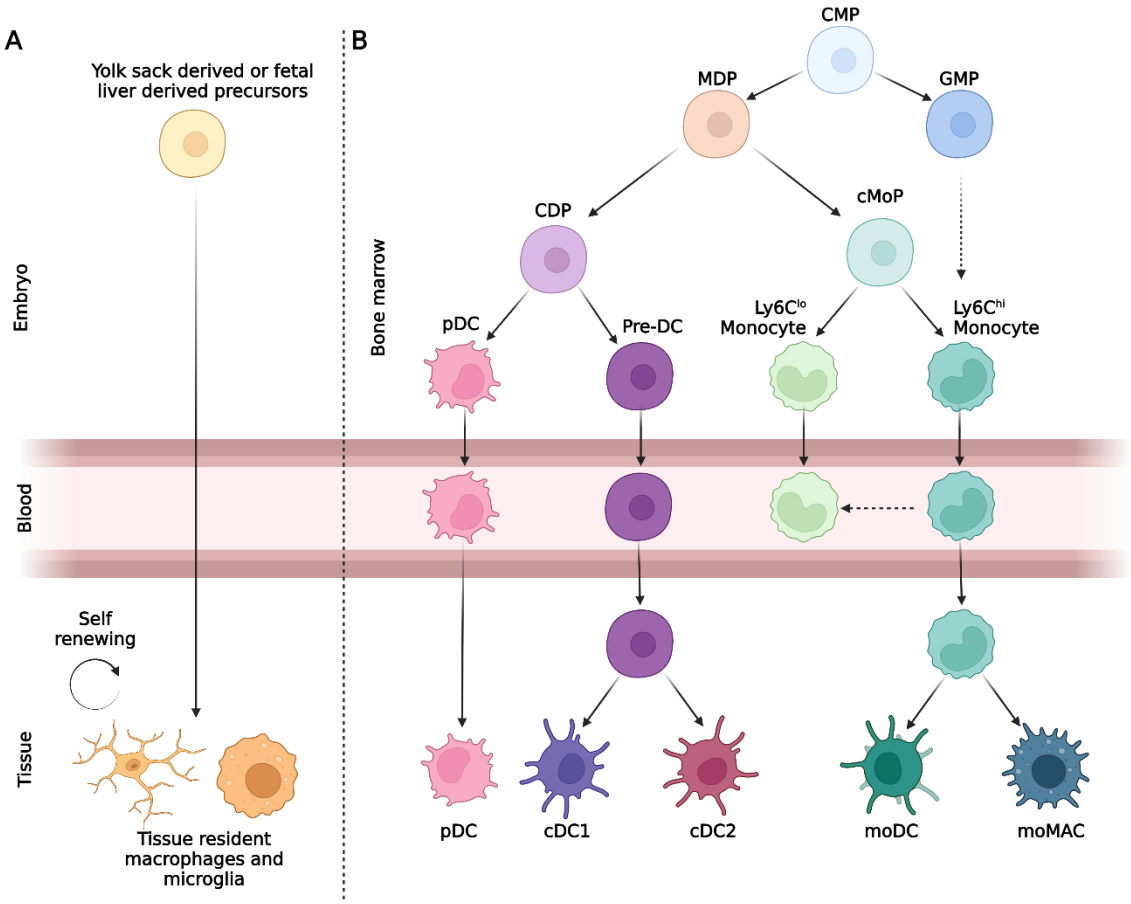

Figure ii: Development of myeloid subsets.

(A) Tissue-resident macrophages and microglia arise from yolk-sac-derived precursors and are self-maintaining. (B) common myeloid progenitor (CMP), which gives rise to the granulocyte-monocyte precursors (GMPs) and monocyte-macrophage DC progenitor (MDP). MDP differentiates into common DC precursors (CDP) or common monocyte progenitors (cMoP). cMoPs give rise to monocyte populations, while CDPs are able to develop into cDCs and pDCs. Made with BioRender.

Recent advancements in single-cell RNA sequencing (scRNA-seq) technology reveal that the process of lineage commitment is likely more complex than shown in Figure iiB. It has been demonstrated that supposedly oligopotent progenitors already exhibit lineage commitment. Moreover, unipotent progenitors can directly emerge from hematopoietic stem cells without having to sequentially progress through defined bipotent precursor stages[70–72]. Additionally, new research has shown that monocytes can also be derived from granulocyte-monocyte precursors (GMPs), which, like MDPs, originate from CMPs (Fig. iiB)[73,74]. These monocytes are functionally distinct from MDP-derived monocytes, and each subset can differentially contribute to peripheral tissue macrophage populations in homeostasis and following challenges[73,74].

While monocytes can differentiate into macrophages, they have only minimal contribution to most tissue-resident macrophages during steady state[75,76]. Some tissue-resident macrophages like Kupfer cells, epidermal Langerhans cells, and microglia arise from primitive myeloid progenitors during embryonic development[77]. These macrophages are derived from progenitors that migrate from the embryonic yolk sack to the tissue around embryonic day 8.5 (Fig. iiA)[78–80]. Various studies have observed that, while most tissue-resident macrophages are gradually replaced by bone marrow-derived monocytes, microglia and certain border-associated macrophages (BAM) populations are self-maintaining during life[80–82].

1.4.2 Tissue-resident macrophages

Tissue-resident macrophages are specialised immune cells strategically located in various tissues throughout the body. They are heterogeneous and have unique functions depending on their location and tissue-specific microenvironments, which influence macrophage gene expression, surface markers, and functional properties[83,84]. For instance, alveolar macrophages in the lungs are specialised for dealing with airborne pathogens, whereas Kupffer cells in the liver are adapted for filtering blood and metabolising lipids. Tissue-resident macrophages are best known as immune sentinels that sense and respond to invading pathogens and challenging surroundings[83]. Upon sensing danger, these macrophages can engulf pathogens, produce pro-inflammatory cytokines, and recruit other immune cells to the site of infection[85]. In addition to their immune functions, tissue-resident macrophages are essential in the development and homeostasis of their host tissues. They participate in various processes, such as efferocytosis and remodelling of tissues during development[84]. Positioned at the interface of tissue homeostasis and disease development, these macrophages can either safeguard against or contribute to diseases when their homeostatic core functions are disrupted (Fig. iii).

The CNS has two significant tissue-resident macrophage populations: microglia and BAMs[86]. BAMs are found at the interface between the CNS and periphery, including the meninges,

perivascular space, and choroid plexus in the ventricles (reviewed in [80]). The research on BAMs started relatively recently, and the exact function of the various BAM populations during homeostasis, inflammation, and neurological disorders remains under investigation. Microglia, on the other hand, are the most well-characterized macrophage population in the CNS. They reside in the brain parenchyma and play a role in various CNS functions, such as glio-, vasculo-, and neurogenesis, as well as synaptic and myelination processes. They achieve this through their process motility, release of soluble factors, and ability to perform phagocytosis[87]. Even in their resting state, the microglia processes are active, constantly sampling their environment. However, upon insult, microglia respond rapidly by migrating to sites of damage[88].

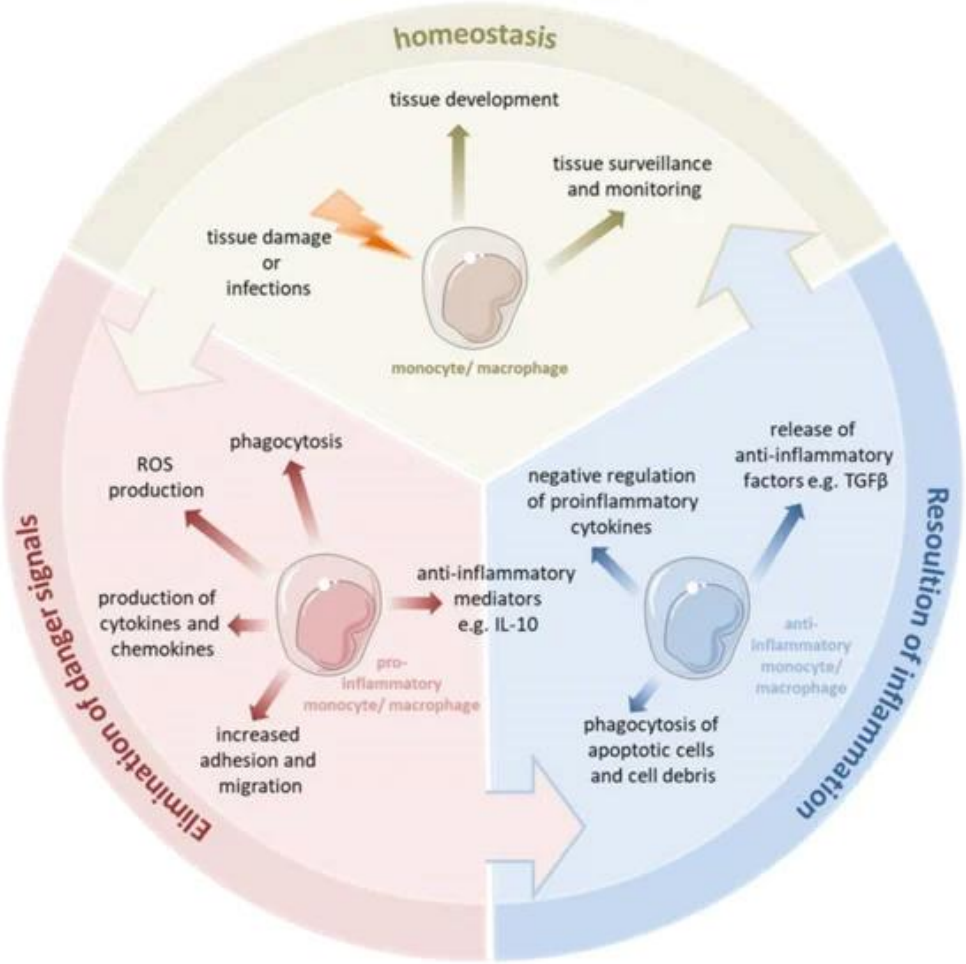

Figure iii: Macrophage and monocyte functions. (From J. Austermann et al., 2022[89])

Monocytes and macrophages play diverse roles in the inflammatory response. They are able to transition from a homeostatic state to a pro-inflammatory state to eliminate pathogens and fight inflammation. In uncomplicated inflammation, they shift from a pro-inflammatory to an anti-inflammatory state, thereby contributing to the resolution of inflammation and the re-establishment of homeostasis. Depending on the kind of signal or pathophysiologic condition, monocytes and macrophages can undergo specific phenotypic polarisation, resulting in distinct functional phenotypes.

Microglia are involved in the pathology of multiple diseases like MS, Parkinson's disease and Alzheimer's disease, amyotrophic lateral sclerosis, Huntington's disease, stroke, epilepsy,

autism spectrum disorder and schizophrenia[16,17,88,90,91]. In individuals with MS, histological assessments have revealed clusters of microglia expressing markers of antigen presentation and phagolysosomal activity in the normal-appearing white matter. This suggests that microglia may play a role in the early stages of lesion development [92]. Microglia expand significantly during the formation of active lesions. As these lesions progress into mixed active and inactive states, microglia are found at their borders while disappearing within the lesion core[15].

Furthermore, it has been shown that in the mouse model EAE, the depletion of microglia and BAMs results in delayed disease onset. This suggests a specific role of these cells in the development of EAE [93]. It has further been shown that microglia acquire MHCII expression during EAE development. However, the deletion of MHCII on microglia and BAMs does not seem to alter EAE pathology[94]. CD40-dependent microglial activation is required for the expansion of encephalitogenic T cells and continual infiltration of leukocytes that sustain chronic disease progression during EAE. Microglia produce cytokines and chemokines important for the recruitment and reactivation of encephalitogenic T cells and the infiltration of monocytes and macrophages[64]. They can also produce anti-inflammatory cytokines like IL-4 and IL-10 during EAE and may have protective and repairing roles in the disease [95].

1.4.3 Monocytes

Monocytes are mononuclear phagocytes that circulate in the bloodstream and play a crucial role in maintaining tissue homeostasis and defending the body against pathogens. They account for 5–10% of all immune cells in the blood and have a short life span of about 1–3 days [67]. During steady state, they exert a homeostatic function and can differentiate into tissue macrophages. During inflammation, monocytes are recruited to the site of inflammation, where they can contribute to the inflammatory response (Fig. iii)[89].

Monocytes can be classified into two distinct sub-populations based on their characteristics.: $CX3CR1^{lo}CCR2^{+}CD43^{-}Ly6C^{+}$ 'classical monocytes' (hereafter $Ly6C^{hi}$ monocytes) and $CX3CR1^{hi}CCR2^{-}CD43^{+}Ly6C^{-}$ 'non-classical' monocytes ($Ly6C^{lo}$ monocytes)[96]. Approximately 90% of the monocytes produced in the bone marrow are $Ly6C^{hi}$ monocytes. During tissue injury, these $Ly6C^{hi}$ monocytes can transport antigens to the LNs and are recruited into the inflamed tissue. Depending on the local cytokine environment, they will differentiate into macrophages or DCs[67,97]. $Ly6C^{lo}$ monocytes, on the other hand, have a patrolling function. They are constantly crawling along the lumen of the vasculature and are involved with early responses to inflammation and tissue repair[98].

It has been has shown that, during steady state, $Ly6C^{hi}$ monocytes are able to infiltrate into tissues (skin, lung, and LNs) without differentiating into macrophages or DCs [97]. Furthermore,

using a fate mapping system, Yona et al. (2013) demonstrated that Ly6C^{hi} monocytes differentiate into Ly6C^{lo} monocytes during steady state conditions[75]. Another study further demonstrated that also under inflammatory conditions, Ly6C^{hi} monocytes can differentiate into Ly6C^{lo} monocytes[99]. Using intravital microscopy, they were able to track both monocyte subsets and show that, during liver injury, Ly6C^{hi} monocytes were recruited to the injury site. After 48 hours, they transitioned into Ly6C^{lo} monocytes, which entered the site of injury and were essential for proper wound healing[99]. Whether this transition of Ly6C^{hi} into Ly6C^{lo} monocytes also happens in other inflammatory models and tissues still needs to be addressed. Furthermore, it has been shown in a model for myocardial infarction that Ly6C^{hi} monocytes can be found early on at the site of inflammation, where they express pro-inflammatory cytokines and help clear debris. While in the later reparative phase, Ly6C^{lo} monocytes can be found, which promote angiogenesis and healing[100]. These studies suggest a tight interplay between monocyte subsets during steady state and inflammatory conditions.

While little is known about the role of Ly6C^{lo} monocytes in the progression of MS and EAE, there is research which demonstrates that the infiltration of Ly6C^{hi} monocytes into the CNS directly correlates with the progression of EAE disease[101–103]. Blocking circulating Ly6C^{hi} monocyte entry into the CNS by inhibiting CCR2 has been found to reduce EAE severity [101,103]. These CNS infiltrating Ly6C^{hi} monocytes are capable of producing inflammatory cytokines and chemokines and participate in the local immune response in EAE[103]. Additionally, these monocytes are able to differentiate into inflammatory DCs and macrophages, which are essential for the polarisation of T_H1 and T_H17 cells and the inflammatory response[96,102,104]. Moreover, they are capable of expressing MHCII, which has been shown to be required during the induction phase of EAE[103,105]. This suggests that Ly6C^{hi} monocytes can also act as antigen-presenting cells during EAE induction.

1.4.4 Dendritic cells (DCs): subsets and functions

DCs play a crucial role in the body's immune system, and they are known to act as messengers between the innate and adaptive immune systems. They are primarily responsible for capturing and presenting foreign antigens, such as viruses, bacteria, and fungi, to B cells and T cells and maintaining tolerance against self-antigens[106–108]. They have a unique shape, with long, branching projections allowing them to interact with many other cells simultaneously[106].

The cDCs are the most abundant DC type during steady state and can be found in almost all tissues. They can be further divided into different subsets based on their function and location[109,110]. Based on their steady state location, the cDCs can be divided into lymphoid tissue-resident (res)DCs and non-lymphoid tissue migratory (mig)DCs. ResDCs are high in CD11c and intermediate in MHCII expression; they are found in the spleen, LNs and Peyer patches[111]. They form dense but dynamic networks surrounding B cell follicles and into the T

cell zone, where they are constantly surveilling antigens and can initiate T cell-dependent immune responses[112].

MigDCs are high in MHCII and intermediate for CD11c expression and can be found in non-lymphoid tissue such as lungs, intestine, and skin. They are strategically located at possible sites of pathogen entry and can migrate to lymphoid tissue under both steady state conditions and during inflammation[109,113]. After antigen uptake, they undergo maturation by upregulating MHCII, costimulatory molecules, and the chemokine receptor (CCR)7, which is crucial for migration. CCR7 guides the migDCs through the lymphatic vessels to the T cell zone in the LNs through the attraction to CCL19/21. Here, they are able to present self- or pathogen antigens to induce tolerance or an immune response, respectively[114,115].

The cDCs can be further divided into two subsets based on their markers and function: $CD8\alpha^+XCR1^+$ cDC1s and $CD11b^+Sirp\alpha^+$ cDC2s. cDC1s are specialised in cross-presenting intracellular pathogens via MHCI to $CD8^+$ T cells, which is essential during antiviral and antitumor immunity. They express high levels of the toll-like receptor (TLR)3 an endosomal pathogen recognition receptor that detects viral double-stranded RNA within dead cell debris internalised by cDC1s[116]. They initiate type 1 immune responses that require the early activation of ILC1s and NK cells and eventually polarise T_H1 cells (Fig. iv)[117]. cDC1s are a major source of IL-12 *in vivo*, which makes them more efficient than cDC2s at inducing IFNγ-producing T_H1 cells. Furthermore, during steady state, cDC1s are capable of producing high levels of TGFβ, allowing them to participate in both central and peripheral tolerance induction. In addition, cDC1s can induce peripheral tolerance towards tissue-associated self-antigens through direct contact with self-reactive T cells, resulting in cell death of the latter[107].

On the other hand, cDC2s are most efficient in presenting antigens from extracellular pathogens on their MHCII and triggering a $CD4^+$ T cell response. They have a pivotal role in immunity against allergens, parasites, and extracellular pathogens or even blood antigens, and they can initiate both type 2 and type 3 immune responses, depending on the stimuli they receive (Fig. iv)[117]. cDC2s are highly heterogeneous and can be further classified into multiple populations across various tissues. A study by Brown et al. 2019, demonstrates two cDC2 populations in the spleen and LNs of mice: $T\text{-}bet^+$ cDC2a and $T\text{-}bet^-$ ($CX3CR1^+$) cDC2b, which have distinct cytokine profiles. The cDC2b population is shown to be more pro-inflammatory by producing higher levels of IL-6 and TNFα and is more potent in inducing Th1 and Th17 differentiation than cDC2a[118].

Besides the cDCs, there are also non-conventional (non-)cDCs, which share features with cDCs but are distinct and also contribute to the immune response. These non-cDCs include plasmacytoid DCs (pDCs), which are known for their production of type I interferons during viral infections[119]. After activation, pDCs express both MHCI and MHCII, which makes them

capable of presenting antigens to both CD8 and CD4 T cells, albeit not as efficiently as cDCs. Antigen presentation by these cells can lead to T cell activation or tolerance depending on the situation[120]. Another unique non-cDC subset is the Langerhans cells, which are mononuclear phagocytes that are seeded from common macrophage precursors in the skin epidermis before birth. Like migDCs, Langerhans cells capture the antigen and have the ability to migrate to skin-draining LNs. This migration allows them to present antigens to naïve T cells, thus initiating an immune response or inducing tolerance (Fig. iv) [121].

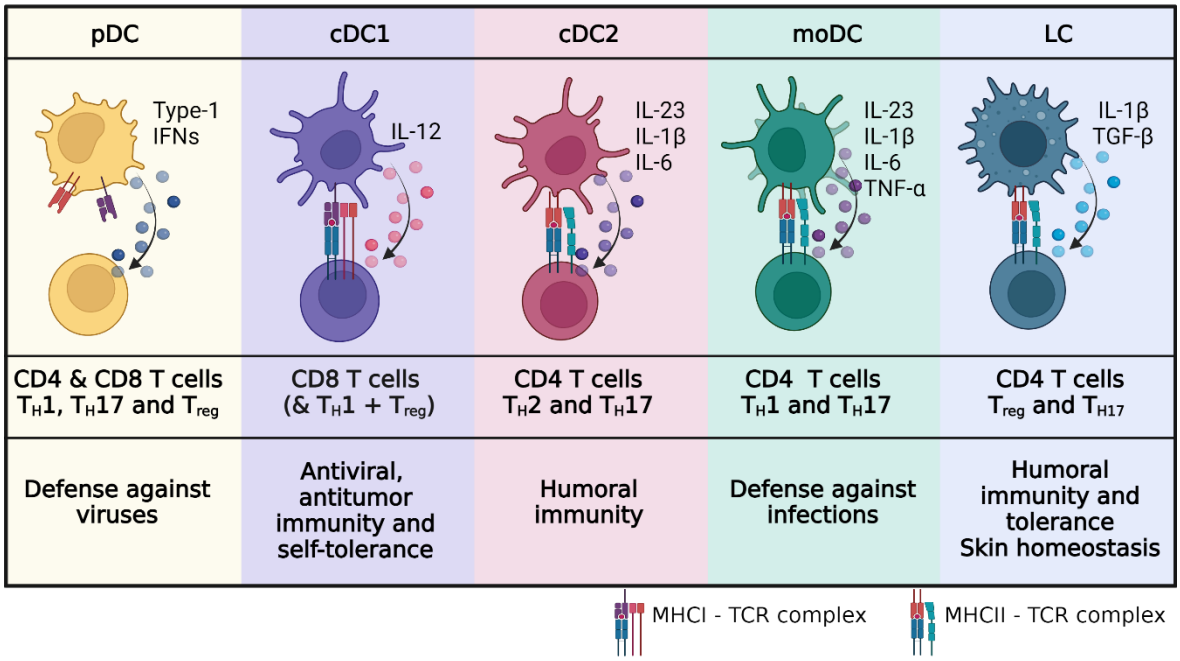

Figure iv: Dendritic cell subsets and their functions.

Five DC subsets are characterised by their cytokine production and function: plasmacytoid DCs (pDC) are known for their role in fighting viral infections by their production of type 1 interferons (IFNs) and they have the capability to present antigens to both CD8 and CD4 T cells, resulting in T_H1, T_H17, and Treg response depending on the situation. cDC1s are known for their abilities to cross-present antigens to CD8 T cells, their production of IL-12, which is important for T_H1 induction and their role in tolerance. cDC2s present antigens via MHCII to CD4 T cells, which together with their production of inflammatory cytokines, is essential for CD4 T cell priming and T_H2 and T_H17 response. Monocyte-derived (mo)DCs appear during inflammation where they can present antigens to CD4 T cells, produce inflammatory cytokines, and induce a T_H1 and T_H17 response. Langerhans Cells (LC) are found in the skin where they capture antigens, which they can present to CD4 T cells. Made in BioRender.

Another subset of non-cDCs is monocyte-derived DCs (moDCs); as the name suggests, these are monocytes which differentiate into DCs and contribute to immune responses. Recent research has indicated that moDCs have the ability to migrate to the T cell area of LNs and appear similar to cDCs and can activate both CD4 and CD8 T cells [122]. These cells demonstrate high activity and superior antigen presentation capabilities compared to other DC types [123]. However, further studies have revealed that moDCs are not able to stimulate T cell proliferation through either direct or indirect antigen presentation. In fact, they have been found to inhibit the ability of cDCs to induce CD4 T cell proliferation through the production of iNOS. Nevertheless, moDCs

have proven to be more effective in inducing a T_H1 and T_H17 response in T cells and inhibiting T_H2 cell polarisation [124]. Furthermore, moDCs have demonstrated greater potency compared to cDCs and pDCs in inducing T_H17 cells *in vivo* (Fig. iv)[125].

cDCs have long been thought of as the main antigen-presenting cells during EAE[126]. However, contradicting research has been published on the role of DCs in EAE. Multiple groups have tried to demonstrate the importance of DCs in EAE by making use of the diphtheria toxin receptor (DTR) mouse model. For this, they used mice that express the human DTR in CD11c-expressing cells. When injected with the toxin, the cells expressing the DTR, $CD11c^+$ cells in this case, will die. It has been demonstrated that depleting DCs with the DTR model slightly reduces EAE but does not affect the differentiation of T_H1 and T_H17 cells [127]. However, other studies contradicted these findings and demonstrated that the ablation of $CD11c^+$ cells lead to a stronger inflammatory T cell response and a more severe EAE [128,129]. The study by Yogev et al. suggests that DCs play a crucial role in inducing tolerance during EAE by promoting Tregs[107,128]. They further hypothesise that other $CD11c^{low}$ cells or macrophages (but not B cells) are capable of antigen presentation and can induce EAE[128]. Another study which focused on the effector phase of EAE by transferring MOG-reactive T_H17 cells into CD11c-DTR mice has shown that depletion of DCs reduces EAE severity. They further show a distinct role for $CD11c^+$ cells in the CNS by attracting pathogenic T cells into the CNS and promoting their survival within the CNS[130]. The contradictory results in these studies on the role of DCs in EAE pathogenesis are unclear, but it might be due to the different roles of DC subsets and their functions during different stages of EAE development.

1.5 The NF-κB Signalling Pathway and its Primary Stimulator

1.5.1 The non-canonical NF-κB signalling pathway

The non-canonical NF-κB signalling pathway regulates many aspects of the immune and stress response[131,132]. The pathway can be activated by receptors that are part of the tumour necrosis factor superfamily, including lymphotoxin β receptor (LTβR), B cell activating factor receptor (BAFF-R), receptor activator of NF-κB (RANK), CD40, and CD27. The non-canonical NF-κB pathway is also a target of certain pathogens, which include several RNA viruses and bacteria[132,133]. The primary stimulator of this pathway is NF-κB-inducing kinase (NIK) which is a MAP3 kinase (*Map3k14*)[131]. During steady state, NIK is associated with tumour necrosis factor receptor-associated factor (TRAF)3, which then recruits an E3 ligase complex that contains TRAF2 and cIAP1&2. The binding of this complex results in the ubiquitination and degradation of NIK by the proteasome[134]. However, activation of the pathway by inflammatory mediators induces the recruitment of the TRAF2&3-cIAP1&2 complex to the receptor. This complex activates cIAP1-cIAP2, which induces TRAF3 degradation and results in the stabilisation and accumulation of NIK in the cytosol of the cell[135,136]. NIK then activates and

cooperates with its downstream target, IκB-specific kinase α (IKKα), to trigger the phosphorylation of p100, leading to p100 ubiquitination and processing. This subsequently results in the generation of active p52 and the translocation of the p52-Relb complex into the nucleus, resulting in the transcription of multiple genes involved in immune response and inflammation[137,138] (Fig. v). There is also a proposed negative feedback mechanism regulating the activation of the non-canonical pathway in which NIK-activated IKKα phosphorylates NIK at its C-terminal, thereby destabilising it[139].

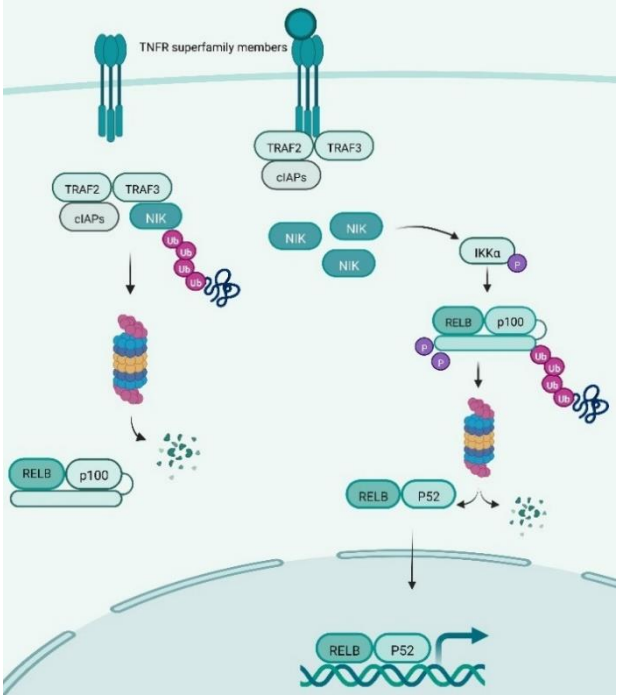

Figure v: The non-canonical NF-κB signalling pathway

1.5.2 The NF-κB Inducing Kinase (NIK)

As mentioned earlier, NIK is the primary activator of the non-canonical NF-κB pathway. NIK is a serine/threonine kinase consisting of four main domains: a TRAF3 binding domain, which contains a lysine (Lys48) whose ubiquitination mediates NIK degradation. The second domain consists of a negative regulatory domain that regulates the TRAF3 binding domain and its interaction with other proteins. The third and largest domain is the kinase domain and lastly, at the C-terminus, the non-catalytic region, which allows protein binding to IKKα and p100 (Fig. vi)[140,141]. Mutations in the NIK gene are associated with immunodeficiency and autoimmune diseases. For example, mutations in NIK have been identified in patients who suffer from combined immunodeficiency. Two known mutations both result in impaired kinase activity ($NIK^{Val345Met}$ & $NIK^{Pro565Arg}$; Fig. vi). These patients display B cell lymphopenia, decreased frequencies of class-switched memory B cells, and impaired B cell survival. Additionally, patients exhibited defects in both follicular helper and memory T cell populations, as well as NK cells [142,143]. Furthermore, NIK has been studied in several types of cancer and genome-wide association studies have shown that NIK is also a susceptibility gene for rheumatoid arthritis and MS [22,141].

Mice with a naturally occurring point mutation in the non-catalytic region of the NIK locus (Fig. vi) were discovered by Miyawaki and colleagues in 1986. Similar to the human mutations that cause combined immunodeficiencies, they found that these mice were immunodeficient and highly susceptible to infections. The mice were named $NIK^{aly/aly}$ mice (aly for Alymphoplasia) since they also lacked LNs and Peyer's patches throughout their body[144]. Further analysis of

the NIK$^{aly/aly}$ mice revealed they lacked clear and defined lymphoid follicles in the spleen. Additionally, the thymus showed an ambiguous cortical-medullary distinction, indicating a potential disruption in its normal functionality[144].

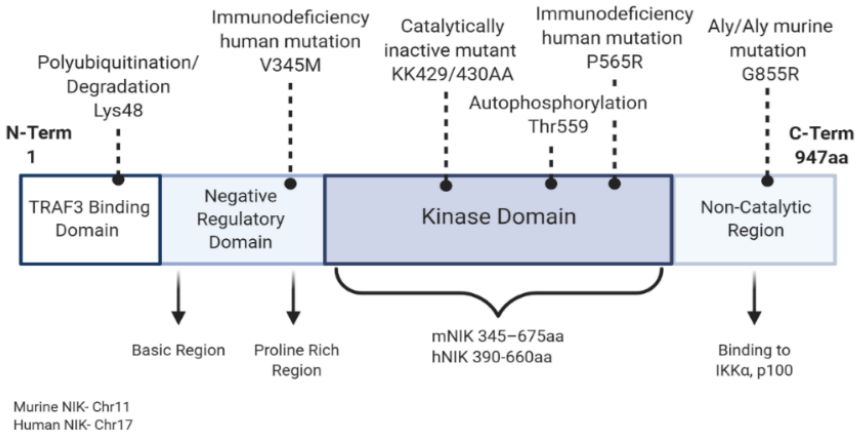

Figure vi: NIK structures and mutations (from Pflug et al., 2020).

NIK is 947 amino acids long and consists of four main domains. Multiple known human mutations are found in different domains, resulting in immunodeficiency. The Aly/Aly mouse mutation in the C-terminal causes alymphoplasia and an immunodeficient phenotype.

It has further been shown that NIK plays an essential role in many different cell types. In B cells, the deletion of NIK results in the defective development of B cells and a reduction of mature B cells. Moreover, deletion of NIK in the germinal centres decreases the numbers of germinal centre B cells and impairs the ability of NIK-deficient B cells to develop into class-switched cells *in vivo*. B cells that lack NIK cannot respond to the survival factor BAFF, a known stimulator of the non-canonical NF-κB pathway [145,146]. NIK also plays an essential role in T cell maturation and activation. When NIK was deleted in T cells, it showed to be critical for maintaining the homeostasis and function of peripheral T cells. Furthermore, the NIK-deficient T cells were unable to differentiate into T_H1 and T_H17 cells[147].

Additionally, NIK has been shown to have an essential role in the development of a subset of macrophages, mainly the Siglec1$^+$ metallophilic marginal zone macrophages in the spleen, which are missing in the NIK$^{aly/aly}$ mice [148]. Further research by Camara et al. demonstrated that RANK and LTβr signalling, two known stimulators of the non-canonical NF-κB pathway, are essential for the development and maintenance of these macrophages. Not only in the spleen but also in the LN, the Siglec1$^+$ macrophages depend on RANK and LTβr signalling and lack of this signalling results in the loss of this macrophage subsets in the spleen and LNs[149]. Furthermore, the lack of NIK or the non-canonical pathway receptors RANK and LTβr in Siglec1$^+$ macrophages results in a defective immune response to viral infections[148,149]. Research into the role of NIK in DCs has demonstrated that it is essential for the cross-presentation of antigens to CD8$^+$ T cells[150]. It was further discovered that NIK in DCs is essential

for regulating intestinal homeostasis, promoting mucosal immunity against pathogens, as well as promoting chronic inflammation associated with inflammatory bowel disease[151].

1.5.3 Non-canonical NF-κB signalling pathway in EAE

The deletion of NIK in mice has been shown to cause resistance to EAE[152,153]. A study by Greter et al. has shown that splenectomised $NIK^{aly/aly}$ mice, which were reconstituted with wild-type hematopoietic systems, were susceptible to EAE. While wild-type mice with normal secondary lymphoid tissues but are reconstituted with $NIK^{aly/aly}$ bone marrow do not develop any EAE disease[153]. This study proves that the defect in cell-mediated immunity in the $NIK^{aly/aly}$ mice is not connected to their lack of secondary lymphoid tissue but that NIK activity is critical for cellular immune function[153]. Further research with cell-specific deletion of NIK has shown that NIK in $CD4^+$ T cells is crucial for the development of EAE[147,154]. A study by Lacher et al. demonstrated that NIK promotes the development of encephalitogenic T cell populations by regulating TCR signalling and F-actin dynamics during immunological synapse formation[154].

It's not well understood how the non-canonical NF-κB pathway impacts monocytes and macrophages in the context of EAE. However, it has been demonstrated that NIK facilitates microglial activation and chemokine induction, which is required for the CNS recruitment of T cells during the later phase of EAE[155]. While more is known about the role of NIK in DCs, conflicting results have been published on its function in DCs during EAE. For example, research with the $NIK^{aly/aly}$ mice has shown the importance of NIK in DCs for effector T cell functions and the development of EAE[156]. Furthermore, a DC-specific deletion of Relb has been shown to protect against EAE through the accumulation of Tregs[157]. Another study has shown that the deletion of $CRL4^{DCAF2}$, a negative regulator of NIK, in CD11c-expressing cells, leads to an overexpression of NIK and IL-23. This further resulted in a more severe EAE characterised by more infiltrating cells into the CNS and an increased number of T_H17 cells[158]. These studies suggest an important role for NIK in DCs. However, a study by Katakam et al., who utilised a more cell-specific model by deleting NIK in CD11c-positive cells, demonstrated that it is dispensable for $CD4^+$ T cell priming and EAE development [159].

1.6 Rationale of the Study

Mutations and polymorphisms in the NIK gene are associated with immunodeficiency and autoimmune diseases, including MS[22,141]. Many studies have focused on the $NIK^{aly/aly}$ mice, which have shown the importance of NIK in lymphoid structure and multiple immune cells. While cell-specific deletions of NIK have focused on DCs, B, and T cells, less is known about the role of the non-canonical NF-κB pathway and NIK in macrophages, monocytes, and monocyte-derived cells. It has been shown that certain $Siglec1^+$ macrophage populations in the LNs and spleen depend on RANK and LTβR signalling, two known receptors of the non-canonical NF-

κB pathway[149]. However, it is still unexplored whether this is specific to NIK signalling and whether other macrophage and myeloid populations, like microglia and monocytes, also depend on NIK during steady state conditions. In addition, numerous studies have shown that NIK has a crucial role in EAE development. Monocytes and DCs have been shown to be important during the development of EAE. However, how they regulate the disease and whether a specific subset of DCs could be involved is still unclear. We therefore wanted to investigate the role of NIK in CX3CR1-expressing cells, which include monocytes macrophages and a subset of cDC2s[160]. Our hypothesis is that NIK in CX3CR1-expressing cells drives autoimmune inflammation in the EAE model, which I examine and confirm in this thesis.

By deleting NIK in CX3CR1-expressing cells, the objectives of this project were:

1. To establish the effect of NIK deficiency in microglia and peripheral myeloid cell subsets in steady state.
2. To determine if NIK in the peripheral or CNS resident CX3CR1-expressing cells is involved in EAE development.
3. To examine the mechanisms of NIK-regulated alterations that play a role in EAE development.

2.

MATERIALS AND METHODS

2.1 Mouse experiments

2.1.1 Mouse strains

$NIK^{fl/fl}$ mice, with LoxP sites flanking exons 4-6, were generated by TaconicArtemis (Fig. M1) and bred with CX3CR1-Cre mice ($NIK^{\Delta CX3CR1}$), CX3CR1-CreERt2 mice[75] ($NIK^{\Delta MG}$) and CD11c-Cre mice[161] ($NIK^{\Delta DC}$). All mice used were on the C57BL/6J background and housed under specific-pathogen-free conditions. Cre-negative and $NIK^{fl/wt}$ Cre-positive littermates were used as controls, and animals (both male and female) were between 8 and 14 weeks of age at the start of the experiment unless otherwise indicated. All animal experiments were performed in accordance with the guidelines from the Central Animal Facility Institution.

2.1.2 Tamoxifen treatment

A 20 mg/mL solution of tamoxifen (Sigma Aldrich) was prepared by suspension in olive oil (Sigma Aldrich) at 37°C for 2 hours on a shaker. Pups of the $NIK^{\Delta MG}$ strain were injected subcutaneously with 2mg of tamoxifen, 2 days apart at P18 and P20 unless otherwise indicated.

2.1.3 Genotyping: DNA isolation and Polymerase Chain Reaction

Ear biopsies were taken at the recommended ages and lysed overnight at 56°C in TENS buffer supplemented with 200 mg/ml proteinase K. DNA was extracted by adding an equal volume of isopropyl alcohol to precipitate the DNA. DNA was pelleted by centrifugation at full speed for 5 min at rt. Afterwards, the supernatant was discarded, and 70% ethanol was added as a washing step. After centrifugation at full speed for 5 min at RT, the supernatant was discarded, the pellet was dried overnight at RT, and DNA was reconstituted in 300ul distilled water and used for polymerase chain reaction (PCR).

PCR was performed in a total volume of 20 µl, containing 1 µl DNA and 19 µl of a polymerase and primer containing master mix. To prepare the master mix, 500 µl REDTaq ReadyMix were supplemented with 5 µl of each primer (Table 1) and filled up with water to a total volume of 950 µl. PCR reactions were performed at the primer-specific annealing temperature. Agarose gels were prepared at 2% in 1x TAE buffer (total volume 300 ml) and supplemented with 12 µl Midori green DNA stain. Amplified DNA fragments were separated by size by agarose gel

electrophoreses at a constant voltage of 130 V. DNA bands were visualised under UV light using the Gel Doc XR+ gel documentation system (Bio-Rad), and band sizes were determined by comparing with the GeneRuler 100 bp plus DNA ladder (Thermo Fisher Scientific).

Table 1: primers used for genotyping

Primer name	Primer sequence (5'-3')	T_{ANN}[°C]	Direction
NIK1 fw	TAT GAA CTG CTC CCG TTT CG	60	sense
NIK2 rev	CCT GTG CAT CAC AGA GTA TAC TAG C	60	anti-sense
NIK4 rev	TTC CTG TGA ACT CAA ACA CTC CC	60	anti-sense
CX3CR1 fw	CCT CTA AGA CTC ACG TGG ACC TG	58	sense
CX3CR1 wt rev	GAC TTC CGA GTT GCG GAG CAC	58	anti-sense
CX3CR1 spec rev	GCC GCC CAC GAC CGG CAA AC	56	sense

2.1.4 Active EAE induction

An emulsion of 50 µg MOG_{35-55} peptide (Gene Script, amino acid sequence: MEVGW-YRSPFSRVVHLYRNGK) and CFA supplemented with 1.1 mg of heat-inactivated Mycobacterium tuberculosis was injected subcutaneously at the base of the tail to immunise mice. 150 ng of pertussis toxin (PTx) was injected intraperitoneally on the same day as the MOG immunisation and again two days later. The mice were weighted and scored daily for clinical signs of EAE (Table). When they reached a score of 4.5 or lost over 20% of body weight, mice were sacrificed according to the animal allowances.

Table 2: Scoring system for clinical signs of EAE.

Symptoms and Behaviour	Score
No symptoms, normal behaviour	0
Decreased tone in the tail tip	0.25
Decreased tail tone	0.5
Tail partially paralysed	0.75
Tail completely paralysed	1.0
Mouse can be turned to the dorsal side but turns back immediately	1.25
Mouse can be turned to the dorsal side but turns back rather easily	1.5
Mouse can be turned to the dorsal side but needs more effort to turn back	1.75
Mouse can be turned to the dorsal side and stays at least 1 s in this position	2.0
Mouse walks with lowered buttocks	2.25
Mouse walks with lowered buttocks and shows wadding gait	2.5
Gait sorely afflicted, but walking movements are still recognisable	2.75
Legs are weak but still move forward	3.0
Partial paralysis of the hind legs	3.25
Paralysis of one hind leg	3.5
Paralysis of both hind legs but mouse still moves forward rather effortlessly	3.75
Mouse shows difficulties with moving forward	4.0
Mouse stays in position and only moves forward with supreme effort	4.25

Mouse does not move forward and bends to one side	4.5
Mouse lies on one side even if turned to the other side	4.75
Mouse lies apathetically on the belly or side, breathing slowly, eyes (almost) closed	5.0
Mouse is dead	6.0

2.1.5 Adoptive transfer EAE

donor mice were immunised for EAE, as described above. At eight dpi, single-cell suspensions of the spleen and dLN (inguinal & para-aortic) were prepared by mechanical dissociation in PBS/2%FCS and filtered through a 70mm cell strainer. Erythrocytes were removed by ACK lysis under sterile conditions. $5x10^6$ cells/ml were then cultured in T cell media containing 15 ng/ml IL-23 (Sino Biological), 10 µg/ml anti-IFNγ (BioXCell), and 20 µg/ml MOG_{35-55} peptide. After four days, cultured cells were washed with PBS, and $5x10^6$ blasting cells were intravenously injected into the recipient mice. The recipients were injected intraperitoneally with 150ng PTx on the same day and two days after the transfer. The mice were scored for clinical symptoms as described above.

2.1.6 2D2 T cell transfer

Single-cell suspensions of the spleen and dLN (inguinal) of 2D2 mice were prepared by mechanical dissociation in PBS/2%FCS and filtered through a 40mm cell strainer. Erythrocytes were removed by ACK lysis. $CD4^+$ cells were purified using the $CD4^+$ T Cell Isolation Kit according to the manufacturer's protocol. Briefly, isolated cells were incubated with a cocktail of biotin-conjugated antibodies, followed by incubation with anti-biotin microbeads. The magnetically labelled non-target cells are depleted by retaining them on an LD column (Milteny) in a magnetic field, and the flow-through was collected. The purified $CD4^+$ T cells were stained with anti-TCR vb11-PE for flow cytometry to check the percentage of 2D2-positive $CD4^+$ T cells. 10^4 2D2 cells were transferred intravenously in the tail of experimental mice one day before MOG-immunisation. Cells from the spleen and dLNs were isolated six days after MOG immunisation.

2.2 Cell biology

2.2.1 Leukocyte Isolation from CNS

CNS isolation: Mice were deeply anaesthetised by inhalation with isoflurane, then transcardially perfused with 15-20mL sterile NaCl prior to organ isolation. Brain and spinal cord were digested in 0,05mg/ml DNase type I and 2mg/ml Collagenase Type II (lymphocyte and microglia analysis) or 1mg/ml Papain (microglia analysis) in HBSS with calcium and magnesium for 30min at 37°C using the gentleMACS Octo Dissociator (Milteny). CNS homogenates were passed through a 70mm cell strainer and put into a discontinuous

30%:37%:70% percoll gradient and centrifuged at 500g without brakes for 45 minutes. Myelin was discarded, and the 70/37% interphase was carefully collected in FACS buffer for flow cytometry analysis.

2.2.2 Myeloid/lymphocyte isolation from peripheral organs

For myeloid cell isolation: spleen and LNs were digested in 1mg/ml Collagenase Type II and 0,1mg/ml DNase Type I in PBS with calcium and magnesium while shaking at 37°C for 30 minutes. EDTA was added to a 10 mM final concentration, and the cell suspension was passed through a 70mm cell strainer. Erythrocytes were removed from the spleen by ACK lysis. The cells were washed with FACS buffer before being collected for flow cytometry.

For lymphocyte isolation: Spleen and LNs were mechanically dissociated in PBS/2%FCS and filtered through a 40mm cell strainer. Erythrocytes were removed from the spleen by ACK lysis. The cells were washed with PBS/2%FCS before being collected for flow cytometry.

2.2.3 Culture of myeloid cells

Cells from the spleen and lymph nodes were isolated with enzymatic digestion, as described above. Myeloid cells were purified using the CD11b microbeads ultrapure (Milteny) according to the manufacturer's protocol. Briefly, isolated cells were incubated with anti-CD11b MACS beads, washed, and then applied to prepared LS columns (Milteny). Columns were washed 3x with MACS buffer before the final elution of $CD11b^+$ cells from the column. $5x10^4$ cells were plated in only T cell media or with 10µg/ml anti-CD40 (BioXCell) or 1µg/ml LPS (Sigma Aldrich) for 1h and 4h.

2.2.4 Flow cytometry

Single-cell suspensions of the different organs were resuspended in FACS buffer with Fc-block for 20-40 minutes at 4°C to block Fc receptors. Cells were incubated with surface antibodies (Table 7&8) in FACS buffer. For intracellular staining, either the Cytofix/Cytoperm solution kit or the Foxp3/Transcription Factor Staining Buffer Set was used according to the manufacturer's instructions. For cytokine staining, cells were reactivated prior to staining in T cell media containing 20 µg/ml MOG_{35-55} peptide with 1 µg/ml Brefeldin A at 37 °C for 6h. Isolated cells from the 2D2 transfer experiment were reactivated prior to staining in T cell media containing 50 ng/ml PMA, 500 ng/ml Ionomycin and 1 µg/ ml Brefeldin A for 4h at 37 °C. After staining, the samples were acquired on a BD Canto II, a BD Aurora for the steady state myeloid analysis, and a BD Symphony for the myeloid analysis after MOG immunisation. Data was analysed using FlowJo V10.8 or Rstudio.

2.2.5 Histology

Brain: Mice were deeply anesthetised by inhalation with isoflurane, then transcardially perfused with ice-cold PBS and then with ice-cold 4% PFA. Brains were post-fixed in 4% PFA overnight and dehydrated in 30% sucrose for three days before being frozen in Tissue-Tek O.C.T (Sakura Finetek). Free-floating 40 mm sagittal sections were used to examine microglia morphology, while embedded 12.5 mm sagittal sections were used to quantify microglia numbers.

Sections were blocked for 1h in D1 blocking buffer at RT, then stained overnight with primary antibodies for microglia using rabbit anti-Iba1. The bound primary antibody was further labelled with the appropriate secondary antibodies. Secondary antibodies were incubated with sections for 1h at RT in D1 blocking buffer: anti-rabbit CF488A. Nuclei were further stained either with Hoechst and mounted with PermaFluor Aqueous Mounting Medium (Thermoscientific) or directly mounted with Fluoroshield mounting media with DAPI (Sigma-Aldrich).

For quantifications of microglia numbers, sections were imaged using a Leica Dmi8 fluorescence microscope with an objective magnification of 20x. Images were acquired from the cortex, hippocampus, and cerebellum. $Iba1^{+}DAPI^{+}$ microglia cell bodies were counted in the FIJI software (NIH). For microglia morphology, images of microglia from layers II/III of the cortex were acquired with a 20x oil immersion objective with 3x zoom and 1 µm increments on a Leica SP8 from the top to the bottom of each slide imaged. Stacks were opened with Imaris 8.4, and processes were semi-automatically traced using the Filament tracing tool. Only cells with a cell body in the centre of the stack were used for analysis. To quantify cell complexity, 3D sholl analysis was used on reconstructed cells.

Spleen and inguinal LNs were carefully dissected and fixed in 4%PFA for 12h at 4°C, followed by two subsequent washes with PBS for another 12h, before being sent to our collaborators Prof. B. Ludewig and L. Onder, who processed the organs for histology, stained the slides with Siglec1, F4/80, B220, and CD3, and acquired images.

2.3 Molecular biology

2.3.1 RNA extraction and qPCR

RNA was extracted from isolated cells using the ReliaPrep™ RNA Cell Miniprep System (Promega) according to the manufacturer's instructions. RNA quality and concentration were determined by measuring absorbance at 260 nm and 280 nm using the NanoQuant Plate™ (Tecan) at an Infinite M200 pro Tecan plate reader (Tecan). cDNA was synthesised using 200–1000 ng of total RNA with the QuantiTect® Reverse Transcription Kit (Qiagen) and

subsequently used for qPCR, which was performed with the StepOnePlus™ Real-Time PCR System (Life Technologies) using SYBR Green. Fold enrichment was calculated using the Delta–Delta CT (2ΔΔCT) method normalised to hypoxanthine-guanine-phosphoribosyltransferase (*HPRT*) as a housekeeping reference. Primers were ordered as QuantiTect Primer Assays (Table 3).

Table 3: Primers used for qPCR

Gene name/ Commercial primers	Company
Mm_Hprt_1_SG QuantiTect Primer Assay	Qiagen (QT00166768)
Mm_Il23a_ 2_SG QuantiTect Primer Assay	Qiagen (QT01663613)
Mm_Il12a_1_SG QuantiTect Primer Assay	Qiagen (QT01048334)
Mm_Il6_1_SG QuantiTect Primer Assay	Qiagen (QT00098875)
Mm_Il1b_2_SG QuantiTect Primer Assay :	Qiagen (QT01048355)
Mm_Il10_1_SG QuantiTect Primer Assay	Qiagen (QT00106169)

2.3.2 Sample preparation for scRNA-seq

Cells from dLN were isolated from mice four days post immunisation as described earlier. to enrich for myeloid cells, T and B cells were removed by using the CD19 microbeads and CD90.2 microbeads MACS (Milteny) according to the manufacturer's protocol. Briefly, isolated cells were incubated with anti-CD90.2 and anti-CD19 MACS beads, washed, and then applied to prepared LD columns. The flow-through and 3x wash steps with MACS buffer were collected as this contained the enriched myeloid cells, while CD90 and CD19 cells were magnetically bound to the column and discarded afterwards.

Isolated myeloid cells were trapped on a BD rhapsody cartridge. Each sample was tagged with a special sample tag in order to allow multiplexing of samples on the same cartridge (4 samples per cartridge). Samples were further processed according to BD rhapsody pipeline. Briefly, after passing a BD rhapsody cartridge, cell capture beads were passed over the cartridge, cells were lysed, and the beads retrieved. Whole transcriptome libraries and sample tag libraries were created using BD WTA Amplification Kit (BD Rhapsody) with random primers followed by amplification and insertion of sequencing adaptors following the BD Rhapsody System mRNA WTA and Sample Tag Library Preparation Protocol (BD Biosciences). Quality control was performed with Invitrogen's Qubit HS assay, and fragment size was determined using Agilent's 2100 Bioanalyzer HS DNA assay. Samples were then sent to Novogene Europe in Cambridge (United Kingdom) for sequencing, and the raw output data was pre-processed according to the BD pipeline.

The resulting raw data was preprocessed according to the Illumina standard protocol, and transcript alignment, counting and demultiplexing were performed using the BD Rhapsody

WTA analysis pipeline, yielding 22,238 called putative cells overall with a mean of 65,437.95 aligned reads per cell.

2.4 Data analysis

2.4.1 UMAP analysis flow cytometry data

Cells were pregated in FlowJo, excluding duplets, dead cells, Neutrophils, NK, B and T cells. The $CD11b^+$ were exported for each sample and further analysed in Rstudio as described in https://f1000research.com/articles/6-748[162]. In short, the packages CATALYST and FlowSOM were used to cluster cells and the nonlinear dimensionality reduction technique, uniform manifold approximation and projection (UMAP), were used to visualise the clusters (5000 cells randomly selected per sample). Differential analysis was done using the diffcyt package[163]. With the false discovery rate (FDR) set to 0,5. Using the test "diffcyt-DA-GLMM" (GLMM = generalised linear mixed models) to test for differences in cluster percentages between two groups and the "diffcyt-DS-LMM" to test for differences in marker expression within clusters. Both methodologies are based on mixed models, and to account for the multiple testing corrections, the Benjamini-Hochberg adjustment was applied to each of the samples using a false discovery rate (FDR) cutoff of 5%. Significance is indicated as follows: * $p < 0.05$, ** $p < 0.01$, ***$p < 0.001$.

2.4.2 scRNA-seq data analysis

Pipeline output was imported into Rstudio software and further analysed with the Seurat package[164]. Steps were followed as described in vignettes/pbmc3k_tutorial.Rmd. cells that contained less than 200 detected genes and a percentage of mitochondrial counts higher than 12% were removed from subsequent. Single-cell counts were normalised by scaling each cell's expression values by its total expression, multiplying by a factor of 10,000, and then applying a log transformation. Dimensionality reduction was performed using Principal Component Analysis (PCA) to identify the principal components that capture the most significant variance in the gene expression data. The first 15 principal components were selected for downstream analysis. A graph-based approach was employed for clustering. First, a shared nearest neighbour (SNN) graph was constructed using the identified principal components. Then, the Louvain algorithm was applied to this graph to identify clusters of cells with similar expression profiles. A resolution parameter of 0.5 was used to determine the granularity of the clustering. Clusters were visualised using the UMAP technique and annotated according to ImmGen's (www.immgen.org) data browser.

The cell signature for antigen presentation was added to the UMAP visualisation using the UCell package. The following genes were included in the signature: *Cd81*, *Cd80*, *Cd40*, *Cd86*, *Ctss*, *Tnfsf9*, *Cd68*, *Mapk14*, *Icam1*, *Ciita*, *Clec4a2*, *Cd74*, *H2-Ab1*, *H2-Aa*, and *Cd274*.

Differential abundance testing was conducted using the Milo package[165]. This method identifies changes in cell population frequencies between conditions, allowing us to detect shifts in cellular composition and abundance in a spatially-aware manner.

To identify differentially expressed genes (DEGs) between control and NIK^CX3 cells, the FindMarkers function was used. DEGs were identified and sorted based on the following criteria: Log2 fold change (Log2FC) less than -0.1 and adjusted p-value (adj.p-value) less than 0.05, or Log2FC greater than 0.1 and adj.p-value less than 0.05. For pathway enrichment analysis, the enrichGO function from the clusterProfiler package[166] was employed.

2.4.3 Statistical analysis

Data are shown either as mean ± SD or ± SEM, as indicated in the figure legends. For the comparison of the two groups, we performed the Mann-Whitney Test or multiple t-tests with the Holm-Sidak method, as indicated in the figure legends. Sholl analysis and EAE disease progression were analysed by 2-way ANOVA with Sidak's Multiple Comparison test. Significance is indicated as follows: * $p < 0.05$, ** $p < 0.01$, ***$p < 0.001$, ****$p<0.0001$.

2.5 Reagents, Buffers, Kits and Antibodies

Table 4: List of chemicals and reagents

Reagent	Supplier
β–Mercaptoethanol	Fluka Chemie GmbH
Adjuvant Complete H37Ra (CFA)	BD Biosciences
Agarose	Biozym
Ammonium chloride (NH_4Cl)	Merck
Bovine Serum Albumin (BSA)	Merck
Brefeldin A	Merck
Collagenase II	Thermo Fisher Scientific
Dithiothreitol (DTT)	Thermo Fisher Scientific
DNase I	Roche
Dulbecco's modified PBS (DPBS)	Merck
Ethanol	AppliChem
Ethylenediaminetetraacetic acid (EDTA)	Merck
Gene ruler 100 bp DNA ladder	Thermo Fisher Scientific
Gibco® Dullbecco's Modified Eagle Medium (DMEM)	Thermo Fisher Scientific
Gibco® Hank's buffered saline solution (HBSS)	Thermo Fisher Scientific
Gibco® Hank's buffered saline solution (HBSS) with Ca^{2+} and Mg^{2+}	Thermo Fisher Scientific
Gibco® MEM non-essential amino acids (NEAA) 100x	Thermo Fisher Scientific

Gibco® RPMI 1640	Thermo Fisher Scientific
Gibco® Sodium pyruvate 100 mM	Thermo Fisher Scientific
GoTaq® qPCR Master Mix	Promega
HEPES	Thermo Fisher Scientific
Interleukin (IL) 23 (P19 &P40 subunits)	Sino Biological
Ionomycin	Merck
Isoflurane	Abbvie
Isopropyl alcohol	AppliChem
L-Glutamine	Thermo Fisher Scientific
Lipopolysaccharide (LPS)	
Methanol	Roth
Midori Green	Nippon Genetics
Mycobacterium tuberculosis Des. H37Ra	BD Biosciences
Myelin oligodendrocyte glycoprotein (MOG) 35-55	GenScript
Olive oil	Merck
Papain	Merck
Paraformaldehyde (PFA) 4%	Santa Cruz
Penicillin/Streptomycin (P/S)	Thermo Fisher Scientific
Percoll	Merck
Pertussis toxin from *Bordatella pertussis*	List Labs
Phorbol Myristate Acetate (PMA)	Merck
Proteinase K	Roche
REDTaq® ReadyMixä	Merck
Roti Histofix 4%	Roth
RPMI 1640	Life Technologies
Single cell multiplexing kit, mouse immune sample tag	BD Biosciences
Sodium chloride (NaCl)	Roth
Sodiumdodecylsulfate (SDS)	AppliChem
Sucrose	Merck
Tamoxifen	Merck
Tris	Merck
Triton X-100	Merck

Table 5: buffers and media

Buffer/Medium	Composition
10x Ammonium-Chloride-Potassium (ACK) lysis buffer (pH 7.4)	150 mM NH_4Cl 100 mM $KHCO_3$ 10 mM EDTA
50x Tris-acetate-EDTA (TAE) buffer (pH 8.3)	2 M Tris 1 M acetic acid 50 mM EDTA pH 8.0
D1 blocking buffer	PBS 0.5% BSA 0.3% Triton X-100
FACS buffer	PBS

	2% FCS 2mM EDTA
MACS buffer	PBS 0.5% BSA 2mM EDTA
PBS-T	PBS 0,1% Triton-X
T cell medium	RPMI 1640 10% FCS 100 U/mL P/S 2 mM L-Glutamine 1 % NEAA 1 mM Sodium pyruvate 1 mM HEPES 50 M -Mercaptoethanol
Tails lysis buffer (TENS)	10 mM Tris 5 mM EDTA (pH 8) 0.2% SDS 200 mM NaCl

Table 6: List of Kits

Kit	Supplier
BD Cytofix/Cytoperm Fixation/Permeabilization Solution Kit	BD Bioscience
Foxp3 / Transcription Factor Staining Buffer Set	eBioscience™
QuantiTect Reverse Transcription Kit	Qiagen
ReliaPrep™ RNA Cell Miniprep System	Promega
CD11b microbeads ultrapure, mouse	Milteny
CD4+ T Cell Isolation Kit, mouse	Milteny
CD90.2 MicroBeads, mouse	Milteny
CD19 MicroBeads, mouse	Milteny

Table 7: List of antibodies and their application

Antibody	Conjugate	Clone	Host	Dilution	Supplier	Application
***InVivo MAb* anti-mouse IFN-γ**	-	R4-6A2	-	1060	BioXCell	blocking
***InVivo MAb* anti-mouse CD40**	-	FGK4.5	-	388	BioXCell	Activating
***InVivo MAb* anti-mouse CD16/CD32**	-	2.4G2	-	100	BioXCell	Blocking (Fc-block)
CD4	BV421	GK1.5	Rat	500	BioLegend	FACS

CD4	PERCP	GK1.5	Rat	1000	BioLegend	FACS
CD8a	FITC	53-6.7	Rat	1000	BioLegend	FACS
CD8a	BV510	53-6.7	Rat	200	BioLegend	FACS
CD44 ebioscience™	FITC	IM7	Rat	1000	Thermo Fisher Scientific	FACS
CD11b	PE-Cy7	M1/70	Rat	1000	BioLegend	FACS
CD11b ebioscience™	eFl450	M1/70	Rat	300	Thermo Fisher Scientific	FACS
CD45	BV510	30-F11	Rat	200	BioLegend	FACS
CD45	BUV805	30-F11	Rat	1000	BD Bioscience	FACS
CD45.1	FITC	A20	Mouse	1000	BioLegend	FACS
CD80	PerCP	16-10A1	Arm. hamster	500	BD Biosciences	FACS
CD86	V450	GL1	Rat	200	BD Biosciences	FACS
CD88	APC	20/70	Rat	500	BioLegend	FACS
CD90.1	PerCP	OX-7	Mouse	1000	BioLegend	FACS
CD90.2	PerCP	53-2.1	Rat	1000	BioLegend	FACS
CX3CR1	PE-CF594		Rat	300		FACS
Ly6C	PerCP	HK1.4	Rat	100	BioLegend	FACS
Ly6C	BV570	HK1.4	Rat	500	BioLegend	FACS
CD19	PE-Cy5	1D3	Rat	800	BD Bioscience	FACS
Ly6G	PE	1A8	Rat	1000	BioLegend	FACS
Ly6G	BV750	1A8	Rat	500	BD Bioscience	FACS
I-A/I-E (MHCII)	BV786	M5/114.15.2	Rat	1000	BD Bioscience	FACS
Sirp1α	PE-Cy7	P84	Rat	500	BioLegend	FACS
TCRβ	APC	H57-597	Arm. Hamster	1000	BioLegend	FACS
TCR vβ11	PE	RR3-15	Rat	400	BD Bioscience	FACS
CD11c	APC	HL3	Arm. Hamster	800	BD Bioscience	FACS

CD11c	APC-R700	N418	Arm. Hamster	500	BD Bioscience	FACS
CD40L (CD154)	APC	MR1	Arm. Hamster	200	BioLegend	FACS
F4/80	BB70-P	T45-2342	Rat	500	BD Bioscience	FACS
IFN-γ ebioscience™	PE-Cy7	XMG1.2	Rat	1000	Thermo Fisher Scientific	FACS
IL-17A ebioscience™	eFl450	eBio17B7	Rat	300	Thermo Fisher Scientific	FACS
GM-CSF	PE	MP1-22E9	Rat	200	BioLegend	FACS
Iba-1	-	Polyclonal	Rabbit	1000	FUJIFILM Wako Pure Chemical Corporation	IHC
Anti-rabbit	CF488A	-	Goat	800	Merck	IHC

Table 8: Antibodies used for FACS Aurora provided by the lab of B. Becher in Zürich.

Antigen	Conjugate	Dilution
Lyve1	AF488	200
NK1.1	BB700	400
CD3	Spark Blue 550	400
B220	APC	200
XCR1	AlexaFlour647	200
CD206	AlexaFlour700	300
Ly6C	APCCy7	400
SiglecF	BV421	300
MHCII	PacificBlue	1000
CD90.2	BV570	400
PDL1	BV605	200
CD11b	BV650	800
CD64	BV711	200
CD88	BV750	200
MerTK	SB780	200
CD45	BUV395	300
CD4	BUV496	800
Ly6G	BUV563	700
CD44	BUV737	400

Sirpa Biotin	BUV805	200
Siglec1	PE	200
CX3CR1	PE-Dazzle594	400
F4/80	PECy5	700
CD11c	PECy5.5	800
Tim-4	PECy7	200
strep	BUV805	200

3.

RESULTS

3.1 The role of NIK in microglia and myeloid cells during steady state

3.1.1 NIK does not affect Microglia state or numbers

Previous research has demonstrated that NIK, although prone to degradation during a steady state, plays an essential role in the development of LNs and various cell types like B cells and macrophages. To investigate the role of NIK in myeloid cells, we created a mouse line that contained LoxP sites flanking exon 4-6 of the NIK gene crossed to the CX3CR1-Cre ($NIK^{\Delta CX3CR1}$). This line allows for the continuous expression of Cre and subsequent deletion of the target gene in all CX3CR1-expressing cells, which include subpopulations of cDC2s, monocytes, macrophages, and microglia[75]. We aimed to analyse the potential influence of the deletion of NIK in microglia in the CNS and myeloid populations in the LNs and spleen during steady state.

Upon analysing the median fluorescent intensity (MFI) of various activation markers on microglia, a slight decrease was measured in the expression of the MHCII, which plays a key role in antigen presentation and $CD4^+$ T cell activation (Fig. 1C). However, no differences were observed in the expression of the co-stimulatory molecules CD40, CD80 and CD86, which participate along with MHCII in antigen presentation[167] (Fig. 1C). Moreover, there seems to be a lower expression of the nucleotidase CD39, which hydrolysis Adenosine Triphosphate (ATP) and Adenosine Diphosphate (ADP), and the phagocytotic marker CD68 [168–170] (Fig. 1C). This indicates that NIK might regulate activation and phagocytosis in microglia.

Microglia, as the primary immune cells in the CNS, play a crucial role during development and maintaining homeostasis. Therefore, our study began by examining the impact of NIK deletion on these cells in the $NIK^{\Delta CX3CR1}$ mice. Microglia were isolated from the CNS (brain and SC combined) of $NIK^{\Delta CX3CR1}$ mice and littermate controls and analysed using flow cytometry. The markers CD45 and CD11b were used to distinguish microglia ($CD45^{int}CD11b^+$) from other immune cell populations ($CD45^{high}$) (Fig. 1A). Our analysis showed no significant difference in the total cell number of $CD45^{high}$, $CD45^{high}CD11b^+$ or microglia between the two groups (Fig. 1B).

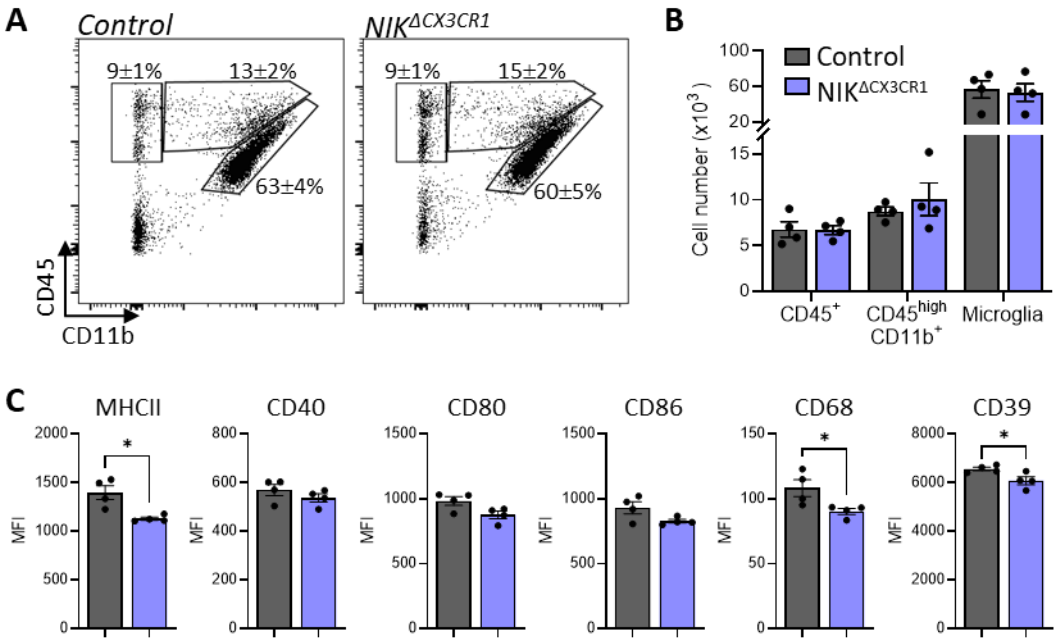

Figure 1: Less activated microglia during steady state in NIK$^{\Delta CX3CR1}$.

*(A) Representative flow cytometry plots of mononuclear cells isolated from the CNS (brain and spinal cord) of NIK$^{\Delta CX3CR1}$ and littermate controls with the mean percentage +/- SEM of each population. (B) Quantification of cell numbers for CD45^{high} lymphocytes, CD45^{high}CD11b^{+} myeloid cells and CD45^{int}CD11b^{+} Microglia. Debris, duplets and dead cells were excluded. (C) The median fluorescent intensity (MFI) of different activation markers on microglia. Data in B-C is shown as mean ± SEM and analysed using two-tailed unpaired Student's t-test(C) or multiple t-test with Šídák's multiple comparisons test . *p < 0.05, **p < 0.01, ***p < 0.001, ****p<0.0001*

Microglia are heterogeneous and may differ both within and among specific brain regions[171,172]. To study microglia in different brain regions, we used immunohistochemistry to stain for ionised calcium-binding adapter molecule 1 (Iba1), a well-described marker for microglia, and 4',6-diamidino-2-fenylindool (DAPI), a nuclear marker, to visualise all cell bodies. The Iba1^{+} microglia were counted in the cortex, brainstem and hippocampus of NIK$^{\Delta CX3CR1}$ and littermate controls, and no differences in the number of Iba1^{+} cells were observed between groups (Fig. 2A, B). We next studied the morphology of microglia, which can provide information about their state and function. During steady state conditions, microglia are ramified with thin processes and radial branching. However, when they become more reactive, they become more amoeboid with thicker processes and reduced branching[173]. We performed 3D reconstruction of Iba1^{+} cells imaged from the upper layers (layers II/III) of the cortex to examine the morphology of the microglia (Fig. 2C). This analysis revealed no differences in the number of branches or dendrites per cell and length of the dendrites (Fig. 2D). Additionally, a sholl analysis to examine the complexity of the microglia, did also not show any differences between NIK$^{\Delta CX3CR1}$ and littermate controls (Fig. 2E). These findings suggest that, besides the slight reduction in the expression of activation markers, the deletion of NIK has minimal effects on the microglia during steady state.

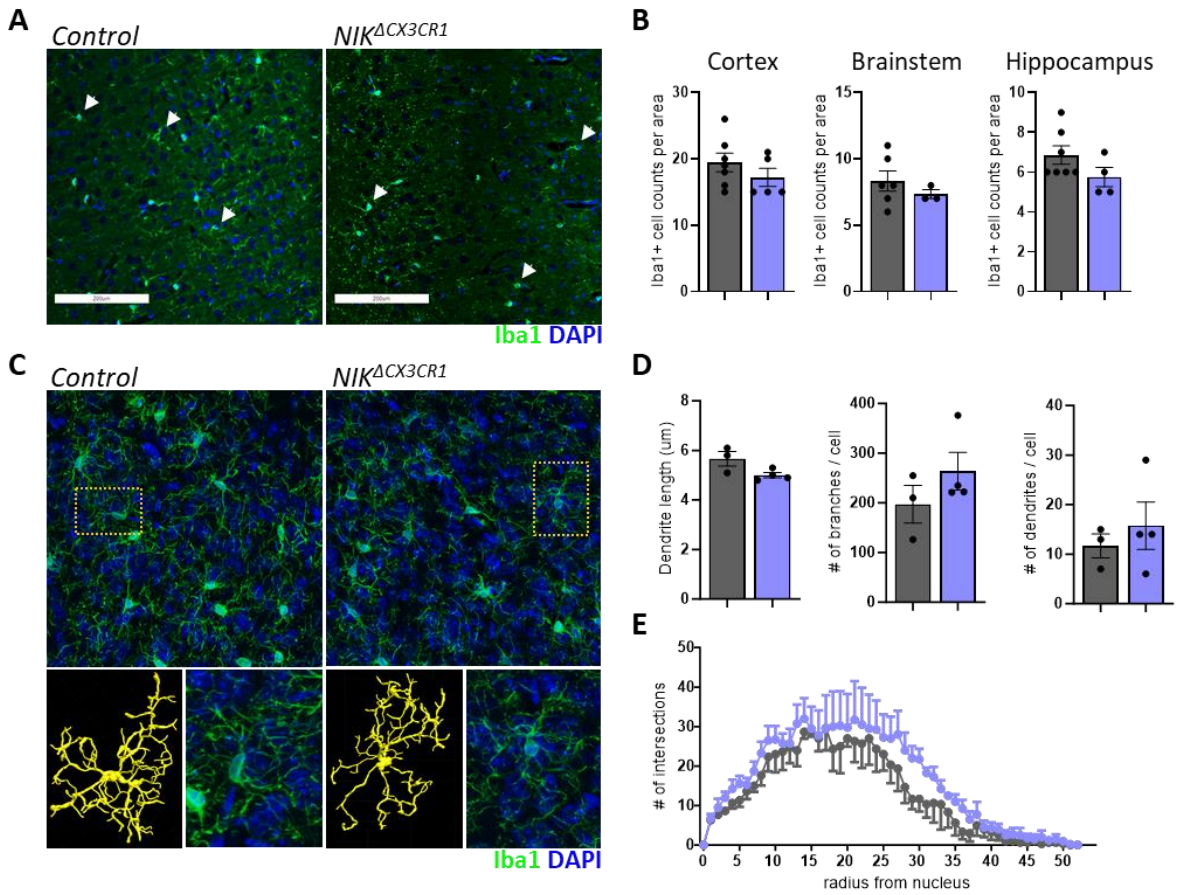

Figure 2: NIK in microglia does not affect the number or morphology of microglia in the brain during steady state.

(A) Immunofluorescence staining for microglia using Iba1 (green) with DAPI (blue) in the cortex in NIK$^{\Delta CX3CR1}$ and littermate controls. White arrows point out Iba1+ cells, scale bar = 200µm. (B) Quantification of microglia numbers in cortex, hippocampus and brainstem. (C) Representative pictures of Iba1+ microglia in the cortex (layer II/III), with a zoom-in of microglia used for reconstruction (in yellow). (D) The length of the microglia dendrites, number of branches and dendrites of reconstructed microglia. (E) Sholl analysis of reconstructed microglia. Each dot represents the average of at least three images(B) or microglia(D-E) per mouse. Data in B, D, and E is shown as mean ± SEM and analysed using two-tailed unpaired Student's t-test (B-D) or two-way ANOVA with Šídák's multiple comparisons test (E).

3.1.2 Siglec1^{+} macrophages in LNs and spleen critically depend on NIK

As previously mentioned, CX3CR1 is also expressed by various myeloid cell subsets in the periphery. Studies have demonstrated that NIK is involved in the development and maintenance of different immune cell populations[145,148]. Additionally, NIK has been shown to be crucial for the development of LNs, as evidenced by the absence of LNs in the NIK$^{aly/aly}$ mice[144]. We wanted to study how the deletion of NIK in CX3CR1-expressing cells would affect the composition of myeloid cells in the dLNs. To achieve this, high-dimensional flow cytometry with 22 markers was used to identify different immune cell populations.

First, we looked into the different subsets of DCs, which are crucial for the initiation of adaptive cell-mediated immunity[109]. A uniform manifold approximation and projection (UMAP) map

was generated to display these various DC subsets in the dLN of NIK$^{\Delta CX3CR1}$ and littermate controls (Fig. 3A). Seven DC clusters were identified using the heatmap: MHCII^{high} CD11c^{low} migDCs and MHCII^{low} CD11c^{high} resDCs which both can be subdivided into XCR1^{+} cDC1s and Sirpa^{+}CD11b^{+} cDC2s. Further subpopulations are Ly6C^{+} monocyte-derived (Mo)DCs, B220^{+}Ly6C^{+} plasmacytoid DCs (pDCs) and CX3CR1^{+} DCs (Fig. 3B). There were no major differences between most DC subsets. However, a slight but significant decrease in migDC2s could be observed (Fig. 3C). This implies that NIK only has a small impact on the composition of DC subsets in CX3CR1 expressing cells during steady state.

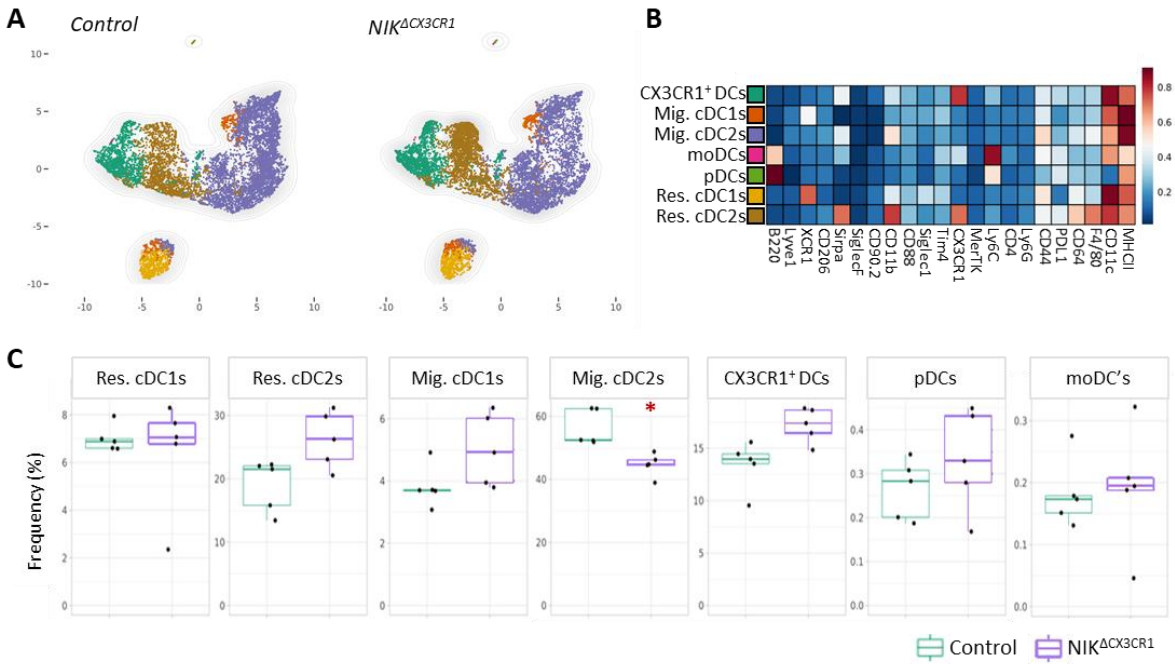

Figure 3: Fewer migratory cDC2s in NIK$^{\Delta CX3CR1}$ mice during steady state.

(A) Uniform manifold approximation and projection (UMAP) map displaying 50,000 randomly sampled cells from the dLN of NIK$^{\Delta CX3CR1}$ and littermate controls analysed by flow cytometry focussing on dendritic cell subsets. (B) A heat map with mean marker expression values for each cluster. (C) Relative frequencies of resident conventional dendritic cells 1&2 (ResDC1&2s), Migratory (Mig)DC1&2, monocyte-derived (mo)DCs, CX3CR1^{+} cDCs and plasmacytoid (p)DCs in the dLN (n=5 per group).

Additionally, a UMAP to display the different monocyte and macrophage populations was generated to investigate the composition of monocyte/macrophage populations in the LNs during steady state (Fig. 4A). We were able to identify three monocyte clusters (ly6C^{hi} and Ly6C^{int} and Ly6C^{lo} mono), a small cDC2 population and four different macrophage clusters (Fig. 4B). There are multiple specialised macrophage populations in the LNs. The first group are the subcapsular sinus (SCS) macrophages, which are characterised by their expression of Sialic Acid Binding Ig Like Lectin 1 (Siglec1) but lack F4/80 expression. They line the SCS and are able to capture and translocate antigens from the lymph and activate B cells[174]. Another group, the medullary sinus macrophages (MSM), are positive for both Siglec1 and F4/80 and, in

addition, express the Lymphatic vessel endothelial hyaluronan receptor 1 (LYVE1). These MSMs are situated between the B cell follicles and the medullary sinuses and are able to clear antigens that filter through the sinuses through their phagocytotic abilities[174,175]. A third macrophage population (MCM) can be found in the medullary cord. These Siglec1^{-}F4/80^{+} MCMs are specialised in clearing plasma cells and provide trophic support to plasma blast and plasma cells[175]. Based on the known markers, we were able to identify SCS macrophages and two MSM-like populations (Fig. 4B). Interestingly, we observed a complete absence of SCS macrophages in the NIK$^{\Delta CX3CR1}$. This loss seems to be compensated by an increase in Ly6C^{hi} and Ly6C^{lo} monocytes and a Siglec^{low} macrophage population (Fig. 4C).

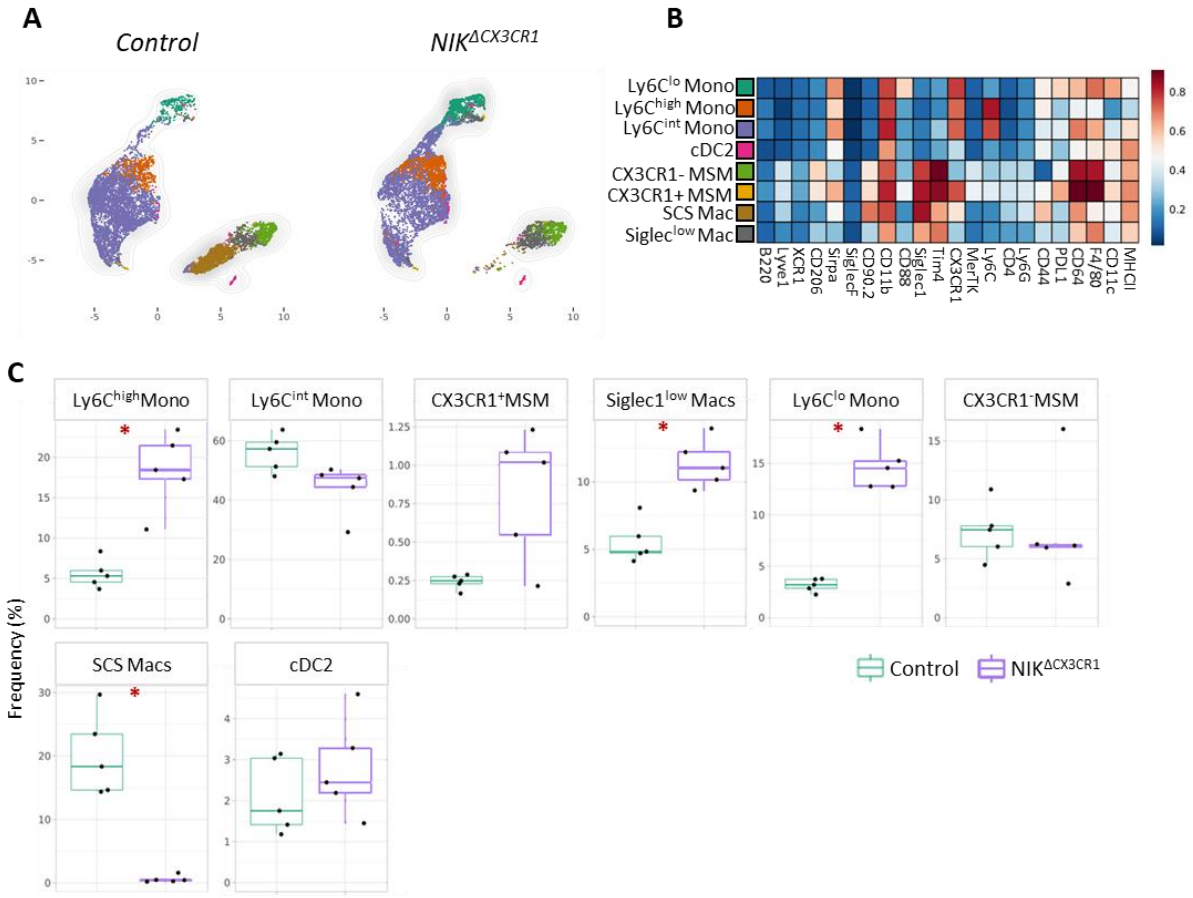

Figure 4: Loss of SCS macrophages and more F4/80^{+} macrophages in the dLN of NIK$^{\Delta CX3CR1}$ mice during steady state.

(A) Uniform manifold approximation and projection (UMAP) map displaying 50,000 randomly sampled cells from the dLN of NIK$^{\Delta CX3CR1}$ and littermate controls analysed by flow cytometry focussing on monocyte and macrophage subsets. (B) A heat map with mean marker expression values for each cluster. (C) Relative frequencies of Ly6C^{high} monocytes (mono), Ly6C^{lo} mono, Ly6C^{int} mono, CX3CR1^{+} medullary sinus macrophages (MSM), Siglec1^{low} Macrophages (Macs), CX3CR1^{-} MSM, sub-capsular sinus (SCS) Macs, cDC2s.

It has been published that isolating SCS macrophages from tissue is challenging since they rapidly die and form apoptotic blebs that bind to interacting cells. This raises the concern that the SCS macrophage population shown in Figure 4 could be Siglec1^{+} apoptotic blebs bound to

other cells[176]. We performed immunohistochemistry to address this issue and confirm the absence of the SCS macrophages in our mice. This technique would also allow the structure of dLNs to be examined. To visualise the different structures, we stained B cells (B220; green) for the B cell follicles in the cortex and T cells (CD4; blue) for the T cell zone in the inner cortex. In addition, F4/80 (red) and Siglec1 (grey) were used to distinguish the different macrophage populations in the LNs (Fig. 5A).

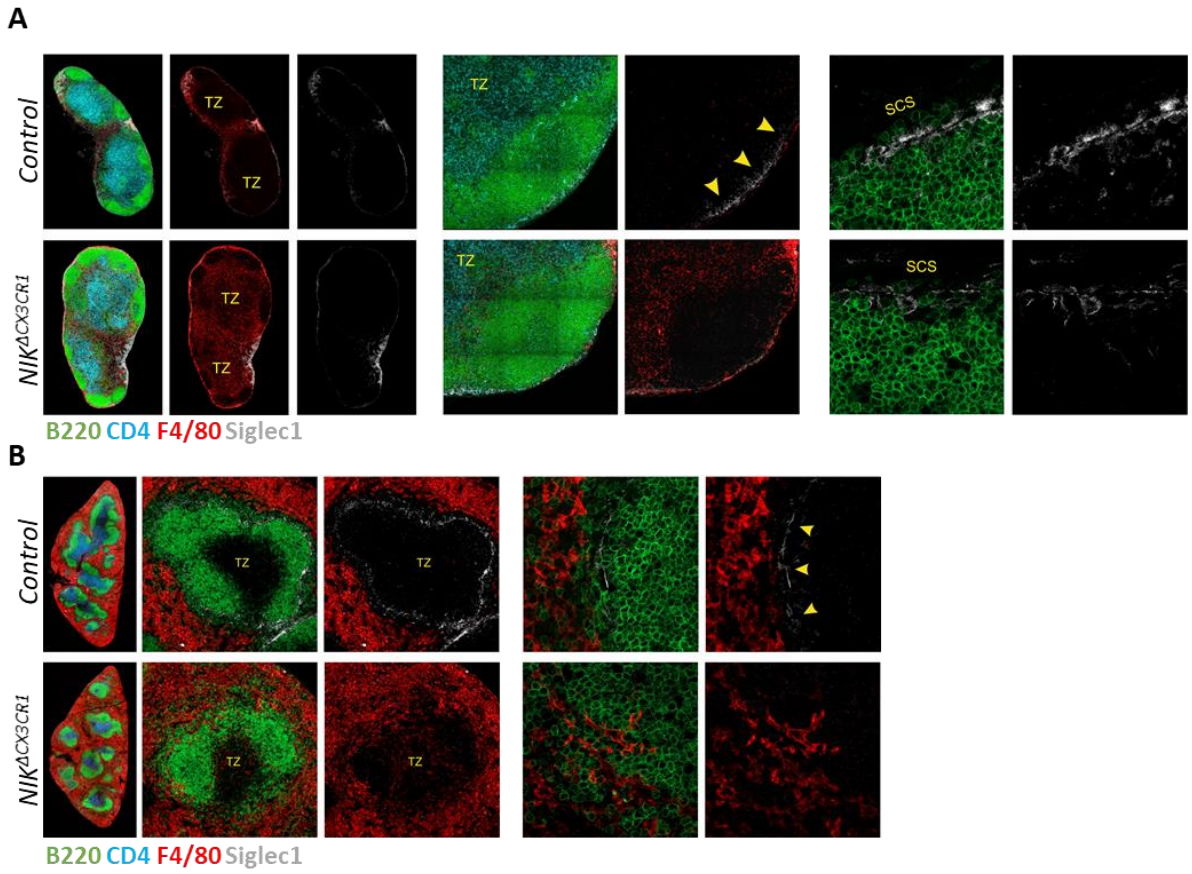

Figure 5: Loss of Siglec1⁺ macrophages and increased F4/80⁺ macrophages in the spleen and LN of NIK$^{\Delta CX3CR1}$ mice.

(A) Histological overview and zoom-in of the inguinal lymph nodes and (B) spleen stained for B220 (green), CD4 (blue), F4/80 (red) and Siglec1 (white) with a zoomed-in view of the sub-capsular sinus (SCS) zone of both NIK$^{\Delta CX3CR1}$ and littermate controls. Arrows indicate the Siglec1⁺ SCS macrophages (A) and marginal metallophilic macrophages (B) TZ= T cell zone SCS= sub-capsular sinus.

There were no noticeable differences in the B-cell follicles and T cell zone (TZ in Fig. 5) between NIK$^{\Delta CX3CR1}$ and littermate controls. However, similar to the data in Figure 4, we did observe a decrease in SCS macrophages, while the Siglec1⁺F4/80⁺ double-positive MSM remained unaffected in NIK$^{\Delta CX3CR1}$ mice compared to the control. Interestingly, we also noted an increase of F4/80⁺ cells in the T cell zone, which could potentially be the Siglec^{low} macrophages and Ly6C^{lo} (F4/80⁺) monocytes that were seen in the flow cytometry data from Figure 4 (Fig.5A).

We studied the spleen to extend these observations to other secondary lymphoid organs. The marginal zone of the spleen consists of Siglec1$^+$ and SIGN-R1$^+$ macrophages, termed marginal metallophilic macrophages (MMM) and marginal zone macrophages (MZM), respectively[177]. We could clearly see a loss of Siglec1$^+$ MMM around the T cell zone in the spleens of NIK$^{\Delta CX3CR1}$ mice (Fig. 5B). Moreover, we observed the same infiltration of F4/80$^+$ cells into the T cell zone as in the LN (Fig. 5B). Based on this data, we hypothesise that NIK has an important role in either the development, maintenance or both of Siglec1$^+$ macrophages in both the spleen and LNs.

3.2 The role of NIK in myeloid cells during autoimmune inflammation

3.2.1 NIK signalling in CX3CR1-expressing cells drives EAE pathology

NIK has been shown to be essential in the development of EAE. This was demonstrated by NIK$^{aly/aly}$ mice, which do not develop any EAE [152]. However, the role of NIK in myeloid cells during EAE is not fully understood yet. Therefore, we wanted to investigate the impact of NIK deletion in CX3CR1-expressing cells on the development of EAE. To achieve this, mice we immunised with MOG_{35-55}/CFA and Ptx and assessed daily for clinical signs of EAE (Fig. 6A). Interestingly, we found that the NIK$^{\Delta CX3CR1}$ mice did not develop any clinical symptoms by looking both at the daily score and overall maximum score (Fig. 6B, C).

EAE pathology involves the infiltration of immune cells into the CNS and the activation of microglia. Therefore, we used flow cytometry to analyse the infiltrating immune cells and microglia during the peak of the disease, day 15. As we suspected, we could observe minimal infiltrating immune cells (CD45^{high}CD11b$^{+/-}$) into the CNS of NIK$^{\Delta CX3CR1}$ mice at this time point, which could explain why the mice did not develop any disease(Fig 6D).

Furthermore, we did not observe any difference in the number of microglia (CD45^{int}CD11b$^+$), and there were no significant changes in the expression of various activation markers, except for a minor increase in CD39. The induction of CD39 on microglia during EAE is thought to be associated with an anti-inflammatory state of the microglia[169]. This suggests that the microglia in the NIK$^{\Delta CX3CR1}$ have a more protective role during EAE. We then examined the composition of myeloid cells (CD11b$^+$CD45^{high}) in the CNS, dLN and spleen during the peak of EAE. Within this population, we could observe a reduction of Ly6C$^+$ inflammatory monocytes in the CNS, while there were no differences in the spleen and dLNs. Additionally, there were no changes in the percentage of Ly6G$^+$ neutrophils in any of the organs (Fig. 6F).

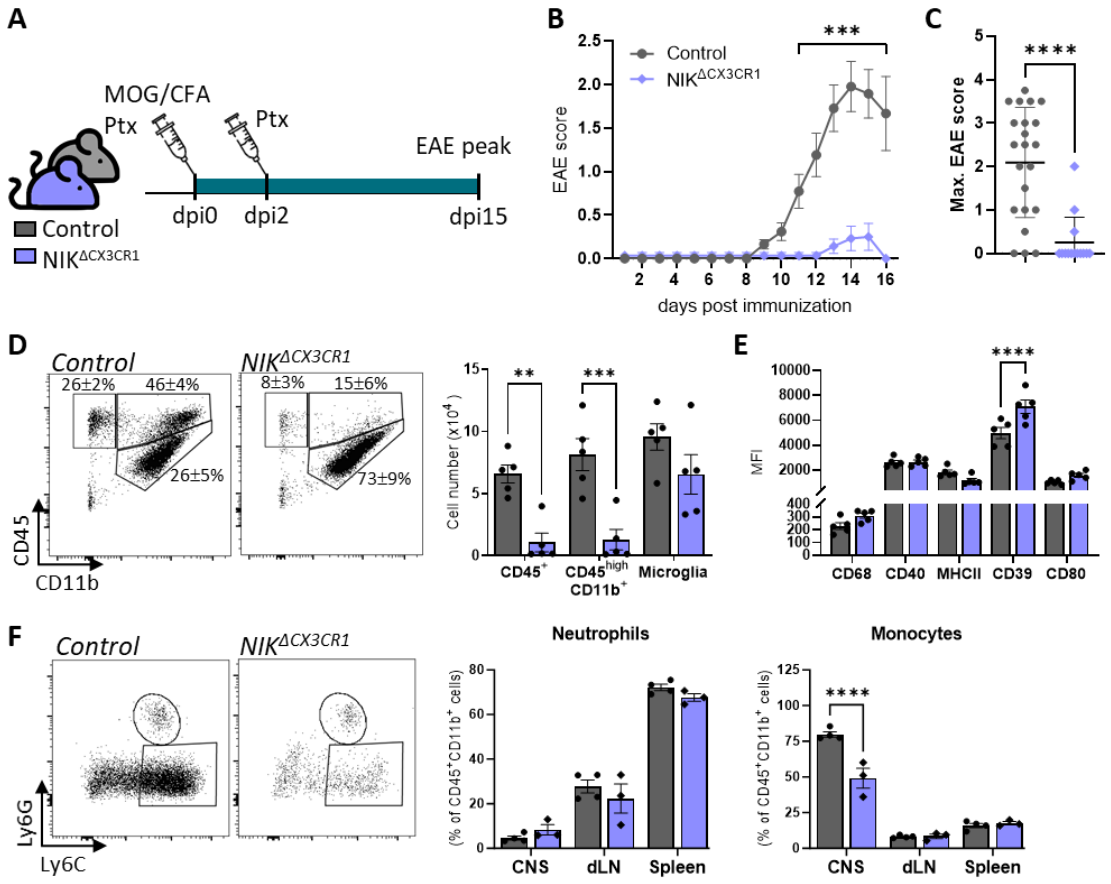

Figure 6: NIK in CX3CR1 expressing cells drives EAE pathology.

*(A) Experimental strategy of MOG immunisation to induce EAE in control and NIK$^{\Delta CX3CR1}$ mice. (B-C) Disease course of NIK$^{\Delta CX3CR1}$ and littermate controls (B) and maximum EAE score (C). Data in B and C is the cumulative data of 3 individual experiments. (D) Representative FACS plots and the number of microglia (CD11b^{+}CD45^{int}) and infiltrating immune cells (CD45^{high} and CD11b^{+}CD45^{high}) into the CNS during the peak of EAE (15dpi). (E) The median fluorescent intensity (MFI) of different activation markers on the microglia population. (F) Representative FACS plots from the CNS and percentages for Ly6G^{+} neutrophils and Ly6C^{+} monocytes in the CNS and dLN, pre-gated on CD45^{+}CD11b^{+} cells. Debris, duplets, and dead cells were excluded before gating on the cell populations shown in D-E. Data in B-E is shown as mean ± SEM and analysed using two-tailed unpaired Student's t test (C) or two-way ANOVA with Šídák's multiple comparisons test. (B, D, E, F). *p < 0.05, **p < 0.01, ***p < 0.001, ****p < 0.0001. dpi=days post-immunization.*

Next, we analysed the T cell compartment during the peak of EAE and their encephalitogenic properties. For this, we subjected the isolated cells from CNS, dLN and spleen to an *ex vivo* MOG antigen recall assay in which the isolated leukocytes were restimulated with MOG for six hours. Flow cytometry was used to gate on CD4^{+}CD90^{+} T cells to look at overall T cell numbers in these organs. These T cells were further gated on CD44, an activation marker, and CD40L, another activation marker which is rapidly upregulated upon antigen-specific interaction with cognate APCs and thus serves as a marker for MOG_{35-55} specific cells. We additionally checked for the cytokine profile of these cells by performing an intracellular cytokine staining for IL-17A, GM-CSF and IFNγ (Fig. 7A).

In the CNS, we observed a significant decrease in infiltrating CD4+ T cells, as well as a reduction in CD40L+ MOG-activated T cells and no cytokine-producing T cells (Fig. 7B). There were no significant changes observed in the dLNs and spleen, but we did notice a trend towards fewer MOG-activated T cells and a slight decrease in cytokine-producing T cells of NIK$^{\Delta CX3CR1}$ mice (Fig. 7C).

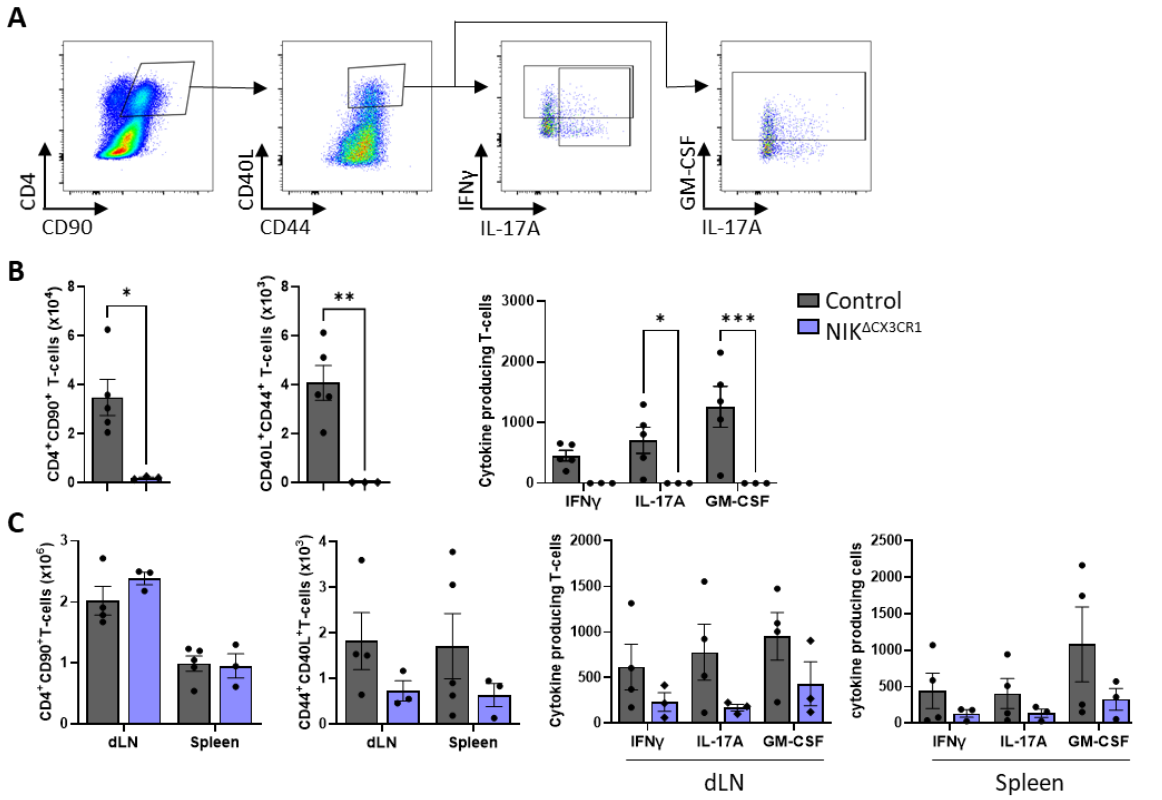

Figure 7: Fewer infiltrating T cells in the CNS during the peak of EAE.

*Single-cell suspensions of mononuclear cells were subjected to a MOG recall assay, and flow cytometry analysis was used to quantify T cell subsets. (A) An example of the gating strategy used to gate for CD4+CD90+ T cells, CD44+CD40L+ MOG reactive T cells, and IL-17A, IFNγ and GM-CSF production by these cells. Duplets and dead cells were excluded. (B) The total cell number of these T cell populations in the CNS (brain + spinal cord) and (C) spleen + dLN of NIK$^{\Delta CX3CR1}$ and control mice. Data in B-C is shown as mean ± SEM and analysed using two-tailed unpaired Student's t test or two-way ANOVA with Šídák's multiple comparisons test. *p < 0.05, **p < 0.01, ***p < 0.001.*

The CX3CR1-Cre targets various myeloid populations, including some CD11c-positive populations, such as a subpopulation of cDC2s and moDCs. It has been reported that mice with a deficiency of NIK in CD11c-expressing cells were fully susceptible to EAE and had a similar disease course compared to wild-type mice[159]. This would suggest that the resistance to EAE observed in our NIK$^{\Delta CX3CR1}$ mice is likely due to NIK deficiency in CX3CR1+CD11c- cells rather than CX3CR1+CD11c+ cells. To validate these findings, we crossed our NIK$^{fl/fl}$ mice with the CD11c-Cre (NIK$^{\Delta CD11c}$) (Fig 8A) and induced EAE in these mice. Contrary to previous reports, our NIK$^{\Delta CD11c}$ mice were almost fully resistant to EAE, similar to the NIK$^{\Delta CX3CR1}$ mice (Fig. 8B, C).

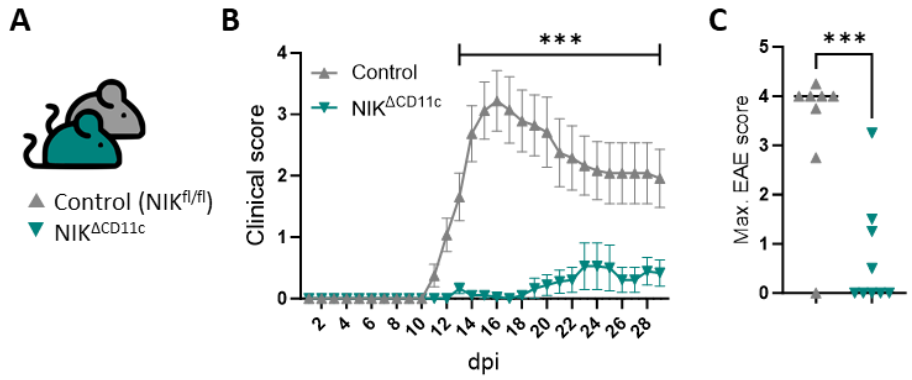

Figure 8: The deletion of NIK in CD11c-expressing cells protects against EAE.

*(A) NIK$^{fl/fl}$ mice were crossed to CD11c-Cre to delete NIK in CD11c-positive cells. (B) The EAE disease development and (C) maximum EAE score in NIK$^{\Delta CD11c}$ mice(n=9) and littermate controls(n=8). Data in B & C is shown as mean ± SEM and analysed using two-tailed unpaired Student's t test (C) or two-way ANOVA with Šídák's multiple comparisons test. (B). *p < 0.05, **p < 0.01, ***p < 0.001. dpi=days post-immunization*

3.2.2 NIK in microglia is redundant during EAE development.

As previously mentioned, microglia play an essential role in immune functions within the CNS and are also targeted by the CX3CR1-Cre. Recent studies reported that NIK in microglia plays a crucial role during the late phase of EAE[155]. We aimed to investigate whether the resistance to EAE observed in NIK$^{\Delta CX3CR1}$ mice could be attributed, at least in part, to the microglia. To achieve this, we crossed the NIK$^{fl/fl}$ with the tamoxifen-inducible CX3CR1-creERt2 (NIK$^{\Delta MG}$). In this system, the Cre-mediated deletion of NIK is only induced after tamoxifen injections. This results in a more specific deletion in microglia and border-associated macrophages (BAMs) due to their long lifespan and self-maintaining capacity, while other myeloid cells are replaced over time[75,178]. The mice were immunised with MOG six weeks after tamoxifen injections, and the clinical EAE score was assessed daily (Fig. 9A).

Surprisingly, our findings showed that the NIK$^{\Delta MG}$ mice were fully susceptible to EAE and had no significant differences in the disease development or the overall maximum EAE score compared to littermate controls (Fig. 9B, C). Using flow cytometry analysis, we did not observe any differences in the percentage or number of infiltrating leukocytes into the CNS during the peak of EAE (Fig. 9D, E), nor any differences in the MFI of various activation markers on microglia (Fig. 9F).

To analyse MOG-activated T cells and the production of IL-17A, GM-CSF, and IFNγ in the infiltrating cells, we subjected the leukocytes to an *ex vivo* MOG antigen recall assay. In this assay, the isolated cells were restimulated with MOG_{35-55} for six hours. No differences were observed in the proportions of $CD4^+$ T cells, MOG-activated T cells or cytokine-producing T cells in the CNS of NIK$^{\Delta MG}$ mice (Fig. 9G-K). This indicates that NIK in microglia and BAMs does

play a role in the development of EAE and does not affect the infiltration of T cell subsets during the peak of EAE.

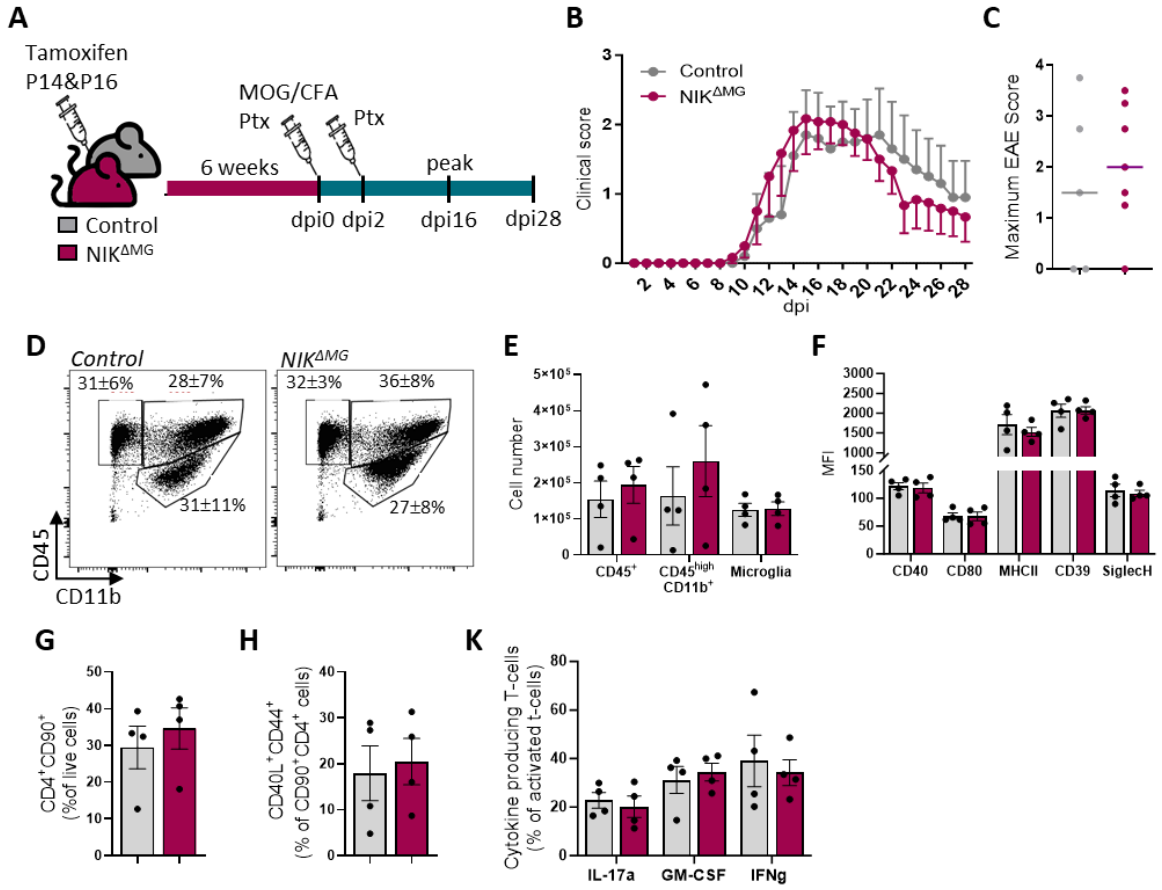

Figure 9: NIK in microglia is redundant for EAE development.

(A) Scheme of the tamoxifen injections and MOG_{35-55} immunisation in $NIK^{\Delta MG}$ and littermate controls. (B) The EAE disease course and (C) maximum EAE score of $NIK^{\Delta MG}$ and littermate controls. (D) representative flow cytometry plots showing the infiltrating cells and microglia in the CNS (brain and spinal cord) during the peak of EAE disease (16 dpi) with the mean percentages and SEM for microglia ($CD11b^{+}CD45^{int}$), infiltrating $CD45^{high}$ and $CD11b^{+}CD45^{high}$ immune cells. (E) The total cell number of these populations. (F) The median fluorescence intensity (MFI) of different activations markers on microglia. (G) The percentages of infiltrating $CD4^{+}CD90^{+}$ T cells, (H) MOG-activated $CD40L^{+}CD44^{+}$ T cells, and (K) cytokine-producing T cells after being subjected to MOG_{35-55} antigen recall assay. Data in graphs are shown as mean ± SEM and analysed using two-tailed unpaired Student's t test (C, G, H) or two-way ANOVA with Šídák's multiple comparisons test (B, E, F, K). dpi=days post-immunization

3.2.3 Impaired T cell priming in the secondary lymphoid organs

Since $NIK^{\Delta MG}$ mice were susceptible to EAE and $NIK^{\Delta CX3CR1}$ mice did not develop any clinical symptoms, we focused on investigating what causes protection against EAE in the periphery of these mice. We hypothesised that the protective effect in the $NIK^{\Delta CX3CR1}$ mice could be primarily because the peripheral CX3CR1 expressing cells lack NIK. And since CX3CR1 is expressed by antigen-presenting cells, we hypothesised that the mice might show defects in T cell priming before the onset of EAE.

We first tested this hypothesis by using the adoptive transfer EAE model. In this model, we avoid the priming step in the NIK$^{\Delta CX3CR1}$ mice by transferring MOG-activated T cells from immunised Ly5.1 wild-type mice into NIK$^{\Delta CX3CR1}$ and control mice(Fig. 10A). The transferred T cells were able to induce the disease in both NIK$^{\Delta CX3CR1}$ mice and control mice. No differences were seen in the clinical score or the overall maximum EAE score (Fig. 10B). These findings demonstrate that transferring MOG-activation T cells from wild-type mice into our NIK$^{\Delta CX3CR1}$ mice is sufficient to induce EAE within this model. This further suggests that there might be a defect in T cell priming in the periphery of these mice.

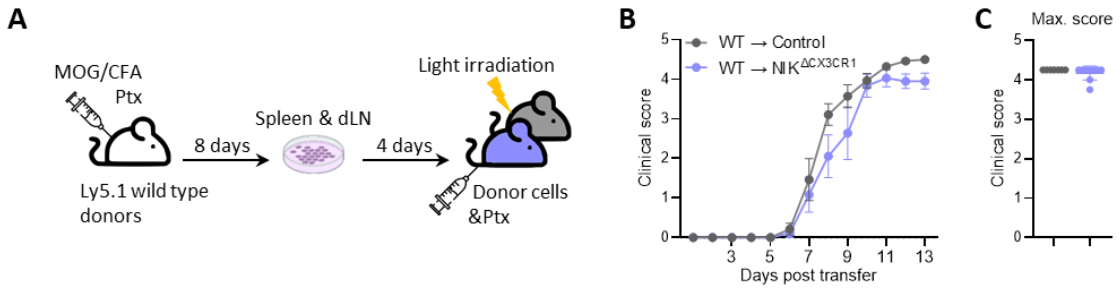

Figure 10: Wild-type MOG-activated T cells are able to induce EAE in NIK$^{\Delta CX3CR1}$ mice.

(A) Scheme of the adoptive transfer EAE model: Ly5.1 wild-type mice were immunised with MOG$_{35-55}$/CFA and Pertussis (Ptx) cells from dLNs and spleen at eight days post injection (dpi) and cultured for four days with MOG$_{35-55}$, IL-23, and anti-IFNγ before being injected into NIK$^{\Delta CX3CR1}$ and littermate controls(A). EAE disease course (B) and maximum EAE score (C) of NIK$^{\Delta CX3CR1}$ and littermate controls after adoptive transfer of MOG activated wildtype T cells. Data in graphs are shown as mean ± SEM and analysed using two-way ANOVA with Šídák's multiple comparisons test (B) or two-tailed unpaired Student's t test (C).

To test if the priming was affected in NIK$^{\Delta CX3CR1}$ mice, we immunised and opened mice eight days after immunisation before the onset of disease (Fig. 11A) . Isolated cells from the dLNs and spleen were subjected to an ex vivo MOG antigen recall assay to investigate T cell activation before mice developed any disease. After restimulation of the cells with MOG, we saw a decrease in the number of CD4$^+$CD90$^+$ T cells in the dLNs but not the spleen of NIK$^{\Delta CX3CR1}$ mice (Fig 11B). Furthermore, a slight decrease of MOG-activated CD40L$^+$CD44$^+$ T cells could be observed, which was only significant in the spleen and not the dLNs (Fig. 11C).

Further looking into the cytokine production among the MOG-activated cells, we could observe a decrease in the percentage of IL-17A and GM-CSF in the dLNs and spleen. In addition, in the spleen, there was also a decrease of the GM-CSF/IFNγ producing T cells (Fig. 11D). A similar decrease of MOG-activated T cells and IL-17A and GM-CSF production was seen 10 days after MOG-immunisation in the spleen of NIK$^{\Delta CX3CR1}$ mice (data not shown). This data suggests that there are fewer encephalitogenic T_H17s and T_H1s in the NIK$^{\Delta CX3CR1}$ mice before EAE onset, which suggests that NIK in CX3CR1 expressing cells is important in regulating effector T cell function during the priming stage in EAE.

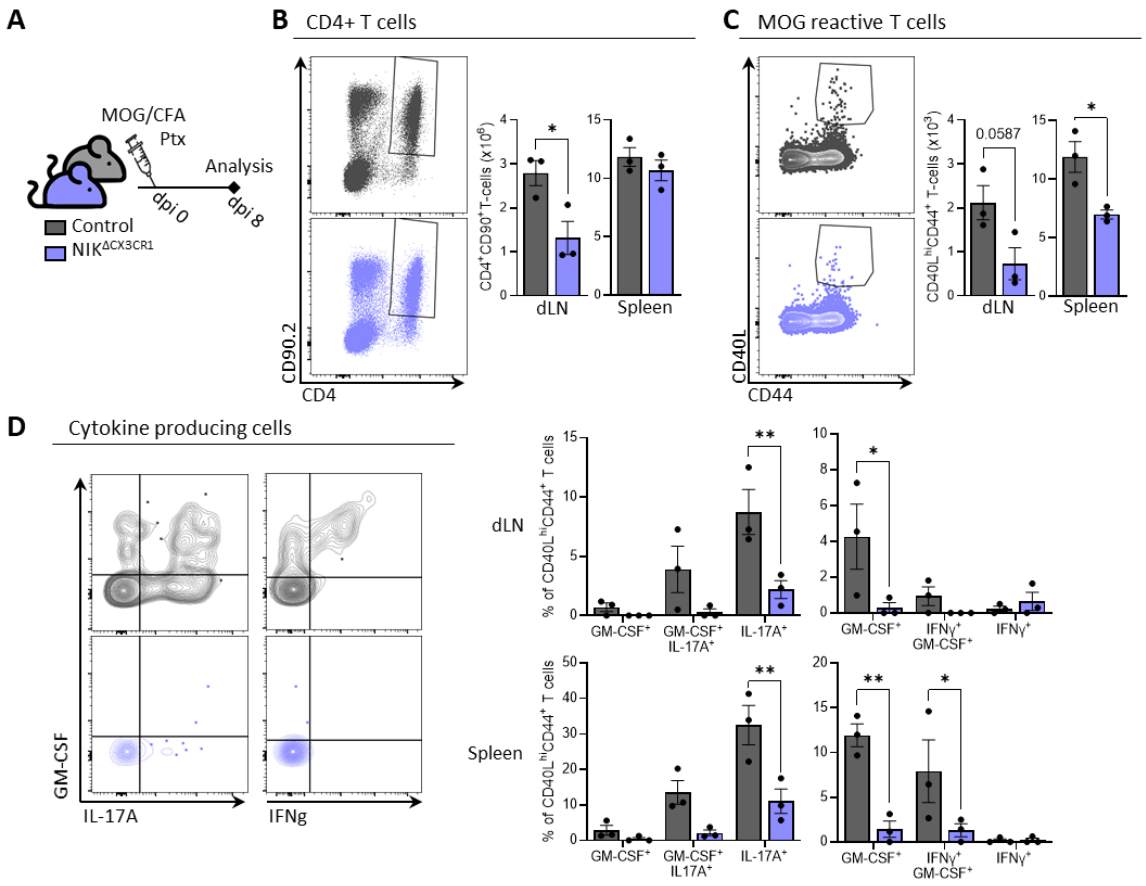

Figure 11: Less cytokine-producing T cells in secondary lymphoid organs before EAE onset.

*(A) Experimental scheme: NIK$^{\Delta CX3CR1}$ and littermate control mice were immunised with MOG$_{35-55}$/CFA and Ptx, and cells were isolated from the spleen and dLN at eight days post immunisation (dpi) for analysis with flow cytometry. (B) representative flow cytometry plots from the spleen and total cell number of CD4$^+$CD90$^+$ T cells and (C) MOG-reactive (CD44$^+$CD40L$^+$) T cells. (D) Representative flow cytometry plots from the spleen and percentages of IL-17A, GM-CSF and IFNγ producing T cells. Pre-gated on live/single cells. Data in graphs are shown as mean ± SEM and analysed using two-tailed unpaired Student's t test (B, C) or two-way ANOVA with Šídák's multiple comparisons test(D). *p < 0.05, **p < 0.01.*

Another priming experiment was performed to strengthen the hypothesis of a defect in the priming of T cells in the NIK$^{\Delta CX3CR1}$ mice. For this, we utilised 2D2 T cells, which are T cells with a transgenic T cell receptor (TCR) specific for the MOG peptide[179]. We adoptively transferred CD90.1$^+$ naive 2D2 T cells into our CD90.2$^+$ NIK$^{\Delta CX3CR1}$ and control mice and followed their fate upon MOG immunisation (Fig. 12A). The congenital marker CD90.1 allowed us to distinguish the 2D2 cells from the CD90.2$^+$ host cells. Significantly fewer 2D2 cells were observed in the spleen of NIK$^{\Delta CX3CR1}$ mice six days after the MOG immunisation, and a similar trend was observed in the dLNs (Fig. 12B). This suggests that the transferred 2D2 cells proliferated less in the NIK$^{\Delta CX3CR1}$ mice. The isolated cells from the spleen and dLN were restimulated *ex vivo* to investigate their cytokine production. Although no significant differences were observed in the production of IFNγ and GM-CSF by the T cells, there was a significant reduction in IL-17A-

producing 2D2 cells in both the spleen and dLNs of the NIK$^{\Delta CX3CR1}$ mice (Fig. 12C). Additionally, the same decrease in IL-17A could be seen in the host cells of the NIK$^{\Delta CX3CR1}$ mice.

These findings further support our hypothesis that the deletion of NIK in CX3CR1-expressing cells impacts their ability to prime T cells, particularly in terms of IL-17A production. The decrease in the production of encephalitogenic cytokines by activated T cells might be a significant factor in the EAE protection observed in NIK$^{\Delta CX3CR1}$ mice.

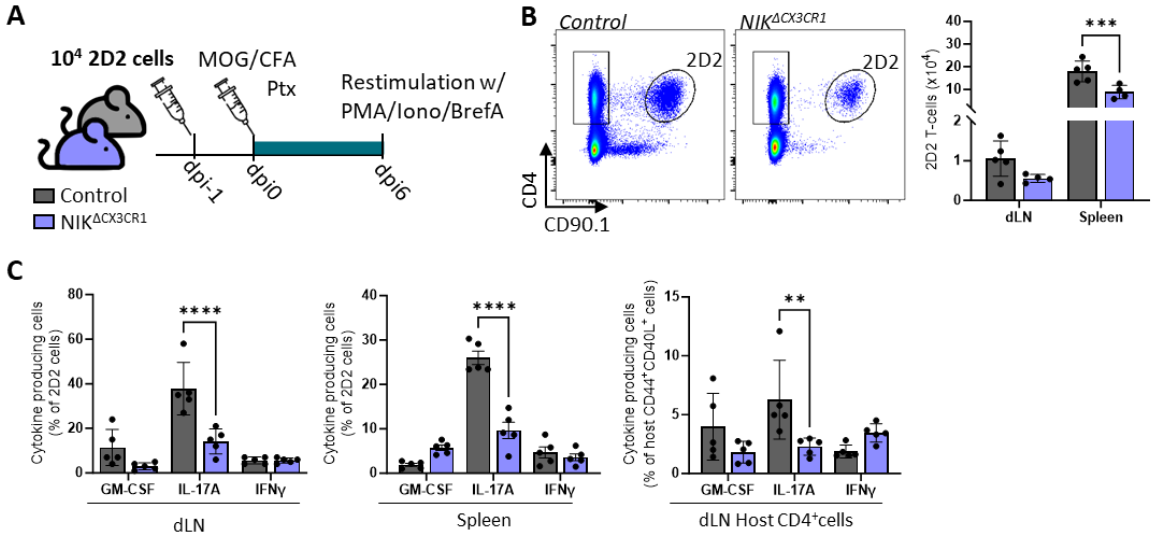

Figure 12: Reduced IL-17A production by 2D2 T cells six days after MOG immunisation.

*(A) 2D2 T cells were transferred into NIK$^{\Delta CX3CR1}$ and littermate controls one day before MOG immunisation. Six days post immunisation, cells were isolated from the spleen and dLN and restimulated with PMA, Ionomycin and Brefeldin A (B) Representative flow cytometry plots of the spleen and the total cell number of transferred CD90.1⁺CD4⁺ 2D2 cells. (C) Percentages of 2D2 T cells that produce IL-17A, GM-CSF or IFNγ in the dLNs and spleen and cytokine-producing CD4+ host cells. duplicates/dead cells were excluded from(B). Data in graphs are shown as mean ± SEM and analysed using two-way ANOVA with Šídák's multiple comparisons test. *p < 0.05, **p < 0.01, ***p < 0.001, ****p < 0.0001. dpi=days post-immunization*

Tregs are a critical component of the immune system, responsible for regulating immune responses and preventing autoimmune diseases such as EAE[180]. Previous research has demonstrated that the deletion of RelB, which is downstream of NIK in the NF-κB pathway, in cells expressing CD11c results in the accumulation of Tregs. This subsequently protects mice from developing EAE[157]. We examined whether Tregs play a role in the protection against EAE in our NIK$^{\Delta CX3CR1}$ mice. There did not seem to be any differences in the percentages of Tregs within all T cells in the spleen and dLNs three- or eight days post-MOG immunisation (Fig. 13A-C). Additionally, the percentage of Tregs during the peak of EAE (15dpi) in the CNS, spleen and dLNs was similar between both groups (Fig. 13D). This suggests that NIK in CX3CR1 expressing cells does not influence the amount of Tregs during EAE.

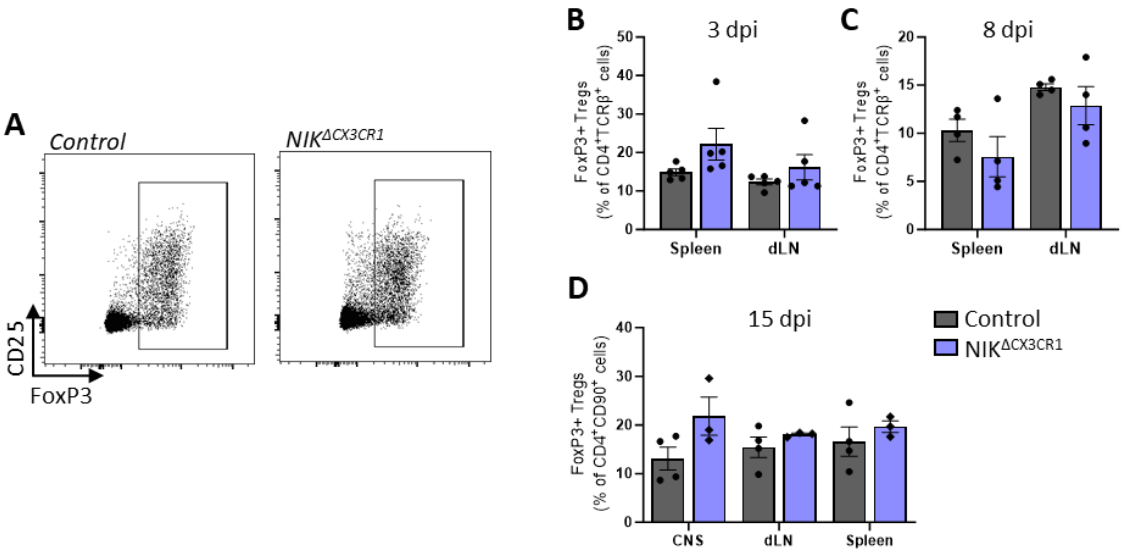

Figure 13: No differences in the percentage of Tregs after MOG immunisation.

*(A) An example of the gating for FoxP3⁺ Tregs in the dLN at eight days post-immunization (dpi) with MOG/CFA and PTx. The percentages of Tregs in the (B) Spleen and dLNsthrre dpi and(C) eight dpi. (D) The percentages of Tregs in the CNS, dLN and spleen during the peak of EAE. Tregs were pre-gated on CD45⁺, TCRβ⁺ or CD90⁺, and CD4⁺ cells, dead cells and duplets were excluded. Data in graphs are shown as mean ± SEM and analysed using two-way ANOVA with Šídák's multiple comparisons test. *p < 0.05, **p < 0.01, ***p < 0.001.*

3.2.4 Reduced expression of activation markers on myeloid subsets before EAE onset

High-dimensional flow cytometry was used to gain a deeper understanding of the myeloid compartment in the dLNs before the onset of EAE (5dpi). We focussed on the CD11b⁺ cells while excluding neutrophils and eosinophils to obtain a clearer overview of the different DC, monocyte, and macrophage populations. A UMAP was generated to represent the diverse myeloid subsets visually, and FlowSom analysis was employed to identify multiple myeloid clusters in both control and NIK$^{\Delta CX3CR1}$ mice (Fig. 14A). The median expression of established cell markers was used to annotate each cell type. Through our analysis, we were able to identify F4/80^{high} macrophages, CD11c^{high} resDC2, MHCII^{high} migDC2, Ly6C^{hi} Ly6C^{int} and Ly6C^{lo} monocytes as well as a CD11c⁺Ly6C⁺ moDC cluster (Fig. 14B). One cluster which had low expression of all markers was unidentified and annotated as “other”.

There seems to be a small shift in some of the clusters of the NIK$^{\Delta CX3CR1}$ mice compared to the control (Fig. 14A). And when looking at the proportions of these clusters, we could observe a significant increase of Ly6C^{lo} monocytes in our NIK$^{\Delta CX3CR1}$ mice. No other significant differences were seen in the proportions of the other clusters (Fig. 14C).

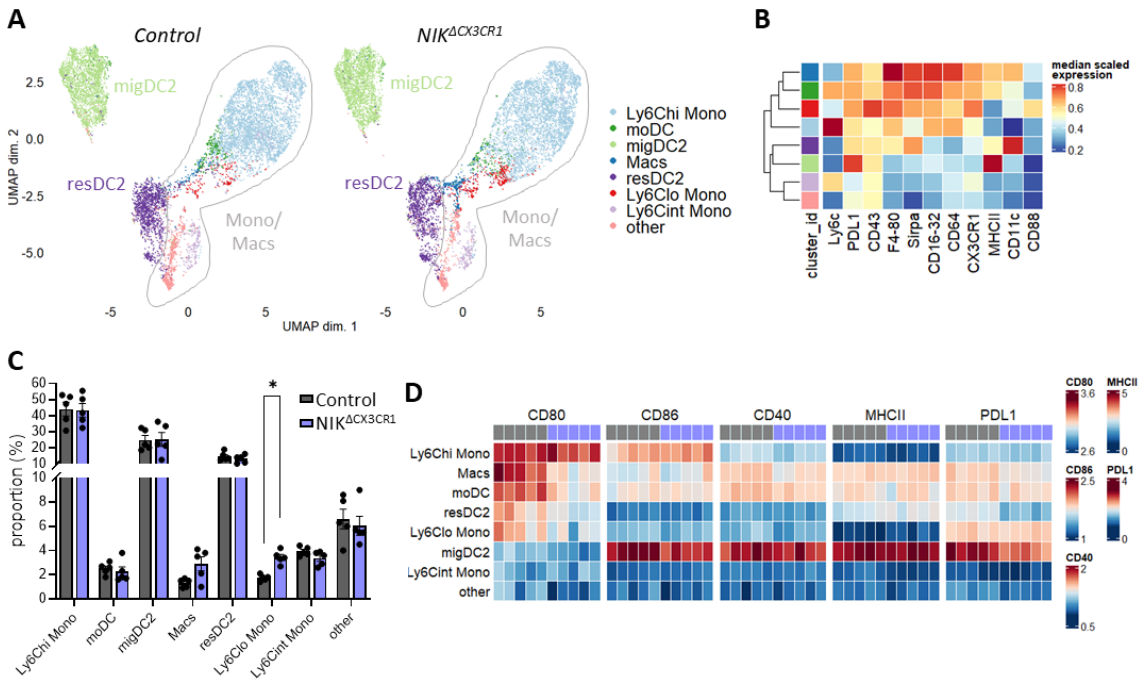

Figure 14: High-dimensional flow cytometry analysis reveals differences in myeloid subsets five days after MOG immunisation.

*(A) UMAP map displaying 50,000 randomly sampled cells from the dLN of NIK$^{\Delta CX3CR1}$ and littermate controls analysed by flow cytometry focussing on CD11b^{+} subsets. (B) Heatmap with median marker expression values for each population shown in the UMAP. (C) Relative frequencies of Ly6C^{high} monocytes (Mono), Ly6C^{int} Mono, Ly6C^{lo} Mono, ResDC2, MigDC2, MoDCs, Macrophages (Mac), other. Pre-gated on CD11b^{+} cells and Dead cells, duplicates, T and B cells, neutrophils and eosinophils were excluded. (D) Median (arcsinh-transformed) expression of CD80 and CD86 (x-axis) across the eight identified myeloid cell populations. Data in C is shown as mean percentage and analysed using two-way ANOVA with Šídák's multiple comparisons test. *p < 0.05.*

CD80 and CD86 are two co-stimulatory molecules found on APCs which interact with CD28 and CTLA-4 on T cells and regulate T cell function. Both CD80 and CD86 have been shown to be increased on mature DCs which is why we analysed the median expression of these markers on our myeloid cell clusters. Here, we could see that most myeloid clusters express CD80 while CD86 is mainly expressed by the migDC clusters (Fig. 14D). When comparing the expression between control and NIK, we could see a significant decrease of CD80 expression in the resDC2 and moDC clusters while CD86 expression is only slightly decreased in the migDC2 cluster (Fig. 14D).

Furthermore, we could not see any differences in the expression levels of MHCII or CD40, an activation marker and known receptor of the non-canonical NF-κB pathway. But a slight decrease in the expression of Programmed death-ligand 1 (PD-L1), a critical molecule in maintaining immune tolerance and regulating T cell responses, could be observed in the migDC2 and cDC2 clusters of NIK$^{\Delta CX3CR1}$ mice (Fig. 14D). This could suggest that our DC

populations are more immature which could affect the priming of T cells and regulating T cell tolerance.

3.2.5 Differences in the proportions of myeloid cell clusters

To get a better understanding of how the deletion of NIK in CX3CR1-expressing cells affects T cell priming and the resistance against EAE, we decided to analyse the differential mRNA expression of these cells. To achieve this, we isolated cells from the dLN of NIK$^{\Delta CX3CR1}$ and littermate control mice four days following MOG immunisation. During this time point, myeloid cells start getting activated and present the MOG peptide to T cells. Since our primary interest was myeloid cells, we enriched for these cells by removing B and T cells (Fig. 15A). We then captured individual cells from each sample using the well-based BD Rhapsody platform. The cells were subsequently sequenced to obtain transcriptomic data at the single-cell level. This approach allowed us to simultaneously analyse gene expression profiles from multiple samples, providing insights into the heterogeneity and diversity of cell populations within each sample.

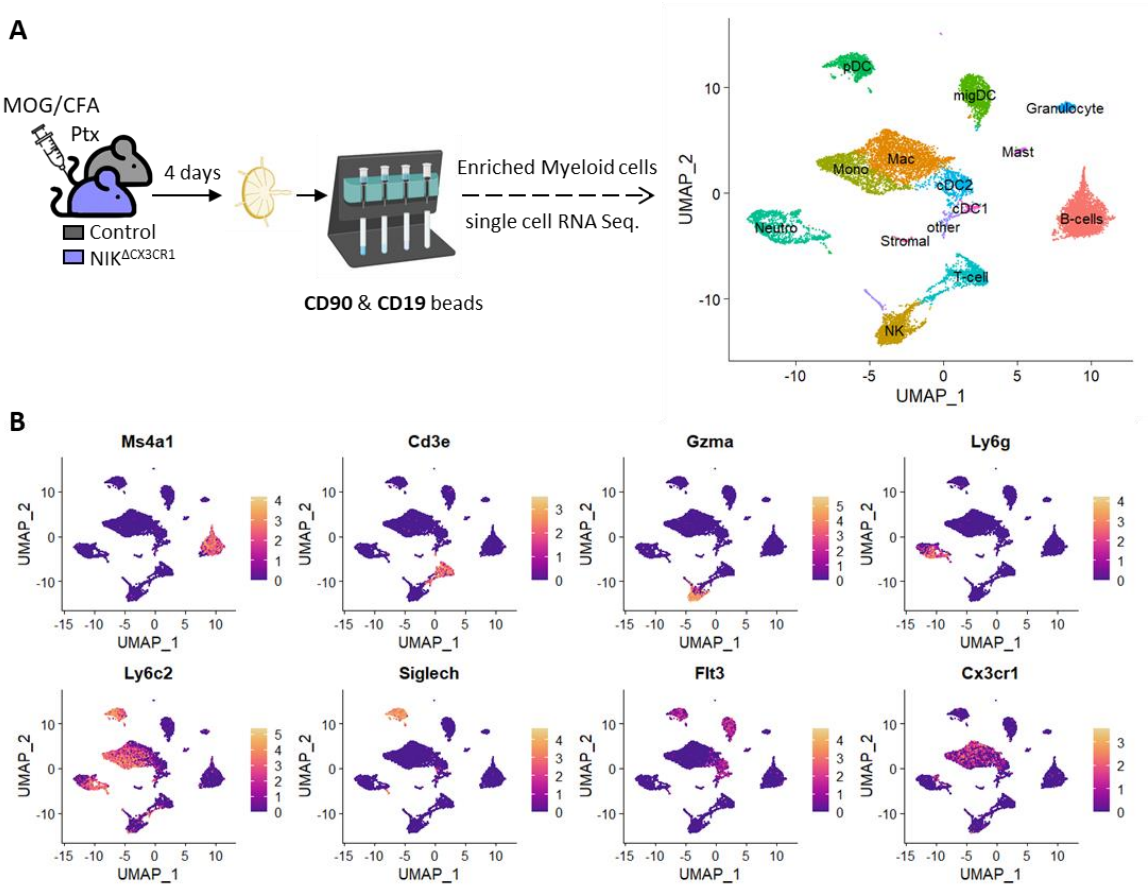

Figure 15: scRNA sequencing strategy and clusters.

(A) Leukocytes were isolated from dLNs four days after MOG immunisation. The cells were enriched for myeloid cells by depleting CD19⁺ & CD90⁺ cells utilising MACS microbeads before scRNA sequencing. Results were analysed in R with the Seurat plugin to visualise UMAP clustering of different cell types. (B) UMAP displaying expression of different cell markers to identify cell type.

The data analysis was conducted using the Seurat package in the R program[164]. The dataset underwent unsupervised clustering analysis to identify distinct cell populations, and the results were visually represented using UMAP (Fig. 15A). The top 20 highly expressed genes per cluster were calculated and used to identify the different cell clusters. This way, we were able to identify 14 cell clusters, and some known markers are shown in Figure 15B, which were used in combination with Immgen to annotate some of the cell clusters. The main clusters which we found were myeloid cells which showed that the enrichment worked. However, there was still some contamination of B and T cells (Fig. 15).

To conduct a more in-depth analysis of the myeloid cells, we focused on the macrophages, monocytes, and cDC populations, as they exhibited the highest CX3CR1 expression and were the clusters where we anticipated the most substantial changes between control and NIK$^{\Delta CX3CR1}$. These particular cell types were filtered, and unsupervised clustering resulted in a UMAP visualisation that revealed nine distinct myeloid cell clusters (Fig. 16A).

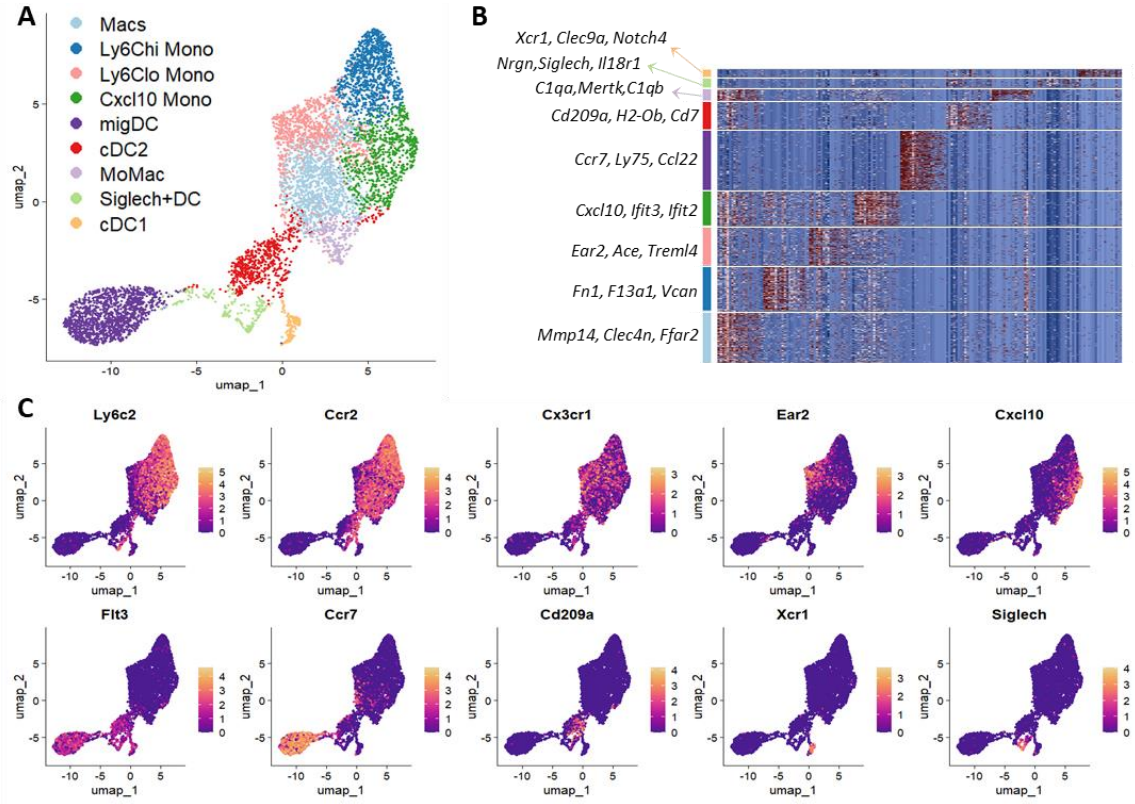

Figure 16: Nine distinct myeloid cell clusters.

(A) UMAP displaying clustering of myeloid cell types of all samples combined. Excluding B-, T-, NK-, mast cells, pDCs, neutrophils, granulocytes and other. (B) Heatmap displaying the top 10 highly expressed markers of each cluster in (A) with three of the top markers per cluster written out. (C) UMAP displaying the expression of different cell markers to identify cell types. Light blue = macrophages (Macs), dark blue = Ly6C^{hi} monocytes(Mono), pink = Ly6C^{lo} Mono, dark green = Cxcl10^{+} Mono, purple =migDCs, red = cDC2s, lilac = monocyte derived (Mo)Macs, light orange = cDC1s, light green = Sox4^{+} DCs. Dimensions = 15 resolution = 0.5

These clusters were further characterised based on their marker genes and annotated with the assistance of Immgen and known literature. We identified two monocyte clusters expressing *Fn1*, *F13a1* and *Vcan* annotated as Ly6C^{hi} Mono and the second monocyte cluster expressing *Ear2*, *Ace*, and *Cd300e* was annotated as Ly6C^{lo} Mono (Fig. 17A-C). Additionally, a third monocyte population expressing *Cxcl10*$^{+}$, *Ifit3,* and *Ifit2*, known to possess a pathogenic phenotype in EAE [181], was identified as Cxcl10 Mono. Furthermore, we could identify a macrophage cluster (Macs) with Immgen based on the top ten marker expressions (incl. *Mmp14*, *Clec4n* and *Ffar2*). Notably, this cluster also shared some monocyte markers like *Ly6c2* and *Ccr2* (Fig. 17B-C). Another cluster sharing both macrophage markers and monocyte markers is the moMac cluster (*C1qa, Mertk, C1qb*), and a similar moMac cluster has been described previously in the context of EAE by Amorim et al.,2022[105].

In addition to the monocyte/macrophage clusters, we could identify four DC clusters which all expressed *Flt3* (Fig. 17C). These clusters were annotated as cDC1s (*Xcr1, Clec9a, Notch4*), cDC2s (*Cd209a, H2-Ob, Cd7*) and migDCs (*Ccr7, Ly75, Ccl22*). The final DC cluster, which expressed *Siglech*, *Nrgn*, and *Il18r,* displayed similarities to a murine Siglech^{+} DC phenotype described by others. These DCs shared characteristics of pDC and cDC2, which are believed to be transitional DCs in the process of transitioning from pre-DC to DC[182,183].

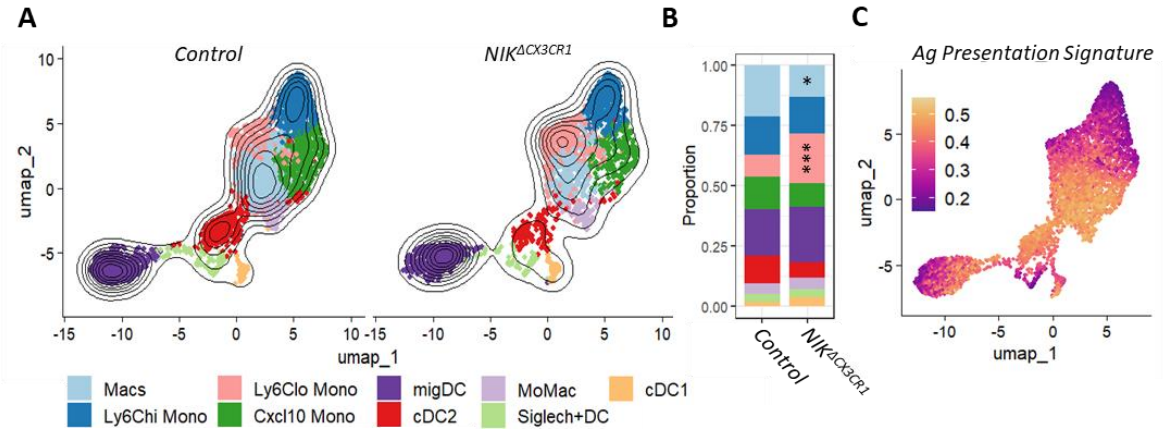

Figure 17: Differences in proportions of myeloid cell compartments.

*(A) Density plots overlaid on the UMAP of control and NIK$^{\Delta CX3CR1}$ displaying clusters in colour. (B) Proportions of each cell type within the UMAP of control (n=4) and NIK$^{\Delta CX3CR1}$ (n=4). (C) Antigen presentation cell signature score projected on UMAP calculated with Ucell. Data in (B) is shown as mean percentage and analysed using two-way ANOVA with Šídák's multiple comparisons test. *p < 0.05, **p < 0.01, ***p < 0.001.*

Upon analysing the UMAPs of the control and NIK$^{\Delta CX3CR1}$ groups, notable changes were observed. A shift in cell clusters was evident when comparing the UMAP of control and NIK$^{\Delta CX3CR1}$ overlaid with a density plot to visualise the distribution of cells. The results indicated a higher presence of Ly6C^{lo} monocytes in NIK$^{\Delta CX3CR1}$, whereas control mice exhibited more macrophages and cDC2s (Fig. 17A). This shift in cell types was further confirmed by analysing

the proportions of each cluster, which also showed a rise in Ly6C^{lo} monocytes and a decline in macrophages (Macs), and cDC2s in our experimental group (Fig. 17B).

Furthermore, analysing the cell signature for antigen presentation projected on our UMAP reveals that the highest score for antigen presentation is within the macrophage and DC clusters, the clusters which are decreased in our NIK$^{\Delta CX3CR1}$ (Fig. 17C). These observations indicate that our NIK$^{\Delta CX3CR1}$ have a decrease of APCs, which might help explain the ameliorated EAE in our mice. At the same time, we see an increase of Ly6C^{lo} monocytes, which are usually found in the vasculature where they are patrolling and play a role in tissue repair and can come into the tissue to differentiate into resident macrophages. However, whether these cells have any role in EAE disease development is yet unknown.

3.2.6 Differentially expressed genes hint towards less antigen presentation and migration

We employed the Milo package to gain deeper insights into the variances between control and NIK on the mRNA level[165]. Milo is a scalable statistical framework that assigns cells to partially overlapping neighbourhoods on a k-nearest neighbour graph and performs differential abundance testing. Through this approach, we were able to identify cell types exhibiting significant variances in abundance between our groups. The cells of our samples were assigned to 536 neighbourhoods (Fig. 18A). At a 10% FDR, we identified 96 differentially abundant neighbourhoods spanning multiple clusters (Fig. 18A-B). While most of these neighbourhoods seem to be in the migDC cluster, there were also some more abundant states in the Ly6C^{lo} monocytes of the NIK$^{\Delta CX3CR1}$ and more abundant neighbourhoods in the macrophage and cDC2 clusters (Fig. 18A-B). This suggests that the migDCs have the most change in mRNA level between control and NIK.

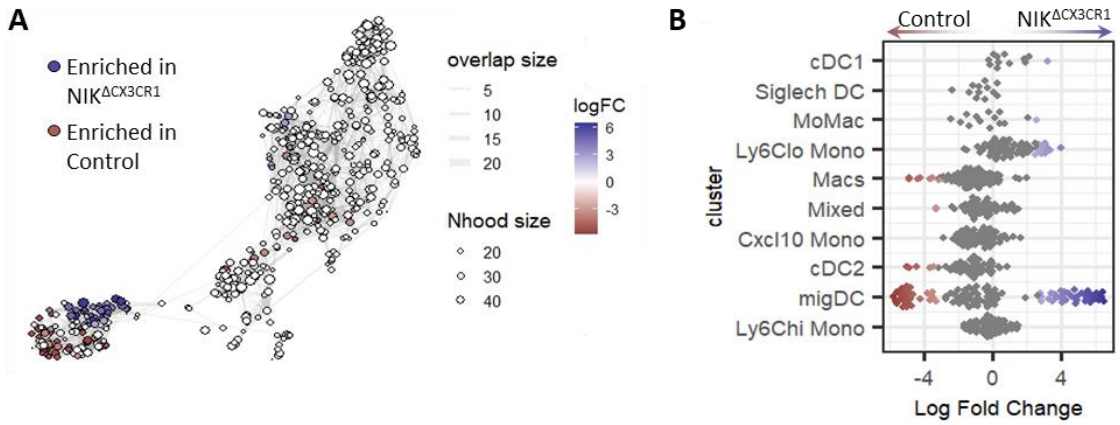

Figure 18: Differentially abundant neighbourhood analysis reveals differences within multiple clusters.
(A) 536 neibourhoods assigned by the Milo package, overlaid on our UMAP of myeloid cell clusters.(B) abundant neighbourhoods across the different myeloid clusters. Red = more abundand in control, Blue = more abundant in NIK$^{\Delta CX3CR1}$. FDR = 10%

An in-depth analysis revealed numerous differentially expressed genes (DEGs) between the control and NIK across various clusters. To gain further insights into the biological implications of these DEGs, we employed the clusterProfiler package to investigate the enrichment of Gene Ontology (GO) terms within our dataset. Our analysis identified several significantly enriched biological processes within the set of DEGs. Specifically, when focusing on DEGs that were significantly downregulated in NIK$^{\Delta CX3CR1}$ myeloid cells (Log2fold < -0.1 and adj.p-value < 0.05), we found notable enrichment in pathways associated with antigen processing and presentation as well as migration and chemotaxis. Furthermore, focussing on the DEGs that were significantly upregulated in NIK$^{\Delta CX3CR1}$ myeloid cells (Log2fold > 0,1 & adj.p-value < 0,05), we found enrichment in biological processes associated with immune response regulation and defence response (Table 9).

Upon further examination of some of the genes involved in these pathways across the various clusters, we found that DEGs involved in migration and chemotaxis (*Aif1*, *Ffar2*, *Thbs1* and *Vegfa*) were mostly reduced in the MoMac, cDC2 and Cxcl10 Mono clusters of NIK$^{\Delta CX3CR1}$ mice (Fig.18D). While some of the DEGs associated with antigen presentation and co-stimmulation, such as *Cd80*, *Cd86*, *Cd274*, *Ciita*, *H2-Ab1*, *H2-DMb1*, and *H2-K1*, showed a slight decrease in the Macs, MoMac, and Cxcl10 Mono clusters (Fig. 3H).

Table 9: Significantly enriched biological processes within myeloid cells from control or NIK$^{\Delta CX3CR1}$

ID	Description	GeneRatio	p.adjust	Enriched in
GO:0060326	**Cell Chemotaxis**	13/162	4,04E-05	Control
GO:0048002	**Antigen Processing And Presentation Of Peptide Antigen**	8/162	4,04E-05	Control
GO:0050900	**Leukocyte Migration**	14/162	4,8E-05	Control
GO:0019882	**Antigen Processing And Presentation**	9/162	5,38E-05	Control
GO:0002764	**Immune Response-Regulating Signaling Pathway**	17/108	5,11E-10	NIK$^{\Delta CX3CR1}$
GO:0002757	**Immune Response-Activating Signaling Pathway**	16/108	2,27E-09	NIK$^{\Delta CX3CR1}$
GO:0002253	**Activation Of Immune Response**	16/108	3,46E-08	NIK$^{\Delta CX3CR1}$

Two other genes that also show decreased expression in the same clusters and have a potential role in regulating antigen presentation are *Tmem176a* and *Tmem176b* (Fig. 19). These genes encode transmembrane proteins that belong to the Membrane-spanning 4A (MS4A) family and both act as cation channels. *Tmem176a/b* have been shown to be important for the intracellular processing of exogenous antigen before loading into the MHCII complex, which in turn affects the priming of CD4+ T cells [184].

When looking into the DEGs enriched in the immune response processes enriched in NIK$^{\Delta CX3CR1}$ myeloid cells, we found two interesting genes: *Tnip3*, which encodes the TNFAIP3 interacting protein 3 and *Otulin* (Fig. 19). Both are negative regulators of the canonical NF-κB pathway and

are believed to be part of the negative feedback regulation of NF-κB activation, inhibiting inflammation [185,186].

Additionally, increased expression levels of the Activating Transcription Factor 3 (*Atf3*) were observed in the monocyte, macrophage and cDC2 clusters (Fig. 19). *Atf3* encodes a transcription factor thought to negatively regulate the transcription of several pro-inflammatory cytokines[187]. Furthermore, the upregulation of *Atf3* in macrophages has been shown to induce a more anti-inflammatory state[188].

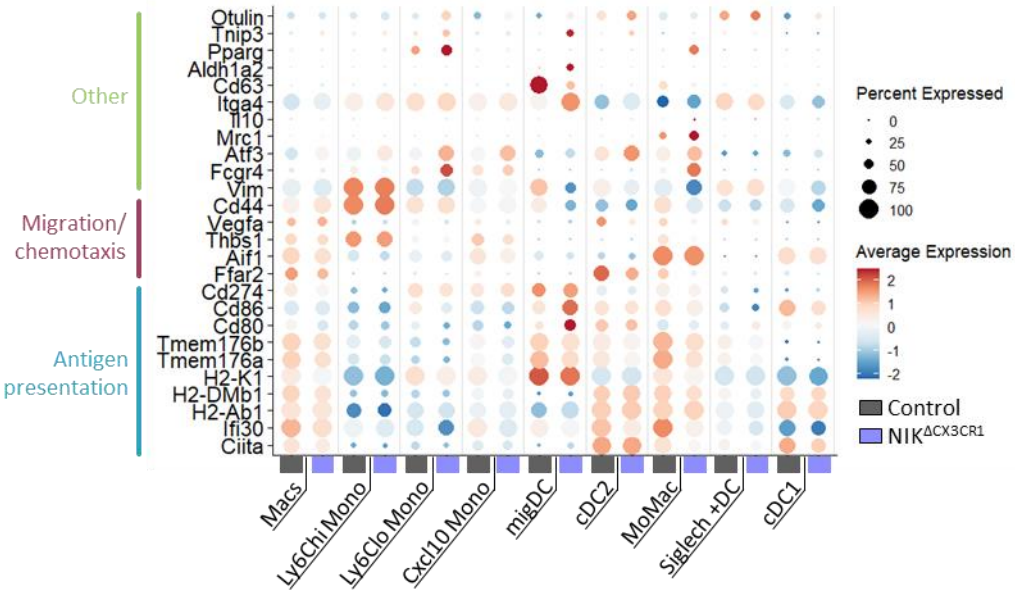

Figure 19: Differentially expressed genes (DEGs) between control and NIK$^{\Delta CX3CR1}$.

Dot plot displaying some selected DEGs (y-axis) and each myeloid cluster of control (grey) or NIK$^{\Delta CX3CR1}$ (lavender) on the x-axis. Average expression in red-high/blue-low gradient of DEGs and percentage of cells expressing said DEG visualised by circle size.

Interestingly, the observed differences in expression appear to be most pronounced in the moMac cluster. This suggests a shift in the inflammatory state of these cells, with the lower expression of *Cd80*/*Cd86* in moMacs indicating a potential shift towards an anti-inflammatory phenotype. This shift is further supported by the increased expression of known anti-inflammatory macrophage markers such as *Mrc1* (CD206) and *Pparg* [189,190] (Fig 19). These findings suggest that the moMacs in the NIK$^{\Delta CX3CR1}$ could play a more protective and suppressive role in EAE compared to the moMacs of control mice.

Since the nearest neighbourhood analysis showed the most differences in abundance within the migDC cluster, we looked a little more into the DEGs within this cluster. We found several genes which have a high expression in the migDC cluster of control mice but almost diminished expression in the migDCs from the NIK$^{\Delta CX3CR1}$ (Fig. 19). Among these, *Cd63* is noteworthy for encoding for a tetraspanin protein which interacts with MHCII in late endosomes and

lysosomes and might have a role in the regulation of endocytic trafficking and antigen presentation[191]. The gene *Vim* encodes a cytoskeletal protein that has been implicated in modulating dendritic cell migration and antigen presentation [192]. Its lower expression may affect the migratory capacity of dendritic cells and their ability to interact with T cells. Interestingly, despite the general trend of reduced gene expression, an upregulation of co-stimulatory genes *Cd80* and *Cd86* was observed in NIK$^{\Delta CX3CR1}$ migDCs, suggesting a more mature phenotype relative to controls (Fig. 19). However, this upregulation did not translate to increased protein levels five days post-immunization (Fig. 15).

One gene which is expressed highly in the migDCs in the NIK$^{\Delta CX3CR1}$ is *Itga4*, a subunit of the integrin Very Late Antigen-4 (VLA-4, α4β1), which is a cell adhesion molecule. It is a cell adhesion molecule that could play a role in the homing of cells into the LNs. It has been shown to play a role in the infiltration of cells into the CNS. Although Itga4 blocking has been found to be protective in EAE and MS, its exact role in dendritic cells remains unknown[193]. Another DEG which could be of interest to our phenotype is *Cd44*. It is known to play a crucial role in T cell activation and was found to be reduced by a lot in the migDCs of NIK$^{\Delta CX3CR1}$(Fig.20E). Previous studies have demonstrated that DCs increase their CD44 expression upon encountering antigens, a process vital for their migration to the T cell zone in the LNs and for the activation of CD4 T cells[194,195].

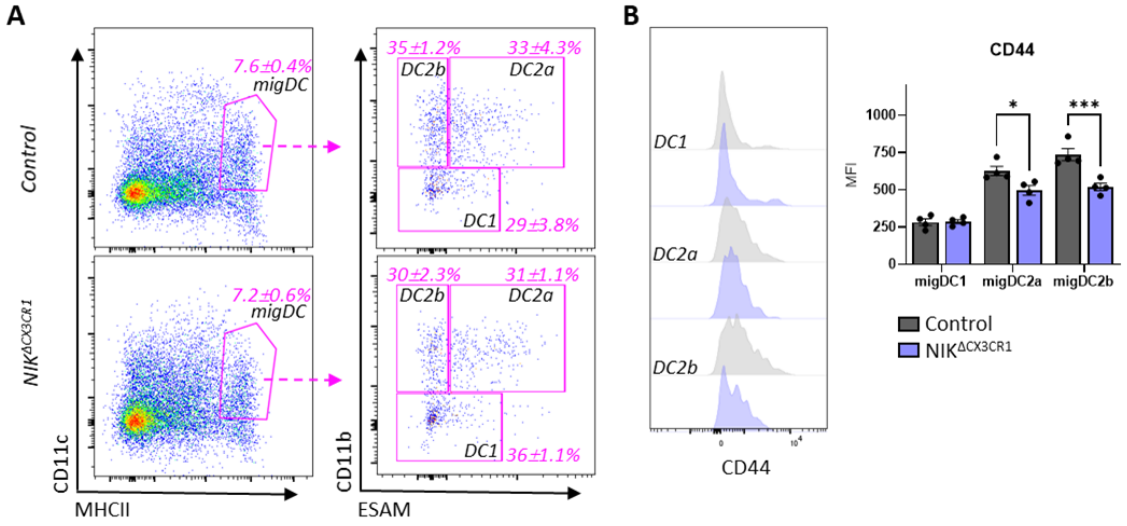

Figure 20: Reduced CD44 expression on migratory DC2s three days post MOG immunisation.

*(A) Gating strategy of MHCIIhighCD11cint migDCs which was gated further for CD11b+ESAM- migDC2b, CD11b+ESAM+ migDC2a and CD11b- migDC1. Mean percentage and SEM are shown in pink for each cluster (n=4 per group). Doublets, dead cells, CD3+/CD19+ cells, eosinophils and neutrophils were excluded. (B) Histogram and the median fluorescent intensity (MFI) of CD44 expression on migDC1, migDC2a and migDC2b. Data in graph B is shown as mean ± SEM and analysed using two-way ANOVA with Šídák's multiple comparisons test. *p < 0.05, **p < 0.01, ***p < 0.001.*

To confirm the decrease of CD44 protein on migDCs, we performed flow cytometry straining three days after MOG immunisation. We identified the migDCs by their high MHCII and intermediate CD11c expression and did not see a difference in the percentage. We used the markers CD11b and ESAM to gate further on migDC1(CD11b-), migDC2a(CD11b+ESAM+), and migDC2b(CD11b+ESAM-) and did not see any significant differences in the percentages of each population (Fig. 20A). Interestingly, when looking at the MFI of CD44 on these populations we could see a decrease in both migDC2a and migDC2b but not migDC1 (Fig. 20B). This confirms our scRNAseq data of decreased Cd44 expression, which could help explain the EAE phenotype.

3.2.7 Reduced production of IL-23 by myeloid cells when NIK is deleted in CX3CR1^{+} cells

Activation of the non-canonical pathway results in the production of several cytokines and chemokines, which are essential for the immune and stress response[133]. Unfortunately, we were unable to detect any mRNA for some of the cytokines we were interested in within our single-cell sequencing experiment. Therefore, we decided to perform an *in vitro* experiment to examine mRNA levels of different cytokines in myeloid cells (Fig. 21A). To achieve this, we isolated CD11b^{+} cells from the LNs and stimulated them for one or four hours with LPS, a bacterial protein which causes a pro-inflammatory response in myeloid cells[196], or anti-CD40, which will bind CD40 and activatea the non-canonical NF-kB pathway[132].

No significant differences were observed in the mRNA levels of the inflammatory cytokines *Il12a*, *Il6* and *Il1b* after stimulation with either anti-CD40 or LPS. However, there was a difference in the production of *Il23a* mRNA. In control cells, we noted an increase of *Il23a* mRNA after stimulating with anti-CD40. Conversely, myeloid cells from NIK-deficient mice exhibited a dramatic reduction of *Il23a* mRNA after both 1h and 4h stimulation (Fig. 21B). The reduction of *Il23a* is consistent with previously published data, where it was demonstrated that NIK in CD11c-positive cells is an essential regulator of IL-23 production[151,158]. Additionally, IL-23 is critical for the induction of EAE and can regulate T cell differentiation into T_H17s[151,197].

In addition to the decrease of *Il23a*, we also observed an increase of *Il10* mRNA 4h after LPS stimulation but not after anti-CD40 (Fig. 21B). IL-10 is an anti-inflammatory cytokine which has been shown to be protective during EAE[198–200]. This suggests that under inflammatory conditions, CD11b^{+} cells from NIK$^{\Delta CX3CR1}$ are more likely to produce the anti-inflammatory cytokine IL-10 rather than the pro-inflammatory IL-23. Together with our previous data, this could help explain the ameliorated EAE phenotype in the NIK$^{\Delta CX3CR1}$ mice.

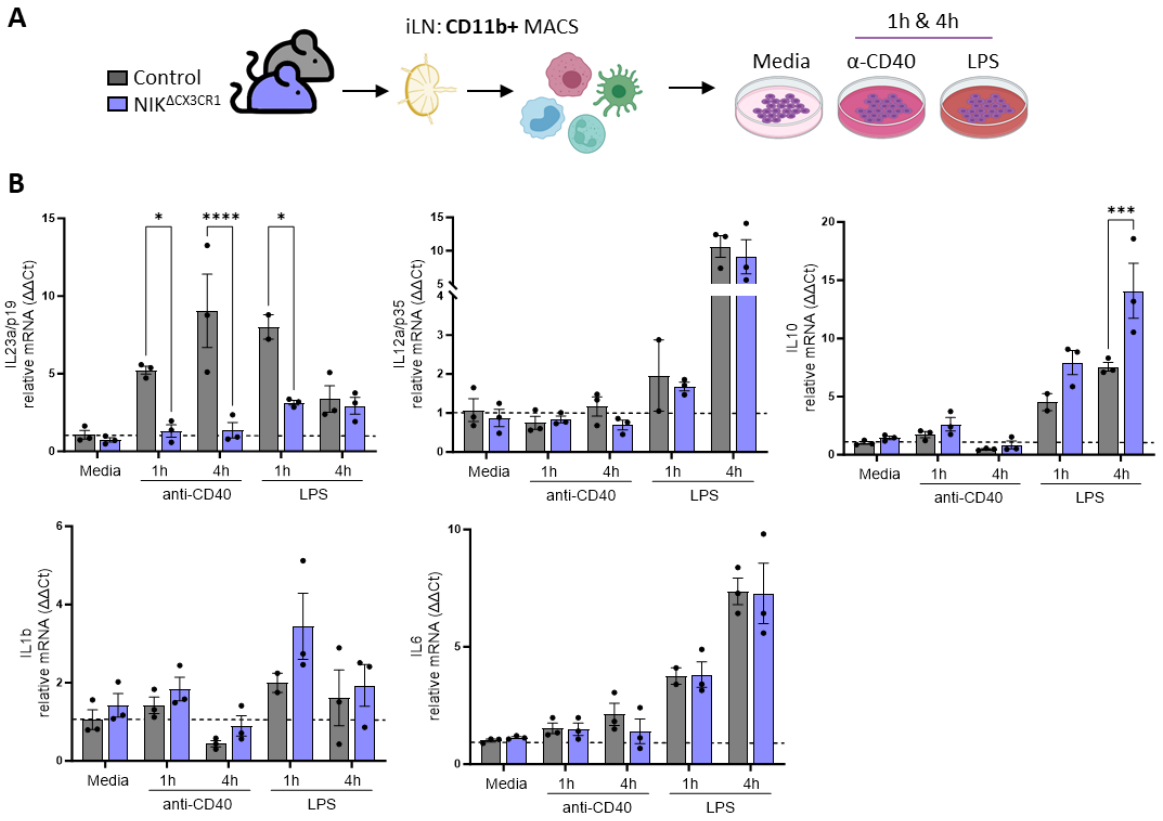

Figure 21: CD11b+ cells from NIK$^{\Delta CX3CR1}$ LNs are unable to produce Il23a mRNA after CD40 stimulation in vitro. *(A) CD11b+ cells were isolated from the LNs of NIK$^{\Delta CX3CR1}$ and littermate controls and were cultured with or without anti-(α)CD40 or LPS for 1 or 4 hours. (B) Relative mRNA levels of different cytokines after different stimulations. mRNA levels of each sample were normalised against the housekeeping gene HPRT and the media control of the corresponding cytokine. Dotted line shows the value of the media control. Data in graphs are shown as mean ± SEM and analysed using two-way ANOVA with Šídák's multiple comparisons test. *p < 0.05, **p < 0.01, ***p < 0.001, ****p < 0.0001.*

To investigate the hypothesis that the absence of IL-23 could account for our EAE phenotype, we opted to employ the passive transfer EAE model. In this experimental setup, cells extracted from the spleen and dLNs of immunised donor mice are cultured under conditions promoting encephalitogenic T_H17 development with the addition of IL-23, MOG and anti-IFNγ. These cells were then transferred into RAG$^{-/-}$ recipients, which are a type of genetically engineered mice that lack mature T and B cells due to a mutation in the *Rag1* gene (Fig. 22A). The aim was to observe whether T cells from immunised NIK$^{\Delta CX3CR1}$ mice would acquire encephalitogenic properties after culturing them with IL-23 and trigger EAE onset in the recipient mice. We could indeed see that the T cells from NIK$^{\Delta CX3CR1}$ donor mice were able to induce EAE in the RAG$^{-/-}$ recipients. However, when comparing the disease score to the recipients who received cells from control mice we could see a significantly reduced score (Fig. 22B). This decrease in score could also be seen when comparing the maximum score and the area under the curve (AUC; Fig. 22C-D). in addition, a significant difference in the time of onset was observed where the recipients receiving cells from NIK$^{\Delta CX3CR1}$ mice developed disease later compared to controls (Fig. 22E).

Our analysis revealed that during the peak of EAE, there were fewer CNS-infiltrating CD4⁺ T cells from NIK$^{\Delta CX3CR1}$ mice compared to controls(Fig. 22F). Interestingly, while a higher proportion of T cells in NIK$^{\Delta CX3CR1}$ mice were reactive to MOG, there were no observed differences in cytokine production from these cells (Fig. 22G-H). These findings suggest that after *in vitro* culture with IL-23, anti-IFNγ, and MOG, T cells from immunised NIK$^{\Delta CX3CR1}$ mice are partially able to induce EAE in RAG$^{-/-}$ recipients with a delayed onset of disease.

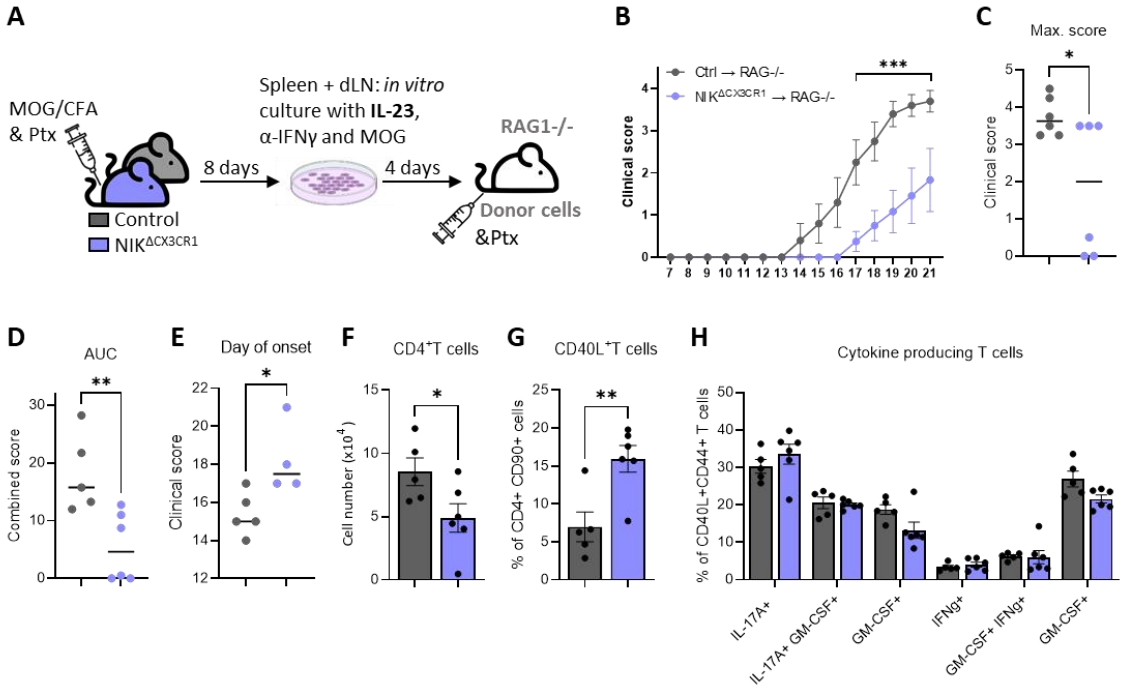

Figure 22: Culturing cells from immunised NIK$^{\Delta CX3CR1}$ mice with IL-23 before transferring into RAG$^{-/-}$ mice partially rescues the EAE phenotype.

*(A) control and NIK were immunised with MOG/CFA and Ptx cells from dLNs and spleen at 8 days post injection (dpi) and cultured for 4 days with MOG, IL-23, and anti-IFNγ before being injected into RAG-/- recipient mice. (B) EAE disease course. (C) Maximum EAE score. (D) Area under the curve (AUC). (E) Day of onset. (F) Total cell number of CNS-infiltrating CD4⁺CD90⁺ T cells during the peak of disease(21dpi). (G) Proportion of CD40L⁺ T cells from CD4⁺CD90⁺ T cells. The proportion of cytokine-producing cells from CD40L⁺ T cells. Data in graphs are shown as mean ± SEM and analysed using two-way ANOVA with Šídák's multiple comparisons test (B, H) or two-tailed unpaired Student's t test(C-G) . *p < 0.05, **p < 0.01, ***p < 0.001*

4.

DISCUSSION

Our research has demonstrated the essential role of NIK in the development of Siglec1^{+} macrophages in the spleen and LNs during steady state conditions. More interestingly, we have demonstrated that several changes occur after deleting NIK in CX3CR1-expressing cells, leading to protection against EAE. The myeloid cell compartment of NIK$^{\Delta CX3CR1}$ mice displays a dysregulation in genes associated with antigen presentation and migration, along with reduced IL-23 production. This results in decreased priming of T cells, leading to reduced production of the inflammatory cytokines IL-17A and, to some extent, GM-CSF. Notably, transferring *ex vivo* MOG/IL-23-activated T cells from immunised NIK$^{\Delta CX3CR1}$ mice into RAG$^{-/-}$ mice was able to recover disease susceptibility in donor mice, as seen by the development of clinical EAE scores, but still with a delayed onset and lower score compared to controls.

4.1 Siglec1^{+} macrophages of the LNs and spleen are dependent on NIK

While we only found minor changes within the DC subsets in the LNs of our NIK$^{\Delta CX3CR1}$ mice, we revealed that NIK$^{\Delta CX3CR1}$ mice lack Siglec1^{+} macrophages, namely the SCS macrophages in the LNs and MMMs in the spleen. This outcome is consistent with prior research on NIK$^{aly/aly}$ mice, which also lack Siglec1^{+} MMMs in the spleen[145]. Additionally, the deletion of RANK or LTβR on Siglec1^{+} cells, two known receptors of the non-canonical NF-κB pathway, also results in the loss of MMMs in the spleen and SSM in the LNs[149]. Our findings and the published data strongly suggests that the non-canonical pathway plays a pivotal role in the development and maintenance of these specific Siglec1^{+} macrophage populations. In line with the study by Camara et al., we observed an increase in F4/80^{+}Siglec1^{-} cells in both LNs and spleen. Our flow cytometry data further revealed an increase in monocytes. This is significant as circulating monocytes have the ability to differentiate into tissue-resident macrophages and replenish them during steady state, which could explain the rise in monocytes we observed[201]. We hypothesise that monocytes enter the LN tissue to replace the missing Siglec1^{+} macrophages. However, since NIK is crucial for the development of these Siglec1^{+} macrophages, monocytes that lack NIK are unable to differentiate into these specific Siglec1^{+} subsets and become F4/80^{+} macrophages instead. This underscores the importance of NIK in the differentiation and homeostasis of Siglec1^{+} macrophages, suggesting that NIK plays a key role in maintaining the balance of these macrophage populations during steady state conditions.

Siglec1 is a viral receptor[202], and the Siglec1^{+} macrophages have been shown to be essential for the immune response during viral infections and viral/antigen-clearing [148,149,203]. They are able to present antigen to B cells and cross-present to cDC1s but are generally considered to be dispensable for T cell responses [203–205]. In the context of EAE, it has been shown that the depletion of Siglec1^{+} cells before EAE induction resulted in normal EAE development[206]. Another study demonstrated that depleting Siglec1+ cells during the full course of EAE reduced the severity of EAE. However, they also show that circulating monocytes and macrophages express Siglec1, and the EAE phenotype is likely due to the loss of these circulating and CNS-infiltrating Siglec1^{+} monocytes[207]. We, therefore, hypothesise that Siglec1^{+} have minimal involvement during EAE and that the resistance we observe in our NIK mice is likely not due to the loss of these cells.

4.2 NIK in Microglia is redundant during EAE

While we did not observe any changes in microglia numbers during steady state, we did observe a slight reduction in the expression of some activation markers like MHCII and CD39 on microglia. This suggests that microglia do not depend on NIK and the non-canonical NF-κB pathway during homeostasis. However, microglia are multifunctional cells. Besides being the primary immune cell in the CNS, they also have functions that regulate neuronal circuits and synaptic pruning[208]. It would be worth exploring whether the deletion of NIK in microglia might affect these processes by investigating the neuronal populations and synapses during development.

Interestingly, a recent study also describing NIK-deficient microglia reported a significant decrease in disease symptoms and fewer infiltrating cells during the later phase of EAE[155]. While we did not observe significant differences during EAE in our mice that lack NIK in microglia, we did observe a similar trend where NIK$^{\Delta MG}$ mice had a decreased score during the recovery phase. However, it should be noted that our study only examined mice at the peak of EAE, during which we did not observe differences in microglia activation or infiltrating cells between NIK$^{\Delta MG}$ and controls. Similarly, Jie et al. (2021) did not report any differences during the peak of EAE but only at the later stages of EAE. Therefore, they hypothesise that NIK in microglia is essential for the second wave of infiltrating cells into the CNS[155]. Based on our data and the findings published by Jie et al., we can confidently conclude that microglia are unlikely to be involved in the resistance against EAE observed in the NIK$^{\Delta CX3CR1}$ mice. Our findings suggest that peripheral CX3CR1-expressing myeloid cells, which lack NIK, are the primary contributors to this resistance.

While both protective and detrimental roles for microglia have been proposed during EAE, it has been shown that microglial activation alone is not sufficient to drive the disease[101]. The recruitment of peripheral monocytes/macrophages and effector T cells to the CNS is necessary

for EAE onset, and the involvement of these different immune cells makes it difficult to fully understand the role of NIK in only microglia in this MS model. Therefore, it would be interesting to use a different model for MS that is less influenced by peripheral immune cells. One option would be the LPC model, which induces focal demyelination in the CNS by directly injecting LPC, a detergent-like compound, into specific brain or spinal cord areas, leading to localised myelin sheath disruption[209,210]. While the model is not dependent on the primary T cell response like EAE, T cells still contribute to activating macrophages and microglia[211]. However, LPC itself has also been shown to activate microglia directly, resulting in a pro-inflammatory response[212]. The cuprizone model is another widely used experimental method to study demyelination and remyelination processes in the CNS. Feeding cuprizone to rodents induces oligodendrocyte loss and subsequent myelin sheath degradation. Notably, unlike the EAE and LPC model, demyelination in the cuprizone model is not dependent on nor accompanied by a T cell-mediated immune response, allowing for the study of mechanisms of de- and remyelination without confounding superimposed inflammatory mechanisms[213,214].

Both of these models have been used to study microglia functions during the de- and remyelination processes, focussing on their protective and damaging properties[210]. Using these models on $NIK^{\Delta MG}$ mice might help us better understand the role of NIK in microglia in MS.

4.3 The Multifaceted Impact of NIK Deletion in DCs on EAE

The CX3CR1-Cre targets multiple cell populations, which include subpopulations of DCs, monocytes, macrophages, and microglia[75]. DCs are critical contributors to immune responses by bridging innate and adaptive immunity. However, the exact role of these cells in EAE is still debated. Studies depleting CD11c-expressing cells during EAE have shown mixed results on the role of DCs during EAE[127–129]. Interestingly, a study by Katakam et al., who utilised a cell-specific deletion of NIK in CD11c-positive cells, demonstrated that it is dispensable for $CD4^+$ T cell priming and EAE development[159]. This study led us to hypothesise that the effect in $NIK^{\Delta CX3CR1}$ mice was most likely not due to DCs but to CX3CR1 expressing cells, which were CD11c negative, like monocytes. However, in our hands, the deletion of NIK in CD11c-Cre resulted in a similar resistance against EAE as seen in the $NIK^{\Delta CX3CR1}$ mice. These results were confirmed by unpublished data from the lab of Burkhard Becher and are further supported by other published data showing a role for NIK in DCs during EAE[156,158]. The discrepancy may be due to differences in experimental protocols, particularly the concentration $MOG_{35–55}$, which was lower in our study. The high concentration of MOG used in the Katakam et al. study might be too high to see a difference in EAE scores.

Considering the similar EAE phenotype in both CD11c-Cre and CX3CR1-Cre mice, we considered the possibility that the effect might stem from $CX3CR1^+CD11c^+$ double-positive

cDC2s and moDCs. Both have been shown to be important in T cell priming, with moDCs promoting T_H polarisation and cDCs promoting T_H priming[124]. A recent study has demonstrated two cDC2 populations in the spleen and LNs of mice: T-bet$^+$ cDC2a and T-bet$^-$ cDC2b. This cDC2b subset expresses CX3CR1 and is shown to be more pro-inflammatory by producing higher levels of IL-6 and TNFα and is more potent in inducing T_H1 and T_H17 differentiation than cDC2a[118]. This suggests that the CX3CR1$^+$ moDC and cDC2b subsets might play a significant role in the observed EAE phenotype. We were unable to identify these subpopulations and most likely have both within the resDC2 cluster of our scRNA-seq data. This is likely also due to the low number of resDC2s in our samples. Furthermore, the cDC2s and moDCs share many markers, especially during inflammation, which makes them difficult to distinguish from each other[215].

The nearest neighbourhood analysis showed the most significant differences in the abundance of cell neighbourhoods within the migDC cluster. The migDC cluster appeared to be divided into two sub-clusters, one more abundant in NIK$^{\Delta CX3CR1}$ mice and the other more abundant in control mice. The increased abundance of one sub-cluster in NIK$^{\Delta CX3CR1}$ mice indicates that these migDCs might have distinct characteristics compared to those in control mice. We indeed were able to see the most DEGs within this migDC cluster, further suggesting distinct characteristics between the control and migDC clusters.

It could be due to the early time point after EAE induction that most of the changes were observed in this cluster since migDCs are some of the first responders to EAE induction[114,115]. Dermal DCs take up the MOG antigen at the injection site and migrate into the T cell zone of the dLN to present it to T cells and initiate T_H response, thereby regulating EAE disease[216]. Although we were unable to find a phenotypical difference associated with the DEGs in the migDC cluster that could help explain our phenotype, we were able to identify certain DEGs that might be involved in different functions, such as antigen presentation, migration and regulating the immune response.

We observed no difference in the percentage of migDCs in the dLNs at different stages of EAE. Additionally, our collaborator's unpublished research has indicated that migDCs from NIK$^{\Delta CD11c}$ mice retained their migration capabilities in an *in vitro* migration assay. Since the CD11c-Cre targets all DCs and the CX3CR1-Cre is only a subpopulation, we hypothesise that the migDCs in NIK$^{\Delta CX3CR1}$ mice would also not exhibit defects in their ability to migrate to the LNs. However, the reduced expression of CD44 suggests that while migDCs are able to migrate to the dLNs, they may struggle to enter the T cell zone and effectively prime T cells[194].

The upregulation of *Aldh1a2*, a key enzyme for generating retinoic acid, suggests that the NIK$^{\Delta CX3CR1}$ migDCs may be more tolerogenic[217]. Retinoic acid has been shown to down-regulate the antigen-presenting capacity of DCs, thereby regulating the T_H1 and T_H17 cell responses

during EAE[217,218]. This shift towards a more tolerogenic state could potentially dampen the inflammatory response, highlighting a novel aspect of how NIK deletion affects immune regulation in EAE. Further research is needed to elucidate the exact mechanisms by which NIK deletion alters migDC function and its implications for EAE pathogenesis.

4.4 Fewer Antigen-Presenting Cells and Their Impact on EAE

We were able to show a reduction in cell clusters that had a signature for antigen presentation in the $NIK^{\Delta CX3CR1}$ mice. This suggests that there were fewer APCs in the dLNs shortly after EAE induction in $NIK^{\Delta CX3CR1}$ mice, which could affect the priming of T cells. We further observed a decrease in the expression of genes involved in antigen processing and presentation in multiple myeloid clusters. The antigen processing and presentation steps are essential during the activation of the immune response during EAE, and any defects in these pathways could play a role in the development of the disease.

In our experiments, we immunised mice with the $MOG_{35–55}$ peptide, which has already been processed and is thought to be loaded directly on the MHCII molecule, skipping the antigen processing step. This would suggest that the DEGs associated with antigen processing might not affect EAE development and T cell priming. However, one of these genes, *Ifi30*, was decreased in most of our clusters. *Ifi30* encodes the gamma-interferon-inducible lysosomal thiol reductase (GILT), which catalyses the reduction of disulfide bonds during antigen processing and is constitutively expressed by many APCs. GILT in APCs has been shown to improve MHCII-restricted antigen presentation and modulate autoimmunity[219]. In the context of EAE, it has been shown that the lack of GILT in mice immunised with the $MOG_{35–55}$ epitope results in diminished clinical disease, suggesting that processing of the endogenous MOG protein is defective in these mice, which is unable to reduce thiol bonds[220]. Thus, the reduced expression of *Ifi30* and other genes involved in antigen presentation and processing in our study may contribute to the overall protection against EAE by impairing antigen processing and subsequent T cell activation.

Also, at the protein level, we observed a reduction in the co-stimulatory molecules CD80 and CD86 in certain APC clusters. These molecules bind to CD28 on T cells, providing the second signal required for T cell activation and proliferation[63]. This is a crucial step in T cell priming, and a decrease in these co-stimulatory molecules on APCs could further explain the reduction in T cell priming we saw before the onset of EAE.

We have observed multiple genes related to activation, antigen presentation and migration. However, we have not observed an apparent loss of these genes that could fully explain the resistance against EAE. We believe that in conjunction with the decrease in antigen-presenting macrophages and cDC2s, along with other subtle changes, this could result in reduced T cell

priming and reduced T_H17 and T_H1 cells. Ultimately, this could lead to resistance against EAE. However, one limitation of our scRNA-seq was that the sequencing was not deep enough to capture mRNA levels of immune regulatory cytokines and chemokines. It would have been beneficial to sort the cells beforehand to remove all neutrophils, B, T, and NK cells. Additionally, deeper sequencing with more reads per cell could provide valuable insights.

4.5 IL-23, an essential cytokine for EAE development.

The cytokine environment plays a crucial role in differentiating T cells into effector T cell subsets. We were able to demonstrate that NIK is essential for the production of *Il23a* mRNA. Previous studies have also confirmed the role of NIK in regulating IL-23 production[151,158]. Specifically, Jie et al. demonstrated that in a colitis model, NIK-activated non-canonical NF-κB triggers the expression of IL-23 in DCs, contributing to the maintenance of T_H17 cells in the gut[151]. IL-23 has further been shown to be indispensable for T cell differentiation into T_H17 cells and the development of EAE[151,197]. Furthermore, research by El-Behi et al. determined that IL-23 induces the production of GM-CSF in T_H17 cells, and GM-CSF production by T_H1 and T_H17 cells is necessary for EAE development[221]. We were indeed able to show the importance of IL-23 in a passive transfer EAE model, where T cells from immunised $NIK^{\Delta CX3CR1}$ mice were cultured with IL-23 before being transferred into $RAG^{-/-}$ mice. This resulted in the development of the disease, albeit with a delayed onset and lower score. This suggests that the lack of IL-23 production by NIK-deficient myeloid cells is at least partly responsible for the resistance observed in the active EAE model.

More interestingly, it has been shown that IL-23 is elevated in MS patients and correlates with T_H17 cells and disease, which makes it an interesting target for the treatment of MS[222]. Furthermore, the inhibition of IL-23 by using antisense oligonucleotides has been shown to down-regulate IL-23 and TNF-α production and up-regulate IL-10 production in moDC cultures from MS patients[223]. It will be fascinating to investigate further which CX3CR1-expressing cells produce IL-23 during EAE and how this production affects disease development. This could open up new avenues for understanding and potentially treating EAE and MS.

4.6 A switch towards a less inflammatory state

In addition to the observed reduction in APCs and the pro-inflammatory cytokine IL-23, our analysis revealed a significant increase in $Ly6C^{lo}$ monocytes within the dLNs of $NIK^{\Delta CX3CR1}$ mice following EAE induction. Typically found in the vasculature, these cells are known for their involvement in early responses to inflammation and tissue repair, constantly crawling along the lumen[98]. Research indicates that $Ly6C^{hi}$ monocytes can differentiate into $Ly6C^{lo}$ monocytes and $Ly6C^{lo}$ macrophages, which are able to infiltrate into the tissue[75,224,225]. The population identified as $Ly6C^{lo}$ monocytes in our study may represent $Ly6C^{lo}$ macrophages or cells in the

transition phase towards becoming Ly6C^{lo} macrophages, as evidenced by the expression of the macrophage marker *Adgre1* (F4/80). Notably, Ly6C^{lo} macrophages have been described as both protective and inflammatory in the context of various disease models[226]. For instance, they have been shown to resolve sciatic nerve injury through efferocytosis[227] and have an anti-inflammatory state in allergic skin and arthritis mouse models[228,229]. Interestingly, we were able to demonstrate an increase in genes associated with anti-inflammatory macrophage in both the Ly6C^{lo} monocyte and the moMac clusters (*Atf3*, *Mrc1*, *Pparg2*, *Il10*) in our scRNA-seq. In addition, *in vitro* stimulation of myeloid cells led to an increase in *Il10* mRNA in our NIK$^{\Delta CX3CR1}$ mice. These anti-inflammatory macrophages might provide a more anti-inflammatory environment, suppressing the activation of other myeloid cells and T cells.

For our studies on myeloid cells, we mainly focused on early time points (3-5 dpi) since this is when the initial activation and priming of T cells starts in the dLNs. However, studies have shown that monocytes and moDCs/moMacs start increasing in percentage in the dLNs and CNS around day six[105]. We did not observe any significant changes in the distribution of these cells at later points in the dLNs (data not shown). However, it might be interesting to investigate whether the lack of NIK in monocytes and monocyte-derived cells affects cell percentage in the CNS or polarises these cell types toward more anti-inflammatory phenotypes at later time points in the dLNs and CNS.

These results suggest that NIK could be involved in the differentiation of Ly6C^{hi} monocytes into macrophages with an antigen-presentation signature during autoimmune inflammation. However, it could also be a secondary effect of the less inflammatory environment.

4.7 Improving cell-specific targeting: options beyond CX3CR1-cre

We have discussed here how the deletion of NIK affects many different cell types in the NIK$^{\Delta CX3CR1}$ mice during EAE. Whether these effects are directly due to the deletion of NIK or due to the environment is unknown. Furthermore, the use of the CX3CR1-cre targets many different subsets, which include subsets of NK and CD8 T cells[75].

To further explore the role of NIK in these different subsets, it would be interesting to use different cre lines to target cDC2s or monocytes specifically. It has been published that MHCII on CCR2-expressing cells is essential during the induction phase of EAE[105]. CCR2 is expressed by similar cells expressing CX3CR1 such as inflammatory monocytes, monocyte-derived APCs, and cDC2s, but excludes tissue-resident macrophages. Deleting NIK with the CCR2-CreERT2 could aid in understanding of whether these cells depend on NIK during EAE. However, more monocyte-specific Cre-line, like Ms4a3-Cre, would be a good option for investigating the role of NIK during EAE in monocytes and monocyte-derived cells. This Cre-line would exclude the cDC2s, tissue-resident macrophages, and other CX3CR1-expressing cells but would include granulocytes, like neutrophils[230].

It is worth noting that the CD11c-cre, commonly used to target cDCs, also targets macrophage and monocyte populations and in a small population of NK, T, and B cells[231]. A study by Loschko et al. has described the *Zbtb46*-Cre, which is expressed by pre-DCs and targets cDC1 and cDC2s with little or no targeting of macrophages and other cells[232,233]. However, for our study, it would be interesting to have the NIK deletion specifically in the cDC2 population, which we hypothesise might be responsible for the priming of T cells after EAE induction. While there are many Cre-lines available to target cDC1s, none are available for cDC2s[231], most likely due to the heterogeneity of this subset and the many markers they share with monocytes and macrophages.

The migDCs are another population that is affected by the NIK deletion during EAE and might be at least partly responsible for the EAE resistance in the $NIK^{\Delta CX3CR1}$ mice. Targeting these cells with the Langerin-Cre, which is expressed by langerin$^+$ Langerhans cells and epidermal DCs[234], would be a great way to explore the role of NIK in these cells during the early stages of EAE.

Investigating the role of NIK using different Cre lines during EAE would provide valuable insights into the specific functions of NIK in various cell types. However, it is likely that the observed protection against EAE in $NIK^{\Delta CX3CR1}$ mice (and $NIK^{\Delta CD11c}$) results from the cumulative effect of NIK deletion across these multiple cell types (cDC2s, moDCs, monocytes, etc). Therefore, studying these different Cre lines could elucidate the distinct and combined contributions of each cell type to the overall protective effect, enhancing our understanding of the role of NIK in EAE pathogenesis and its potential as a therapeutic target.

4.8 NIK as a potential target in MS

Given its role as a key regulator in the non-canonical NF-κB pathway, which is involved in immune regulation and inflammation, targeting NIK represents a novel therapeutic strategy for MS and other autoimmune diseases. Under normal conditions, NIK levels are kept low in most cell types, which helps maintain cellular homeostasis. The fact that mice and humans with mutations in NIK can survive suggests that NIK is not essential for life, making it a viable target for therapeutic intervention without causing severe systemic effects. This characteristic makes NIK an attractive target for treating autoimmune diseases, where precise modulation of the immune response is required.

Recent research has highlighted the potential of NIK inhibition in various therapeutic contexts[235]. For example, NIK inhibition has shown promise as a target for cancer therapy due to its role in cell survival and proliferation[236]. Moreover, NIK inhibitors have been suggested for the treatment of sepsis, given their ability to modulate inflammatory responses[237]. Notably, a genome-wide association study identified NIK as a susceptibility gene for MS, directly linking it to the pathogenesis of this autoimmune disease[23]. This suggests that NIK inhibitors could be

a potential therapeutic intervention during MS pathology, offering a ray of hope in the treatment of autoimmune diseases.

Our study demonstrates that NIK is crucial during the initial phase of EAE development and that deleting NIK in CX3CR1 cells prevents the disease in mice. However, MS is typically diagnosed only after symptoms appear, by which time inflammation has already commenced in the CNS. Consequently, it would be valuable to investigate the effects of deleting NIK after the initial priming phase, either through the inducible CX3CR1-CreERT2 system or by using NIK inhibitors. This research could potentially lead to significant advancements in the treatment of autoimmune diseases, underscoring the urgency of further research in this area.

4.9 Conclusion

In conclusion, our investigation into the resistance of our mice against EAE has revealed a multitude of subtle changes within the myeloid cell compartment. The observed reduction in APCs and reduced expression of activation markers such as CD80 may account for the decrease in T cell priming, while the diminished production of *Il23a* mRNA in myeloid cells following stimulation could explain the decrease in encephalitogenic T_H17 cells. Additionally, an increase of $Ly6C^{lo}$ monocytes/macrophages was observed during both steady state and after EAE induction. These $ly6C^{lo}$ monocytes/macrophages have a more tissue repair-oriented phenotype and may play a protective role during EAE. These findings suggest that a complex signature of subtle changes collectively contributes to the significant effect of EAE resistance in our mice. Moreover, this highlights the intricate nature of the immune system and the pathophysiology of diseases such as MS, emphasising the multifactorial nature of immune responses and disease pathology. Recognising the interconnected factors involved in autoimmune conditions highlights the necessity for a comprehensive and multifaceted approach to understanding and addressing diseases like MS.

5.

SUMMARY

The NF-κB inducing kinase (NIK) is a primary stimulator of the non-canonical NF-κB signalling pathway, which regulates many aspects of the immune response. Mutations in the NIK/Map3k14 gene have been associated with various autoimmune diseases, including multiple sclerosis (MS) and mice with germline deletion of NIK are resistant to experimental autoimmune encephalomyelitis (EAE). We found that NIK has a minimal effect on the number and activation state of microglia in the CNS during steady state. However, the $NIK^{\Delta CX3CR1}$ mice lack a specific $CD169^{+}$ macrophage population in the spleen and LNs, suggesting an essential role for the non-canonical NF-κB pathway in the development and maintenance of cells. More interestingly, our research revealed that $NIK^{\Delta CX3CR1}$ mice exhibit resistance to EAE, with fewer immune cells infiltrating the CNS and a reduced number of activated microglia. Intriguingly, when NIK is selectively deleted in microglia using the tamoxifen-inducible CX3CR1-CreERt2 line ($NIK^{\Delta MG}$), the resistance against EAE diminishes. This suggests that the protective effects observed in $NIK^{\Delta CX3CR1}$ mice are not due to the absence of NIK in microglia but rather in other peripheral CX3CR1-positive cells. We further observed a reduction in the priming of T cells in the dLNs before the onset of EAE in the $NIK^{\Delta CX3CR1}$ mice. The myeloid cell compartment of $NIK^{\Delta CX3CR1}$ mice displayed a dysregulation in genes associated with antigen presentation and migration, along with reduced IL-23 production. Given the crucial role of IL-23 in EAE, we hypothesised that the reduced levels of IL-23 in the $NIK^{\Delta CX3CR1}$ mice could be responsible for protection against EAE. Indeed, stimulating cells from MOG-immunised $NIK^{\Delta CX3CR1}$ mice with IL-23 before transferring them to $RAG^{-/-}$ mice partly restored the EAE in these mice.

Our findings indicate that NIK plays a critical role in the development and function of certain macrophages during steady state and has a crucial role in the progression of EAE by regulating many aspects of myeloid cell activation. The multitude of subtle changes within the myeloid cell compartment, such as alterations in antigen presentation genes, reduced IL-23 production, and upregulation of anti-inflammatory genes, collectively contribute to the significant EAE resistance observed in our mice. These insights provide a deeper understanding of the intricate mechanisms of immune regulation by NIK and highlight potential therapeutic targets for autoimmune diseases such as MS, offering a ray of hope for future treatments.

6.

ZUSAMMENFASSUNG

Die NF-κB-induzierende Kinase (NIK) ist ein primärer Stimulator des nicht-kanonischen NF-κB-Signalwegs, der viele Aspekte der Immunreaktion reguliert. Mutationen im NIK/*Map3k14*-Gen wurden mit verschiedenen Autoimmunerkrankungen in Verbindung gebracht, darunter auch mit Multipler Sklerose (MS), und Mäuse mit einer Keimbahndeletion von NIK sind resistent gegen experimentelle autoimmune Enzephalomyelitis (EAE). Wir haben herausgefunden, dass NIK nur einen minimalen Einfluss auf die Anzahl und den Aktivierungszustand der Mikroglia im ZNS im Ruhezustand hat. Allerdings fehlt den $NIK^{\Delta CX3CR1}$-Mäusen eine spezifische $CD169^{+}$ Makrophagenpopulation in der Milz und den Lymphknoten, was auf eine wesentliche Rolle des nicht-kanonischen NF-κB-Signalwegs bei der Entwicklung und Erhaltung von Zellen hindeutet.

Noch interessanter ist, dass unsere Forschung ergab, dass $NIK^{\Delta CX3CR1}$-Mäuse eine Resistenz gegen EAE aufweisen, wobei weniger Immunzellen in das ZNS eindringen und die Zahl der aktivierten Mikroglia reduziert ist. Interessanterweise nimmt die Resistenz gegen EAE ab, wenn NIK selektiv in Mikroglia unter Verwendung der Tamoxifen-induzierbaren CX3CR1-CreERt2-Linie ($NIK^{\Delta MG}$) entfernt wird. Dies deutet darauf hin, dass die in $NIK^{\Delta CX3CR1}$-Mäusen beobachtete schützende Wirkung nicht auf das Fehlen von NIK in Mikroglia, sondern in anderen peripheren CX3CR1-positiven Zellen zurückzuführen ist. Darüber hinaus beobachteten wir in den $NIK^{\Delta CX3CR1}$-Mäusen eine Verringerung des Primings von T-Zellen in den dLNs vor dem Ausbruch der EAE. Das myeloische Zellkompartiment der $NIK^{\Delta CX3CR1}$-Mäuse wies eine Dysregulation in Genen auf, die mit der Antigenpräsentation und migration zusammenhängen, sowie eine verminderte IL-23-Produktion. Angesichts der entscheidenden Rolle von IL-23 bei EAE stellten wir die Hypothese auf, dass die verringerte IL-23-Produktion in $NIK^{\Delta CX3CR1}$-Mäusen für den Schutz vor EAE verantwortlich sein könnte. Tatsächlich führte die Stimulierung von Zellen aus MOG-immunisierten $NIK^{\Delta CX3CR1}$-Mäusen mit IL-23 vor dem Transfer in $RAG^{-/-}$-Mäuse zu einer teilweisen Wiederherstellung der EAE in diesen Mäusen.

Unsere Ergebnisse deuten darauf hin, dass NIK eine kritische Rolle bei der Entwicklung und Funktion bestimmter Makrophagen während der Homöostase spielt und eine entscheidende Rolle beim Fortschreiten der EAE einnimmt, indem es viele Aspekte der myeloischen Zellaktivierung reguliert. Die Vielzahl subtiler Veränderungen innerhalb des myeloischen Zellkompartiments, wie z. B. Veränderungen in den Genen für die Antigenpräsentation, eine verringerte IL-23-Produktion und die Hochregulierung entzündungshemmender Gene, tragen gemeinsam zu der bei unseren Mäusen beobachteten signifikanten EAE-Resistenz bei. Diese

Erkenntnisse ermöglichen ein tieferes Verständnis der komplizierten Mechanismen der Immunregulierung durch NIK und weisen auf potenzielle therapeutische Ziele für Autoimmunerkrankungen wie MS hin, die einen Hoffnungsschimmer für künftige Behandlungen darstellen.

7.

REFERENCES

1. GITTO, L. Living with Multiple Sclerosis in Europe: Pharmacological Treatments, Cost of Illness, and Health-Related Quality of Life Across Countries. in *Multiple Sclerosis: Perspectives in Treatment and Pathogenesis* 17–37 (Codon Publications, 2017). doi:10.15586/codon.multiplesclerosis.2017.ch2.

2. Walton, C. *et al.* Rising prevalence of multiple sclerosis worldwide: Insights from the Atlas of MS, third edition. *Multiple Sclerosis Journal* **26**, 1816–1821 (2020).

3. Steinman, L. Assessment of animal models for MS and demyelinating disease in the design of rational therapy. *Neuron* vol. 24 511–514 Preprint at https://doi.org/10.1016/S0896-6273(00)81107-1 (1999).

4. Dobson, R. & Giovannoni, G. Multiple sclerosis – a review. *European Journal of Neurology* vol. 26 27–40 Preprint at https://doi.org/10.1111/ene.13819 (2019).

5. Baecher-Allan, C., Kaskow, B. J. & Weiner, H. L. Multiple Sclerosis: Mechanisms and Immunotherapy. *Neuron* vol. 97 742–768 Preprint at https://doi.org/10.1016/j.neuron.2018.01.021 (2018).

6. Dendrou, C. A., Fugger, L. & Friese, M. A. Immunopathology of multiple sclerosis. *Nature Reviews Immunology* vol. 15 545–558 Preprint at https://doi.org/10.1038/nri3871 (2015).

7. Ford, H. Clinical presentation and diagnosis of multiple sclerosis. *Clinical Medicine, Journal of the Royal College of Physicians of London* **20**, 380–383 (2020).

8. Hemmer, B., Kerschensteiner, M. & Korn, T. Role of the innate and adaptive immune responses in the course of multiple sclerosis. *The Lancet Neurology* vol. 14 406–419 Preprint at https://doi.org/10.1016/S1474-4422(14)70305-9 (2015).

9. Lassmann, H. Multiple sclerosis pathology. *Cold Spring Harbor Perspectives in Medicine* vol. 8 Preprint at https://doi.org/10.1101/cshperspect.a028936 (2018).

10. Kunkl, M., Frascolla, S., Amormino, C., Volpe, E. & Tuosto, L. T Helper Cells: The Modulators of Inflammation in Multiple Sclerosis. *Cells* vol. 9 Preprint at https://doi.org/10.3390/cells9020482 (2020).

11. Volpe, E., Battistini, L. & Borsellino, G. Advances in T Helper 17 Cell Biology: Pathogenic Role and Potential Therapy in Multiple Sclerosis. *Mediators Inflamm* **2015**, 475158 (2015).

12. Kaskow, B. J. & Baecher-Allan, C. Effector t cells in multiple sclerosis. *Cold Spring Harb Perspect Med* **8**, (2018).

13. Cruciani, C. *et al.* T-Cell Specificity Influences Disease Heterogeneity in Multiple Sclerosis. *Neurology(R) neuroimmunology & neuroinflammation* **8**, (2021).

14. Comi, G. *et al.* Role of B Cells in Multiple Sclerosis and Related Disorders. *Annals of Neurology* vol. 89 13–23 Preprint at https://doi.org/10.1002/ana.25927 (2021).

15. Healy, L. M., Stratton, J. A., Kuhlmann, T. & Antel, J. The role of glial cells in multiple sclerosis disease progression. *Nat Rev Neurol* **18**, 237–248 (2022).

16. Luo, C. *et al.* The role of microglia in multiple sclerosis. *Neuropsychiatric Disease and Treatment* vol. 13 1661–1667 Preprint at https://doi.org/10.2147/NDT.S140634 (2017).

17. Benveniste, E. N. Role of macrophages/microglia in multiple sclerosis and experimental allergic encephalomyelitis. *J Mol Med* **75**, 165–173 (1997).

18. Zrzavy, T. *et al.* Loss of 'homeostatic' microglia and patterns of their activation in active multiple sclerosis. *Brain* **140**, 1900–1913 (2017).

19. Stys, P. K., Zamponi, G. W., Van Minnen, J. & Geurts, J. J. G. Will the real multiple sclerosis please stand up? *Nature Reviews Neuroscience 2012 13:7* **13**, 507–514 (2012).

20. Titus, H. E. *et al.* Pre-clinical and Clinical Implications of "Inside-Out" vs. "Outside-In" Paradigms in Multiple Sclerosis Etiopathogenesis. *Frontiers in Cellular Neuroscience* vol. 14 Preprint at https://doi.org/10.3389/fncel.2020.599717 (2020).

21. Olsson, T., Barcellos, L. F. & Alfredsson, L. Interactions between genetic, lifestyle and environmental risk factors for multiple sclerosis. *Nature Reviews Neurology* vol. 13 26–36 Preprint at https://doi.org/10.1038/nrneurol.2016.187 (2016).

22. Hussman, J. P. *et al.* GWAS analysis implicates NF-κB-mediated induction of inflammatory T cells in multiple sclerosis. *Genes Immun* **17**, 305–312 (2016).

23. Beecham, A. H. *et al.* Analysis of immune-related loci identifies 48 new susceptibility variants for multiple sclerosis. *Nat Genet* **45**, 1353–1362 (2013).

24. Sintzel, M. B., Rametta, M. & Reder, A. T. Vitamin D and Multiple Sclerosis: A Comprehensive Review. *Neurology and Therapy* vol. 7 59–85 Preprint at https://doi.org/10.1007/s40120-017-0086-4 (2018).

25. Soldan, S. S. & Lieberman, P. M. Epstein–Barr virus and multiple sclerosis. *Nature Reviews Microbiology* vol. 21 51–64 Preprint at https://doi.org/10.1038/s41579-022-00770-5 (2023).

26. Bar-Or, A. *et al.* Epstein–Barr Virus in Multiple Sclerosis: Theory and Emerging Immunotherapies. *Trends in Molecular Medicine* vol. 26 296–310 Preprint at https://doi.org/10.1016/j.molmed.2019.11.003 (2020).

27. Bjornevik, K., Münz, C., Cohen, J. I. & Ascherio, A. Epstein–Barr virus as a leading cause of multiple sclerosis: mechanisms and implications. *Nat Rev Neurol* **19**, 160–171 (2023).

28. Bjornevik, K. *et al.* Longitudinal analysis reveals high prevalence of Epstein-Barr virus associated with multiple sclerosis. *Science (1979)* **375**, 296–301 (2022).

29. Yang, J. H., Rempe, T., Whitmire, N., Dunn-Pirio, A. & Graves, J. S. Therapeutic Advances in Multiple Sclerosis. *Front Neurol* **13**, 824926 (2022).

30. Filipi, M. & Jack, S. Interferons in the Treatment of Multiple Sclerosis: A Clinical Efficacy, Safety, and Tolerability Update. *Int J MS Care* **22**, 165–172 (2020).

31. Krämer, J., Bar-Or, A., Turner, T. J. & Wiendl, H. Bruton tyrosine kinase inhibitors for multiple sclerosis. *Nat Rev Neurol* **19**, 289–304 (2023).

32. McGinley, M. P. & Cohen, J. A. Sphingosine 1-phosphate receptor modulators in multiple sclerosis and other conditions. *The Lancet* vol. 398 1184–1194 Preprint at https://doi.org/10.1016/S0140-6736(21)00244-0 (2021).

33. Brandstadter, R. & Katz Sand, I. The use of natalizumab for multiple sclerosis. *Neuropsychiatr Dis Treat* **13**, 1691–1702 (2017).

34. Miyazaki, Y. & Niino, M. B-cell depletion therapy for multiple sclerosis. *Immunological Medicine* vol. 45 54–62 Preprint at https://doi.org/10.1080/25785826.2021.1952543 (2022).

35. Kornek, B. *et al.* Multiple Sclerosis and Chronic Autoimmune Encephalomyelitis : A Comparative Quantitative Study of Axonal Injury in Active, Inactive, and Remyelinated Lesions. *Am J Pathol* **157**, 267 (2000).

36. Uchimura, I. & Shiraki, H. A contribution to the classification and the pathogenesis of demylelinating excephalomyelitis: With special reference to the centirm, nervoos system lesions caused by preventive inoculation against rabies. *J Neuropathol Exp Neurol* **16**, 139–208 (1957).

37. Stuart, G. & Krikorian, K. S. The neuro-paralytic accidents of anti-rabies treatment. *Ann Trop Med Parasitol* **22**, 327–377 (1928).

38. Rivers, T. M., Sprunt, D. H. & Berry, G. P. Observations on attempts to produce acute disseminated encephalomyelitis in monkeys. *Journal of Experimental Medicine* **58**, 39–52 (1933).

39. Kipp, M., Nyamoya, S., Hochstrasser, T. & Amor, S. Multiple sclerosis animal models: a clinical and histopathological perspective. *Brain Pathology* vol. 27 123–137 Preprint at https://doi.org/10.1111/bpa.12454 (2017).

40. Lassmann, H. & Bradl, M. Multiple sclerosis: experimental models and reality. *Acta Neuropathologica* vol. 133 223–244 Preprint at https://doi.org/10.1007/s00401-016-1631-4 (2017).

41. Baker, D. & Amor, S. Experimental autoimmune encephalomyelitis is a good model of multiple sclerosis if used wisely. *Multiple Sclerosis and Related Disorders* vol. 3 555–564 Preprint at https://doi.org/10.1016/j.msard.2014.05.002 (2014).

42. Constantinescu, C. S., Farooqi, N., O'Brien, K. & Gran, B. Experimental autoimmune encephalomyelitis (EAE) as a model for multiple sclerosis (MS). *British Journal of Pharmacology* vol. 164 1079–1106 Preprint at https://doi.org/10.1111/j.1476-5381.2011.01302.x (2011).

43. Lu, C. *et al.* Pertussis toxin induces angiogenesis in brain microvascular endothelial cells. *J Neurosci Res* **86**, 2624–2640 (2008).

44. Jansson, L., Olsson, T., Höjeberg, B. & Holmdahl, R. Chronic experimental autoimmune encephalomyelitis induced by the 89-101 myelin basic protein peptide in B10RIII (H-2r) mice. *Eur J Immunol* **21**, 693–9 (1991).

45. J. van der Star, B. *et al.* In Vitro and In Vivo Models of Multiple Sclerosis. *CNS Neurol Disord Drug Targets* **11**, 570–588 (2012).

46. Bernard, C. C. A. EXPERIMENTAL AUTOIMMUNE ENCEPHALO-MYELITIS IN MICE: GENETIC CONTROL OF SUSCEPTIBILITY. *Int J Immunogenet* **3**, 263–274 (1976).

47. PATERSON, P. Y. Transfer of allergic encephalomyelitis in rats by means of lymph node cells. *J Exp Med* **111**, 119–136 (1960).

48. Ben-Nun, A., Wekerle, H. & Cohen, I. R. The rapid isolation of clonable antigen-specific T lymphocyte lines capable of mediating autoimmune encephalomyelitis. *Eur J Immunol* **11**, 195–199 (1981).

49. Ben-nun, A., Wekerle, H. & Cohen, I. R. Vaccination against autoimmune encephalomyelitis with T-lymphocite line cells reactive against myelin basic protein. *Nature* **292**, 60–61 (1981).

50. Gold, R., Linington, C. & Lassmann, H. Understanding pathogenesis and therapy of multiple sclerosis via animal models: 70 Years of merits and culprits in experimental autoimmune encephalomyelitis research. *Brain* vol. 129 1953–1971 Preprint at https://doi.org/10.1093/brain/awl075 (2006).

51. Ben-nun, A. *et al.* From classic to spontaneous and humanized models of multiple sclerosis : Impact on understanding pathogenesis and drug development. *J Autoimmun* (2014) doi:10.1016/j.jaut.2014.06.004.

52. Jensen, P. E. Recent advances in antigen processing and presentation. *Nature Immunology* vol. 8 1041–1048 Preprint at https://doi.org/10.1038/ni1516 (2007).

53. Hewitt, E. W. The MHC class I antigen presentation pathway: Strategies for viral immune evasion. *Immunology* vol. 110 163–169 Preprint at https://doi.org/10.1046/j.1365-2567.2003.01738.x (2003).

54. Roche, P. A. & Furuta, K. The ins and outs of MHC class II-mediated antigen processing and presentation. *Nat Rev Immunol* **15**, 203–216 (2015).

55. Pishesha, N., Harmand, T. J. & Ploegh, H. L. A guide to antigen processing and presentation. *Nat Rev Immunol* **22**, 751–764 (2022).

56. Stuart, L. M. & Ezekowitz, R. A. B. Phagocytosis: Elegant complexity. *Immunity* vol. 22 539–550 Preprint at https://doi.org/10.1016/j.immuni.2005.05.002 (2005).

57. Tse, S. M. L. *et al.* Differential role of actin, clathrin, and dynamin in Fcγ receptor-mediated endocytosis and phagocytosis. *Journal of Biological Chemistry* **278**, 3331–3338 (2003).

58. Neefjes, J., Jongsma, M. L. M., Paul, P. & Bakke, O. Towards a systems understanding of MHC class i and MHC class II antigen presentation. *Nature Reviews Immunology* vol. 11 823–836 Preprint at https://doi.org/10.1038/nri3084 (2011).

59. Sanderson, F. *et al.* Accumulation of HLA-DM, a regulator of antigen presentation, in MHC class II compartments. *Science* **266**, 1566–9 (1994).

60. Vyas, J. M., Van Der Veen, A. G. & Ploegh, H. L. The known unknowns of antigen processing and presentation. *Nature Reviews Immunology* vol. 8 607–618 Preprint at https://doi.org/10.1038/nri2368 (2008).

61. Bretscher, P. A. A two-step, two-signal model for the primary activation of precursor helper T cells. *Proc Natl Acad Sci U S A* **96**, 185–190 (1999).

62. Chitnis, T. & Khoury, S. J. Role of costimulatory pathways in the pathogenesis of multiple sclerosis and experimental autoimmune encephalomyelitis. *Journal of Allergy and Clinical Immunology* vol. 112 837–849 Preprint at https://doi.org/10.1016/j.jaci.2003.08.025 (2003).

63. Magee, C. N., Boenisch, O. & Najafian, N. The role of costimulatory molecules in directing the functional differentiation of alloreactive T helper cells. *American Journal of Transplantation* vol. 12 2588–2600 Preprint at https://doi.org/10.1111/j.1600-6143.2012.04180.x (2012).

64. Chastain, E. M. L., Duncan, D. S., Rodgers, J. M. & Miller, S. D. The role of antigen presenting cells in multiple sclerosis. *Biochimica et Biophysica Acta - Molecular Basis of Disease* vol. 1812 265–274 Preprint at https://doi.org/10.1016/j.bbadis.2010.07.008 (2011).

65. Kenneth, M., Weaver, C. *Janeway ' S 9 Th Edition*. *America* (2017).

66. Guilliams, M., Mildner, A. & Yona, S. Review Developmental and Functional Heterogeneity of Monocytes. *Immunity* **49**, 595–613 (2018).

67. Ginhoux, F. & Jung, S. Monocytes and macrophages: Developmental pathways and tissue homeostasis. *Nature Reviews Immunology* vol. 14 392–404 Preprint at https://doi.org/10.1038/nri3671 (2014).

68. Hettinger, J. *et al.* Origin of monocytes and macrophages in a committed progenitor. *Nat Immunol* **14**, 821–830 (2013).

69. Puhr, S., Lee, J., Zvezdova, E., Zhou, Y. J. & Liu, K. Dendritic cell development-History, advances, and open questions. *Seminars in Immunology* vol. 27 388–396 Preprint at https://doi.org/10.1016/j.smim.2016.03.012 (2015).

70. Naik, S. H. *et al.* Diverse and heritable lineage imprinting of early haematopoietic progenitors. *Nature* **496**, 229–232 (2013).

71. Velten, L. *et al.* Human haematopoietic stem cell lineage commitment is a continuous process. *Nat Cell Biol* **19**, 271–281 (2017).

72. Perié, L. & Duffy, K. R. Retracing the *in vivo* haematopoietic tree using single-cell methods. *FEBS Lett* **590**, 4068–4083 (2016).

73. Yáñez, A. *et al.* Granulocyte-Monocyte Progenitors and Monocyte-Dendritic Cell Progenitors Independently Produce Functionally Distinct Monocytes. *Immunity* **47**, 890-902.e4 (2017).

74. Trzebanski, S. *et al.* Classical monocyte ontogeny dictates their functions and fates as tissue macrophages. *Immunity* **57**, 1225-1242.e6 (2024).

75. Yona, S. *et al.* Fate Mapping Reveals Origins and Dynamics of Monocytes and Tissue Macrophages under Homeostasis. *Immunity* **38**, 79–91 (2013).

76. Hashimoto, D. *et al.* Tissue-resident macrophages self-maintain locally throughout adult life with minimal contribution from circulating monocytes. *Immunity* **38**, 792–804 (2013).

77. Schulz, C. *et al.* A lineage of myeloid cells independent of myb and hematopoietic stem cells. *Science (1979)* **335**, 86–90 (2012).

78. Ginhoux, F. *et al.* Fate mapping analysis reveals that adult microglia derive from primitive macrophages. *Science (1979)* **330**, 841–845 (2010).

79. Alliot, F., Godin, I. & Pessac, B. Microglia derive from progenitors, originating from the yolk sac, and which proliferate in the brain. *Developmental Brain Research* **117**, 145–152 (1999).

80. Mildenberger, W., Stifter, S. A. & Greter, M. Diversity and function of brain-associated macrophages. *Current Opinion in Immunology* vol. 76 102181 Preprint at https://doi.org/10.1016/j.coi.2022.102181 (2022).

81. Bruttger, J. *et al.* Genetic Cell Ablation Reveals Clusters of Local Self-Renewing Microglia in the Mammalian Central Nervous System. *Immunity* **43**, 92–106 (2015).

82. Ajami, B., Bennett, J. L., Krieger, C., Tetzlaff, W. & Rossi, F. M. V. Local self-renewal can sustain CNS microglia maintenance and function throughout adult life. *Nat Neurosci* **10**, 1538–1543 (2007).

83. Davies, L. C., Jenkins, S. J., Allen, J. E. & Taylor, P. R. Tissue-resident macrophages. *Nature Immunology* vol. 14 986–995 Preprint at https://doi.org/10.1038/ni.2705 (2013).

84. Mass, E., Nimmerjahn, F., Kierdorf, K. & Schlitzer, A. Tissue-specific macrophages: how they develop and choreograph tissue biology. *Nat Rev Immunol* **23**, 563–579 (2023).

85. Lazarov, T., Juarez-Carreño, S., Cox, N. & Geissmann, F. Physiology and diseases of tissue-resident macrophages. *Nature* **618**, 698–707 (2023).

86. Prinz, M., Jung, S. & Priller, J. Microglia Biology: One Century of Evolving Concepts. *Cell* vol. 179 292–311 Preprint at https://doi.org/10.1016/j.cell.2019.08.053 (2019).

87. Paolicelli, R. C. *et al.* Microglia states and nomenclature: A field at its crossroads. *Neuron* vol. 110 3458–3483 Preprint at https://doi.org/10.1016/j.neuron.2022.10.020 (2022).

88. Hoogland, I. C. M., Houbolt, C., van Westerloo, D. J., van Gool, W. A. & van de Beek, D. Systemic inflammation and microglial activation: systematic review of animal experiments. *J Neuroinflammation* **12**, 114 (2015).

89. Austermann, J., Roth, J. & Barczyk-Kahlert, K. The Good and the Bad: Monocytes' and Macrophages' Diverse Functions in Inflammation. *Cells* **11**, 1979 (2022).

90. Frakes, A. E. *et al.* Microglia induce motor neuron death via the classical NF-κB pathway in amyotrophic lateral sclerosis. *Neuron* **81**, 1009–1023 (2014).

91. Xu, Y., Jin, M.-Z., Yang, Z.-Y. & Jin, W.-L. Microglia in neurodegenerative diseases. *Neural Regen Res* **16**, 270–280 (2021).

92. Singh, S. *et al.* Microglial nodules in early multiple sclerosis white matter are associated with degenerating axons. *Acta Neuropathol* **125**, 595–608 (2013).

93. Montilla, A. *et al.* Microglia and meningeal macrophages depletion delays the onset of experimental autoimmune encephalomyelitis. *Cell Death Dis* **14**, 1–13 (2023).

94. Wolf, Y. *et al.* Microglial MHC class II is dispensable for experimental autoimmune encephalomyelitis and cuprizone-induced demyelination. *Eur J Immunol* **48**, 1308–1318 (2018).

95. Plastini, M. J., Desu, H. L. & Brambilla, R. Dynamic Responses of Microglia in Animal Models of Multiple Sclerosis. *Frontiers in Cellular Neuroscience* vol. 14 571814 Preprint at https://doi.org/10.3389/fncel.2020.00269 (2020).

96. Geissmann, F., Jung, S. & Littman, D. R. Blood monocytes consist of two principal subsets with distinct migratory properties. *Immunity* **19**, 71–82 (2003).

97. Jakubzick, C. *et al.* Minimal differentiation of classical monocytes as they survey steady-state tissues and transport antigen to lymph nodes. *Immunity* **39**, 599–610 (2013).

98. Kratofil, R. M., Kubes, P. & Deniset, J. F. Monocyte conversion during inflammation and injury. *Arteriosclerosis, Thrombosis, and Vascular Biology* vol. 37 35–42 Preprint at https://doi.org/10.1161/ATVBAHA.116.308198 (2017).

99. Dal-Secco, D. *et al.* A dynamic spectrum of monocytes arising from the in situ reprogramming of CCR2+ monocytes at a site of sterile injury. *Journal of Experimental Medicine* **212**, 447–456 (2015).

100. Nahrendorf, M. *et al.* The healing myocardium sequentially mobilizes two monocyte subsets with divergent and complementary functions. *Journal of Experimental Medicine* **204**, 3037–3047 (2007).

101. Ajami, B., Bennett, J. L., Krieger, C., McNagny, K. M. & Rossi, F. M. V. Infiltrating monocytes trigger EAE progression, but do not contribute to the resident microglia pool. *Nat Neurosci* **14**, 1142–1150 (2011).

102. King, I. L., Dickendesher, T. L. & Segal, B. M. Circulating Ly-6C+ myeloid precursors migrate to the CNS and play a pathogenic role during autoimmune demyelinating disease. *Blood* **113**, 3190–3197 (2009).

103. Mildner, A. *et al.* CCR2+Ly-6Chi monocytes are crucial for the effector phase of autoimmunity in the central nervous system. *Brain* **132**, 2487–2500 (2009).

104. Monaghan, K. L., Zheng, W., Hu, G. & Wan, E. C. K. Monocytes and Monocyte-Derived Antigen-Presenting Cells Have Distinct Gene Signatures in Experimental Model of Multiple Sclerosis. *Front Immunol* **10**, 2779 (2019).

105. Amorim, A. *et al.* IFNγ and GM-CSF control complementary differentiation programs in the monocyte-to-phagocyte transition during neuroinflammation. *Nat Immunol* **23**, 217–228 (2022).

106. Shortman, K. & Naik, S. H. Steady-state and inflammatory dendritic-cell development. *Nature Reviews Immunology* vol. 7 19–30 Preprint at https://doi.org/10.1038/nri1996 (2007).

107. Waisman, A., Lukas, D., Clausen, B. E. & Yogev, N. Dendritic cells as gatekeepers of tolerance. *Seminars in Immunopathology* vol. 39 153–163 Preprint at https://doi.org/10.1007/s00281-016-0583-z (2017).

108. Steinman, R. M., Hawiger, D. & Nussenzweig, M. C. Tolerogenic dendritic cells. *Annual Review of Immunology* vol. 21 685–711 Preprint at https://doi.org/10.1146/annurev.immunol.21.120601.141040 (2003).

109. Guilliams, M. *et al.* Unsupervised High-Dimensional Analysis Aligns Dendritic Cells across Tissues and Species. *Immunity* **45**, 669–684 (2016).

110. Miller, J. C. *et al.* Deciphering the transcriptional network of the dendritic cell lineage. *Nat Immunol* **13**, 888–899 (2012).

111. Hilligan, K. L. & Ronchese, F. Antigen presentation by dendritic cells and their instruction of CD4+ T helper cell responses. *Cellular and Molecular Immunology* vol. 17 587–599 Preprint at https://doi.org/10.1038/s41423-020-0465-0 (2020).

112. Lindquist, R. L. *et al.* Visualizing dendritic cell networks in vivo. *Nat Immunol* **5**, 1243–1250 (2004).

113. Ohl, L. *et al.* CCR7 governs skin dendritic cell migration under inflammatory and steady-state conditions. *Immunity* **21**, 279–288 (2004).

114. Cabeza-Cabrerizo, M., Cardoso, A., Minutti, C. M., Pereira Da Costa, M. & Reis E Sousa, C. Dendritic Cells Revisited. *Annual Review of Immunology* vol. 39 131–166 Preprint at https://doi.org/10.1146/annurev-immunol-061020-053707 (2021).

115. Randolph, G. J., Ochando, J. & Partida-Sánchez, S. Migration of dendritic cell subsets and their precursors. *Annual Review of Immunology* vol. 26 293–316 Preprint at https://doi.org/10.1146/annurev.immunol.26.021607.090254 (2008).

116. O, S. *et al.* Toll-like receptor 3 promotes cross-priming to virus-infected cells. *Nature* **433**, (2005).

117. Durai, V. & Murphy, K. M. Functions of Murine Dendritic Cells. *Immunity* vol. 45 719–736 Preprint at https://doi.org/10.1016/j.immuni.2016.10.010 (2016).

118. Brown, C. C. *et al.* Transcriptional Basis of Mouse and Human Dendritic Cell Heterogeneity. *Cell* **179**, 846-863.e24 (2019).

119. Ye, Y., Gaugler, B., Mohty, M. & Malard, F. Plasmacytoid dendritic cell biology and its role in immune-mediated diseases. *Clinical and Translational Immunology* vol. 9 Preprint at https://doi.org/10.1002/cti2.1139 (2020).

120. Swiecki, M. & Colonna, M. The multifaceted biology of plasmacytoid dendritic cells. *Nat Rev Immunol* **15**, 471–485 (2015).

121. West, H. C. & Bennett, C. L. Redefining the role of langerhans cells as immune regulators within the skin. *Frontiers in Immunology* vol. 8 1941 Preprint at https://doi.org/10.3389/fimmu.2017.01941 (2018).

122. Segura, E. & Amigorena, S. Inflammatory dendritic cells in mice and humans. *Trends in Immunology* vol. 34 440–445 Preprint at https://doi.org/10.1016/j.it.2013.06.001 (2013).

123. Cheong, C. *et al.* Microbial stimulation fully differentiates monocytes to DC-SIGN/CD209+ dendritic cells for immune T cell areas. *Cell* **143**, 416–429 (2010).

124. Chow, K. V., Lew, A. M., Sutherland, R. M. & Zhan, Y. Monocyte-Derived Dendritic Cells Promote Th Polarization, whereas Conventional Dendritic Cells Promote Th Proliferation. *The Journal of Immunology* **196**, 624–636 (2016).

125. Ko, H.-J. *et al.* GM-CSF–Responsive Monocyte-Derived Dendritic Cells Are Pivotal in Th17 Pathogenesis. *The Journal of Immunology* **192**, 2202–2209 (2014).

126. Hilligan, K. L. & Ronchese, F. Antigen presentation by dendritic cells and their instruction of CD4+ T helper cell responses. *Cellular and Molecular Immunology* vol. 17 587–599 Preprint at https://doi.org/10.1038/s41423-020-0465-0 (2020).

127. Isaksson, M., Lundgren, B. A., Ahlgren, K. M., Kämpe, O. & Lobell, A. Conditional DC depletion does not affect priming of encephalitogenic Th cells in EAE. *Eur J Immunol* **42**, 2555–2563 (2012).

128. Yogev, N. *et al.* Dendritic cells ameliorate autoimmunity in the cns by controlling the homeostasis of PD-1 receptor+ regulatory T cells. *Immunity* **37**, 264–275 (2012).

129. Luu, T., Cheung, J. F., Baccon, J. & Waldner, H. Priming of myelin-specific T cells in the absence of dendritic cells results in accelerated development of Experimental Autoimmune... *PLoS One* **16**, (2021).

130. Paterka, M. *et al.* Gatekeeper role of brain antigen-presenting CD11c + cells in neuroinflammation . *EMBO J* **35**, 89–101 (2016).

131. Sun, S.-C. & Ley, S. C. New insights into NF-kappaB regulation and function. *Trends Immunol* **29**, 469–78 (2008).

132. Sun, S.-C. The noncanonical NF-κB pathway. *Immunol Rev* **246**, 125–140 (2012).

133. Sun, S. C. The non-canonical NF-κB pathway in immunity and inflammation. *Nature Reviews Immunology* vol. 17 545–558 Preprint at https://doi.org/10.1038/nri.2017.52 (2017).

134. Zarnegar, B. J. *et al.* Noncanonical NF-κB activation requires coordinated assembly of a regulatory complex of the adaptors cIAP1, cIAP2, TRAF2 and TRAF3 and the kinase NIK. *Nat Immunol* **9**, 1371–1378 (2008).

135. Liao, G., Zhang, M., Harhaj, E. W. & Sun, S.-C. Regulation of the NF-kappaB-inducing kinase by tumor necrosis factor receptor-associated factor 3-induced degradation. *J Biol Chem* **279**, 26243–50 (2004).

136. Vallabhapurapu, S. *et al.* Nonredundant and complementary functions of TRAF2 and TRAF3 in a ubiquitination cascade that activates NIK-dependent alternative NF-κB signaling. *Nat Immunol* **9**, 1364–1370 (2008).

137. Shih, R.-H., Wang, C.-Y. & Yang, C.-M. NF-kappaB Signaling Pathways in Neurological Inflammation: A Mini Review. *Front Mol Neurosci* **8**, 77 (2015).

138. Xiao, G., Harhaj, E. W. & Sun, S. C. NF-κB-inducing kinase regulates the processing of NF-κB2 p100. *Mol Cell* **7**, 401–409 (2001).

139. Razani, B. *et al.* Negative feedback in noncanonical NF-κB signaling modulates NIK stability through IKKα-mediated phosphorylation. *Sci Signal* **3**, ra41 (2010).

140. Liu, J. *et al.* Structure of the nuclear factor κB-inducing kinase (NIK) kinase domain reveals a constitutively active conformation. *Journal of Biological Chemistry* **287**, 27326–27334 (2012).

141. Pflug, K. M. & Sitcheran, R. Targeting NF-κB-inducing kinase (NIK) in immunity, inflammation, and cancer. *Int J Mol Sci* **21**, 1–19 (2020).

142. Schlechter, N. *et al.* Exome sequencing identifies a novel MAP3K14 mutation in recessive atypical combined immunodeficiency. *Front Immunol* **8**, (2017).

143. Willmann, K. L. *et al.* Biallelic loss-of-function mutation in NIK causes a primary immunodeficiency with multifaceted aberrant lymphoid immunity. *Nat Commun* **5**, (2014).

144. Miyawaki, S. *et al.* A new mutation,aly, that induces a generalized lack of lymph nodes accompanied by immunodeficiency in mice. *Eur J Immunol* **24**, 429–434 (1994).

145. Hahn, M., Macht, A., Waisman, A. & Hövelmeyer, N. NF-κB-inducing kinase is essential for B-cell maintenance in mice. *Eur J Immunol* **46**, 732–741 (2016).

146. Brightbill, H. D. *et al.* Conditional Deletion of NF-κB-Inducing Kinase (NIK) in Adult Mice Disrupts Mature B Cell Survival and Activation. *J Immunol* **195**, 953–64 (2015).

147. Li, Y. *et al.* Cell intrinsic role of NF-κB-inducing kinase in regulating T cell-mediated immune and autoimmune responses. *Sci Rep* **6**, 1–11 (2016).

148. Hamdan, T. A. *et al.* Map3k14 as a Regulator of Innate and Adaptive Immune Response during Acute Viral Infection. *Pathogens* **9**, 96 (2020).

149. Camara, A. *et al.* CD169+ macrophages in lymph node and spleen critically depend on dual RANK and LTbetaR signaling. *Proc Natl Acad Sci U S A* **119**, (2022).

150. Lind, E. F. *et al.* Dendritic Cells Require the NF-κB2 Pathway for Cross-Presentation of Soluble Antigens. *The Journal of Immunology* **181**, 354–363 (2008).

151. Jie, Z. *et al.* NIK signaling axis regulates dendritic cell function in intestinal immunity and homeostasis. *Nat Immunol* **19**, 1224–1235 (2018).

152. Jin, W., Zhou, X.-F., Yu, J., Cheng, X. & Sun, S.-C. Regulation of Th17 cell differentiation and EAE induction by MAP3K NIK. *Blood* **113**, 6603–6610 (2009).

153. Greter, M., Hofmann, J. & Becher, B. Neo-lymphoid aggregates in the adult liver can initiate potent cell-mediated immunity. *PLoS Biol* **7**, 1000109 (2009).

154. Lacher, S. M. *et al.* NF-κB inducing kinase (NIK) is an essential post-transcriptional regulator of T-cell activation affecting F-actin dynamics and TCR signaling. *J Autoimmun* **94**, 110–121 (2018).

155. Jie, Z. *et al.* Microglia promote autoimmune inflammation via the noncanonical NF-κB pathway. *Sci Adv* **7**, (2021).

156. Hofmann, J., Mair, F., Greter, M., Schmidt-Supprian, M. & Becher, B. NIK signaling in dendritic cells but not in T cells is required for the development of effector T cells and cell-mediated immune responses. *J Exp Med* **208**, 1917–29 (2011).

157. Andreas, N. *et al.* RelB Deficiency in Dendritic Cells Protects from Autoimmune Inflammation Due to Spontaneous Accumulation of Tissue T Regulatory Cells. *The Journal of Immunology* **203**, 2602–2613 (2019).

158. Huang, T. *et al.* CRL4DCAF2 negatively regulates IL-23 production in dendritic cells and limits the development of psoriasis. *Journal of Experimental Medicine* **215**, 1999–2017 (2018).

159. Katakam, A. K. *et al.* Dendritic cells require NIK for CD40-dependent cross-priming of CD8+ T cells. *Proc Natl Acad Sci U S A* **112**, 14664–14669 (2015).

160. Jung, S. *et al.* Analysis of Fractalkine Receptor CX 3 CR1 Function by Targeted Deletion and Green Fluorescent Protein Reporter Gene Insertion . *Mol Cell Biol* **20**, 4106–4114 (2000).

161. Caton, M. L., Smith-Raska, M. R. & Reizis, B. Notch-RBP-J signaling controls the homeostasis of CD8- dendritic cells in the spleen. *Journal of Experimental Medicine* **204**, 1653–1664 (2007).

162. Nowicka, M. *et al.* CyTOF workflow: differential discovery in high-throughput high-dimensional cytometry datasets. *F1000Res* **6**, 748 (2019).

163. Weber, L. M., Nowicka, M., Soneson, C. & Robinson, M. D. diffcyt: Differential discovery in high-dimensional cytometry via high-resolution clustering. *Commun Biol* **2**, 183 (2019).

164. Hao, Y. *et al.* Dictionary learning for integrative, multimodal and scalable single-cell analysis. *Nat Biotechnol* **42**, 293–304 (2023).

165. Dann, E., Henderson, N. C., Teichmann, S. A., Morgan, M. D. & Marioni, J. C. Differential abundance testing on single-cell data using k-nearest neighbor graphs. *Nat Biotechnol* **40**, 245–253 (2022).

166. Wu, T. *et al.* clusterProfiler 4.0: A universal enrichment tool for interpreting omics data. *Innovation* **2**, 100141 (2021).

167. Almolda, B., Gonzalez, B. & Castellano, B. Antigen presentation in EAE: Role of microglia, macrophages and dendritic cells. *Frontiers in Bioscience* vol. 16 1157–1171 Preprint at https://doi.org/10.2741/3781 (2011).

168. Matyash, M., Zabiegalov, O., Wendt, S., Matyash, V. & Kettenmann, H. The adenosine generating enzymes CD39/CD73 control microglial processes ramification in the mouse brain. *PLoS One* **12**, (2017).

169. Jakovljevic, M. *et al.* Induction of NTPDase1/CD39 by reactive microglia and macrophages is associated with the functional state during EAE. *Front Neurosci* **13**, (2019).

170. Lier, J., Streit, W. J. & Bechmann, I. Beyond activation: Characterizing microglial functional phenotypes. *Cells* vol. 10 2236 Preprint at https://doi.org/10.3390/cells10092236 (2021).

171. Tan, Y. L., Yuan, Y. & Tian, L. Microglial regional heterogeneity and its role in the brain. *Molecular Psychiatry* vol. 25 351–367 Preprint at https://doi.org/10.1038/s41380-019-0609-8 (2020).

172. De Biase, L. M. & Bonci, A. Region-Specific Phenotypes of Microglia: The Role of Local Regulatory Cues. *Neuroscientist* vol. 25 314–333 Preprint at https://doi.org/10.1177/1073858418800996 (2019).

173. Tay, T. L., Savage, J. C., Hui, C. W., Bisht, K. & Tremblay, M. È. Microglia across the lifespan: from origin to function in brain development, plasticity and cognition. *Journal of Physiology* **595**, 1929–1945 (2017).

174. Moran, I., Grootveld, A. K., Nguyen, A. & Phan, T. G. Subcapsular Sinus Macrophages: The Seat of Innate and Adaptive Memory in Murine Lymph Nodes. *Trends in Immunology* vol. 40 35–48 Preprint at https://doi.org/10.1016/j.it.2018.11.004 (2019).

175. Gray, E. E. & Cyster, J. G. Lymph Node Macrophages. *J Innate Immun* **4**, 424 (2012).

176. Gray, E. E., Friend, S., Suzuki, K., Phan, T. G. & Cyster, J. G. Subcapsular Sinus Macrophage Fragmentation and CD169+ Bleb Acquisition by Closely Associated IL-17-Committed Innate-Like Lymphocytes. *PLoS One* **7**, e38258 (2012).

177. Den Haan, J. M. M. & Kraal, G. Innate immune functions of macrophage subpopulations in the spleen. *Journal of Innate Immunity* vol. 4 437–445 Preprint at https://doi.org/10.1159/000335216 (2012).

178. Wolf, Y., Yona, S., Kim, K. W. & Jung, S. Microglia, seen from the CX3CR1 angle. *Front Cell Neurosci* (2013) doi:10.3389/fncel.2013.00026.

179. Bettelli, E. *et al.* Myelin oligodendrocyte glycoprotein-specific T cell receptor transgenic mice develop spontaneous autoimmune optic neuritis. *J Exp Med* **197**, 1073–81 (2003).

180. Vandenbark, A. A. & Offner, H. Critical evaluation of regulatory T cells in autoimmunity: are the most potent regulatory specificities being ignored? *Immunology* **125**, 1–13 (2008).

181. Giladi, A. *et al.* Cxcl10 + monocytes define a pathogenic subset in the central nervous system during autoimmune neuroinflammation. *Nat Immunol* **21**, 525–534 (2020).

182. Leylek, R. *et al.* Integrated Cross-Species Analysis Identifies a Conserved Transitional Dendritic Cell Population. *Cell Rep* **29**, 3736-3750.e8 (2019).

183. Lukowski, S. W. *et al.* Absence of Batf3 reveals a new dimension of cell state heterogeneity within conventional dendritic cells. *iScience* **24**, 102402 (2021).

184. Lancien, M. *et al.* Dendritic Cells Require TMEM176A/B Ion Channels for Optimal MHC Class II Antigen Presentation to Naive CD4+ T Cells. *The Journal of Immunology* **207**, 421–435 (2021).

185. Bachmaier, K. *et al.* E3 ubiquitin ligase Cblb regulates the acute inflammatory response underlying lung injury. *Nat Med* **13**, 920–926 (2007).

186. Wullaert, A. *et al.* LIND/ABIN-3 is a novel lipopolysaccharide-inducible inhibitor of NF-κB activation. *Journal of Biological Chemistry* **282**, 81–90 (2007).

187. Thompson, M. R., Xu, D. & Williams, B. R. G. ATF3 transcription factor and its emerging roles in immunity and cancer. *Journal of Molecular Medicine* vol. 87 1053–1060 Preprint at https://doi.org/10.1007/s00109-009-0520-x (2009).

188. Sha, H., Zhang, D., Zhang, Y., Wen, Y. & Wang, Y. ATF3 promotes migration and M1/M2 polarization of macrophages by activating tenascin-C via Wnt/β-catenin pathway. *Mol Med Rep* **16**, 3641–3647 (2017).

189. Sica, A. & Mantovani, A. Macrophage plasticity and polarization: In vivo veritas. *Journal of Clinical Investigation* vol. 122 787–795 Preprint at https://doi.org/10.1172/JCI59643 (2012).

190. Croasdell, A. *et al.* PPAR *γ* and the Innate Immune System Mediate the Resolution of Inflammation. *PPAR Res* **2015**, 1–20 (2015).

191. Pols, M. S. & Klumperman, J. Trafficking and function of the tetraspanin CD63. *Experimental Cell Research* vol. 315 1584–1592 Preprint at https://doi.org/10.1016/j.yexcr.2008.09.020 (2009).

192. Tsui, C. *et al.* Dynamic reorganisation of intermediate filaments coordinates early B-cell activation. *Life Sci Alliance* **1**, e201800060 (2018).

193. Jurberg, A. D. *et al.* VLA-4 as a Central Target for Modulating Neuroinflammatory Disorders. *NeuroImmunoModulation* vol. 28 213–221 Preprint at https://doi.org/10.1159/000518721 (2021).

194. Weiss, J. M. *et al.* An essential role for CD44 variant isoforms in epidermal langerhans cell and blood dendritic cell function. *Journal of Cell Biology* **137**, 1137–1147 (1997).

195. Termeer, C. *et al.* Targeting dendritic cells with CD44 monoclonal antibodies selectively inhibits the proliferation of naive CD4+ T-helper cells by induction of FAS-independent T-cell apoptosis. *Immunology* **109**, 32–40 (2003).

196. Page, M. J., Kell, D. B. & Pretorius, E. The Role of Lipopolysaccharide-Induced Cell Signalling in Chronic Inflammation. *Chronic Stress* vol. 6 Preprint at https://doi.org/10.1177/24705470221076390 (2022).

197. Cua, D. J. *et al.* Interleukin-23 rather than interleukin-12 is the critical cytokine for autoimmune inflammation of the brain. *Nature* **421**, 744–748 (2003).

198. Samoilova, E. B., Horton, J. L. & Chen, Y. Acceleration of experimental autoimmune encephalomyelitis in interleukin-10-deficient mice: roles of interleukin-10 in disease progression and recovery. *Cell Immunol* **188**, 118–24 (1998).

199. Cua, D. J., Groux, H., Hinton, D. R., Stohlman, S. A. & Coffman, R. L. Transgenic interleukin 10 prevents induction of experimental autoimmune encephalomyelitis. *J Exp Med* **189**, 1005–10 (1999).

200. Bettelli, E. *et al.* IL-10 Is Critical in the Regulation of Autoimmune Encephalomyelitis as Demonstrated by Studies of IL-10- and IL-4-Deficient and Transgenic Mice. *The Journal of Immunology* **161**, 3299–3306 (1998).

201. Trzebanski, S. & Jung, S. Plasticity of monocyte development and monocyte fates. *Immunology Letters* vol. 227 66–78 Preprint at https://doi.org/10.1016/j.imlet.2020.07.007 (2020).

202. Sewald, X. *et al.* Retroviruses use CD169-mediated trans-infection of permissive lymphocytes to establish infection. *Science* **350**, 563–567 (2015).

203. Grabowska, J., Lopez-Venegas, M. A., Affandi, A. J. & Den Haan, J. M. M. CD169+ macrophages capture and dendritic cells instruct: The interplay of the gatekeeper and the general of the immune system. *Frontiers in Immunology* vol. 9 2472 Preprint at https://doi.org/10.3389/fimmu.2018.02472 (2018).

204. Aichele, P. *et al.* Macrophages of the Splenic Marginal Zone Are Essential for Trapping of Blood-Borne Particulate Antigen but Dispensable for Induction of Specific T Cell Responses. *The Journal of Immunology* **171**, 1148–1155 (2003).

205. Winkelmann, E. R. *et al.* Subcapsular sinus macrophages limit dissemination of West Nile virus particles after inoculation but are not essential for the development of West Nile virus-specific T cell responses. *Virology* **450–451**, 278–289 (2014).

206. Miyake, Y. *et al.* Critical role of macrophages in the marginal zone in the suppression of immune responses to apoptotic cell-associated antigens. *Journal of Clinical Investigation* **117**, 2268–2278 (2007).

207. Bogie, J. F. J. *et al.* CD169 is a marker for highly pathogenic phagocytes in multiple sclerosis. *Multiple Sclerosis Journal* **24**, 290–300 (2018).

208. Sominsky, L., De Luca, S. & Spencer, S. J. Microglia: Key players in neurodevelopment and neuronal plasticity. *Int J Biochem Cell Biol* **94**, 56–60 (2018).

209. Chu, T. *et al.* Dynamic response of microglia/macrophage polarization following demyelination in mice. *J Neuroinflammation* **16**, 188 (2019).

210. Plastini, M. J., Desu, H. L. & Brambilla, R. Dynamic Responses of Microglia in Animal Models of Multiple Sclerosis. *Front Cell Neurosci* **14**, 571814 (2020).

211. Ghasemlou, N., Jeong, S. Y., Lacroix, S. & David, S. T cells contribute to lysophosphatidylcholine-induced macrophage activation and demyelination in the CNS. *Glia* **55**, 294–302 (2007).

212. Schilling, T., Lechmann, F., Rückert, B. & Eder, C. Physiological mechanisms of lysophosphatidylcholine-induced de-ramification of murine microglia. *Journal of Physiology* **557**, 105–120 (2004).

213. Gudi, V., Gingele, S., Skripuletz, T. & Stangel, M. Glial response during cuprizone-induced de- and remyelination in the CNS: Lessons learned. *Frontiers in Cellular Neuroscience* vol. 8 Preprint at https://doi.org/10.3389/fncel.2014.00073 (2014).

214. Sen, M. K., Mahns, D. A., Coorssen, J. R. & Shortland, P. J. The roles of microglia and astrocytes in phagocytosis and myelination: Insights from the cuprizone model of multiple sclerosis. *GLIA* vol. 70 1215–1250 Preprint at https://doi.org/10.1002/glia.24148 (2022).

215. Backer, R. A., Probst, H. C. & Clausen, B. E. Classical DC2 subsets and monocyte-derived DC: Delineating the developmental and functional relationship. *European Journal of Immunology* vol. 53 Preprint at https://doi.org/10.1002/eji.202149548 (2023).

216. King, I. L., Kroenke, M. A. & Segal, B. M. GM-CSF-dependent, CD103+ dermal dendritic cells play a critical role in Th effector cell differentiation after subcutaneous immunization. *Journal of Experimental Medicine* **207**, 953–961 (2010).

217. Oliveira, L. D. M., Teixeira, F. M. E. & Sato, M. N. Impact of Retinoic Acid on Immune Cells and Inflammatory Diseases. *Mediators of Inflammation* vol. 2018 3067126 Preprint at https://doi.org/10.1155/2018/3067126 (2018).

218. Di Caro, V. *et al.* Retinoic acid-producing, ex-vivo-generated human tolerogenic dendritic cells induce the proliferation of immunosuppressive B lymphocytes. *Clin Exp Immunol* **174**, 302–17 (2013).

219. Rausch, M. P. & Hastings, K. T. Diverse cellular and organismal functions of the lysosomal thiol reductase GILT. *Molecular Immunology* vol. 68 124–128 Preprint at https://doi.org/10.1016/j.molimm.2015.06.008 (2015).

220. Bergman, C. M. *et al.* A Switch in Pathogenic Mechanism in Myelin Oligodendrocyte Glycoprotein-Induced EAE in GILT-Free Mice. *J Immunol* **188**, 6001 (2012).

221. El-Behi, M. *et al.* The encephalitogenicity of TH 17 cells is dependent on IL-1- and IL-23-induced production of the cytokine GM-CSF. *Nat Immunol* **12**, 568–575 (2011).

222. Shajarian, M. *et al.* IL-23 plasma level measurement in relapsing remitting multiple sclerosis (RRMS) patients compared to healthy subjects. *Immunol Invest* **44**, 36–44 (2015).

223. Vaknin-dembinsky, A., Balashov, K. & Weiner, H. L. Down-Regulation of IL-23 by Antisense Oligos Increases. 1–7 (2006).

224. Miyake, K. *et al.* Single-cell transcriptomics identifies the differentiation trajectory from inflammatory monocytes to pro-resolving macrophages in a mouse skin allergy model. *Nat Commun* **15**, 1666 (20z24).

225. Auffray, C. *et al.* Monitoring of blood vessels and tissues by a population of monocytes with patrolling behavior. *Science (1979)* **317**, 666–670 (2007).

226. Li, Y. H. *et al.* Occurrences and Functions of Ly6Chi and Ly6Clo Macrophages in Health and Disease. *Frontiers in Immunology* vol. 13 Preprint at https://doi.org/10.3389/fimmu.2022.901672 (2022).

227. Kalinski, A. L. *et al.* Analysis of the immune response to sciatic nerve injury identifies efferocytosis as a key mechanism of nerve debridement. *Elife* **9**, 1–41 (2020).

228. Brunet, A. *et al.* NR4A1-dependent Ly6Clow monocytes contribute to reducing joint inflammation in arthritic mice through Treg cells. *Eur J Immunol* **46**, 2789–2800 (2016).

229. Egawa, M. *et al.* Inflammatory monocytes recruited to allergic skin acquire an anti-inflammatory M2 phenotype via basophil-derived interleukin-4. *Immunity* **38**, 570–80 (2013).

230. Liu, Z. *et al.* Fate Mapping via Ms4a3-Expression History Traces Monocyte-Derived Cells. *Cell* **178**, 1509-1525.e19 (2019).

231. Dalod, M. & Scheu, S. Dendritic cell functions in vivo: A user's guide to current and next-generation mutant mouse models. *European Journal of Immunology* vol. 52 1712–1749 Preprint at https://doi.org/10.1002/eji.202149513 (2022).

232. Loschko, J. *et al.* Absence of MHC class II on cDCs results in microbialdependent intestinal inflammation. *Journal of Experimental Medicine* **213**, 517–534 (2016).

233. Satpathy, A. T. *et al.* Zbtb46 expression distinguishes classical dendritic cells and their committed progenitors from other immune lineages. *Journal of Experimental Medicine* **209**, 1135–1152 (2012).

234. Zahner, S. P. *et al.* Conditional Deletion of TGF-βR1 Using Langerin-Cre Mice Results in Langerhans Cell Deficiency and Reduced Contact Hypersensitivity. *The Journal of Immunology* **187**, 5069–5076 (2011).

235. Cheng, J. *et al.* Pharmacological inhibition of NF-κB-inducing kinase (NIK) with small molecules for the treatment of human diseases. *RSC Med Chem* **12**, 552–565 (2021).

236. Li, M. Y. *et al.* TRAF3 Loss-of-Function Reveals the Non-Canonical NF-Kb Pathway As a Therapeutic Target in Diffuse Large B-Cell Lymphoma . *Blood* **140**, 2042–2043 (2022).

237. Zhang, N. *et al.* Design, Synthesis, and Biological Evaluation of a Novel NIK Inhibitor with Anti-Inflammatory and Hepatoprotective Effects for Sepsis Treatment. *J Med Chem* **67**, 5617–5641 (2024).

8.

ACKNOWLEDGEMENTS

[redacted]

[redacted]

[redacted]

[redacted]

[redacted]

9.

EIDESSTATTLICHE VERSICHERUNG

Hiermit versichere ich, dass ich die von mir vorgelegte Dissertation angefertigt, die benutzten Quellen und Hilfsmittel vollständig angegeben und die Stellen der Arbeit, einschließlich Tabellen und Abbildungen, die andere Werke im Wortlaut oder dem Sinn nach entnommen sind, in jedem Einzelfall als Entlehnung kenntlich gemacht habe; dass diese Dissertation noch keiner anderen Fakultät oder Universität zur Prüfung vorgelegen hat, dass sie noch nicht veröffentlicht worden ist, sowie dass ich eine solche Veröffentlichung vor Abschluss des Promotionsverfahrens nicht vornehmen werde. Die Bestimmungen dieser Promotionsordnung sind mir bekannt. Die von mir vorgelegte Dissertation ist von Herrn Prof. Dr. Ari Waisman betreut worden.

Mainz, July 2024

Nishada Ramphal

10.

CURRICULUM VITAE

NISHADA S.K. RAMPHAL, MSc

[redacted]

EDUCATION

May 2018- present **Doctoral candidate | JGU Mainz,**

Supervisor [redacted]

» Thesis topic: The role of the NF-kB inducing kinase in microglia and other myeloid populations during EAE

Sept. 2014- **Master of Science | University of Amsterdam**

June 2017 » Major in Biomedical Sciences - Neurobiology: Molecular Neurosciences

Sept 2010- **Bachelor of Applied Sciences**| Hogeschool Utrecht

July 2014 » Major in Biomolecular Sciences

»Minor in Biomolecular and Neuroscience, Vrije Universiteit Amsterdam (VU)

RESEARCH EXPERIENCE

Oct. 2015 - **Master thesis | UCSD | Neurobiology**

June 2016 Supervisors: [redacted]

» Topic: The potential link between hippocampus-specific deletion of LGL and the manifestation of autism-like behaviour in mice.

»Techniques: Mouse behavioural experiments | WB | *in vitro* cell culture | Tissue clearing

Dec. 2014 - **Master Internship | University Utrecht | Cell biology of the neuron**

July 2015

»Topic: Investigating the function of EML2, an unidentified microtubule-associated protein, in the early stages of axon development

»Techniques: Primary rat hipp. culture | ICC | Confocal & live cell imaging & analysis | WB | Cloning | Transfection

Feb. 2014 - June 2014 **Bachelor thesis | RadboudUMC Nijmegen, LGEM Neurochemistry**

»Topic: Phosphorylated α-synuclein as a biomarker to distinguish Parkinson's disease from other Parkinsonian diseases.

»Techniques: ELISA | WB | human material

Feb. 2013 - June 2013 **Bachelor Internship | NIN Amsterdam | Neuroregeneration**

» Topic: The effect of ENTPD2 expression in Olfactory Ensheating Cells on ATPase toxicity during spinal cord injury

»Techniques: SC isolation rat | IHC | Confocal imaging & analysis | Glia Neuron co-cultures | qPCR

CERTIFICATES

June 2015 **Laboratory Animal Sciences (Article 9, NL) / FELASA B (DE)**

» Article necessary to work with animals for research purposes within the European Union (EU) (including 8ECT of lectures each year, needed to keep the FELASA valid in Germany)

STIPENDS & AWARDS:

May 2018 **Focus in Translational Neuroscience Mainz Stipendium** (Until April 2020)

Oct. 2022 **Aegean Travel award**

CONFERENCE PRESENTATIONS

May 2024 **Ramphal NS**, Waisman A. *The role of the NF-kB inducing kinase in microglia and other myeloid populations during EAE.* Poster presentation: EMBO Microglia in Health and Disease. Genova, Italy.

Sept. 2023 **Ramphal NS**, Waisman A. *The role of the NF-kB inducing kinase in microglia and other myeloid populations during EAE.* Poster presentation: ISNI 2023. Quebec, Canada.

July 2023 **Ramphal NS**, Waisman A. *The role of the NF-kB inducing kinase in microglia and other myeloid populations during EAE.* Poster presentation: GLIA 2023. Berlin, Germany.

Oct.2022 **Ramphal NS**, Waisman A. *The role of the NF-kB inducing kinase in myeloid populations during EAE.* Poster presentation: Aegean conferences: Autoimmunity: Mechanisms and Novel Treatments. Chania, Greece.

March 2022 **Ramphal NS**, Waisman A. *The role of the NF-kB inducing kinase in myeloid populations during steady state and EAE.* Poster presentation: Keystone symposium: Myeloid cells: from birth to immunity and disease. Banff, Canada.

11.

PUBLICATIONS

2020 Mohebiany AN, **Ramphal NS**, Karram K, Di Liberto G, Novkovic T, Klein M, Marini F, Kreutzfeldt M, Härtner F, Lacher SM, Bopp T, Mittmann T, Merkler D, Waisman A. *Microglial A20 Protects the Brain from CD8 T-Cell-Mediated Immunopathology*. Cell Reports. PMID: 32023471